THE SYNERGIC INFLUENCE OF NANOSILICA AND CARBON NANO TUBE ON FRESH AND HARDENED PROPERTIESOF HIGH VOLUME FLY ASH SELF-COMPACTING CONCRETES

Vahid JALILZADIAN NASL

Master Thesis
Department of Civil Engineering
Structural Division
Assoc. Prof. Dr. Abdulkadir Cuneyt AYDIN
2015

UNIVERSITY OF ATATURK
GRADUATE SCHOOL OF NATURAL AND APPLIED SCIENCES

MASTER THESIS

THE SYNERGIC INFLUENCE OF NANOSILICA AND CARBON NANO TUBE ON FRESH AND HARDENED PROPERTIES OF HIGH VOLUME FLY ASH SELF-COMPACTING CONCRETES

Vahid JALILZADIANNASL

DEPARTMENT OF CIVIL ENGINEERING
Structural Division

ERZURUM
2015

TURKISH REPUBLIC
ATATURK UNIVERSITY
GRADUTE SCHOOL of NATURAL and
APPLIED SCIENCES

THESIS APPROVAL FORM

THE SYNERGIC INFLUENCE OF NANOSILICA AND CARBON NANO TUBE ON FRESH AND HARDENED PROPERTIES OF HIGH VOLUME FLY ASH SELF-COMPACTING CONCRETES

This study, prepared by Vahid JALILZADIANNASL, under supervision of Assoc Prof. Dr. Abdulkadir Cüneyt AYDIN, has been approved on the date of 03 / 12 / 2015 as Master Thesis, in the Structural Division of Civil Engineering Department, by the below-named thesis committee with ~~majority~~/unanimously (.3./.3.).

President : Prof. Dr. Rüstem GÜL Signature :

Member : Assoc. Prof. Dr. Abdulkadir Cüneyt AYDIN Signature :

Member : Assist. Prof. Dr. Merve SAĞIROĞLU Signature :

The above-mentioned result;
Has been approved in accordance with Institute Administrative Committee on the date of .10. /..12.. / 2015 and resolution number 50 /.1656..

Prof. Dr. Ertan YILDIRIM
Institute Director

Note: Reproduction of authentic or quoted notifications, charts, figures and images of this thesis is subject to provisions of Law on Intellectual and Artistic Works law number 5846.

ÖZET

Yüksek Lisans Tezi

YÜKSEK ORANDA UÇUCU KÜL İÇEREN KENDİLİĞİNDEN YERLEŞEN BETONLARIN TAZE VE SERTLEŞMİŞ ÖZELLİKLERİNE NANO SİLİKA VE KARBON NANO TÜPLERİN ETKİSİ

Vahid JALILZADIAN NASL

Atatürk Üniversitesi
Fen Bilimleri Enstitüsü
İnşaat Mühendisliği Anabilim Dalı
Yapı Bilim Dalı

Danışman: Doç. Dr. Abdulkadir Cüneyt AYDIN

Nano silika (NS), karbon nano tüp (CNT) ve uçucu kül (FA) ün ayrık, ikili ya da üçlü kompozisyonlar halinde kendiliğinden yerleşen betonların (SCC) taze ve sertleşmiş özelliklerine etkisi bu çalışma kapsamında araştırılmıştır. Mevcut çalışmaların ışığında oran ve seviyeleri belirlenen bu katkılar çimentodan eksiltme yapmak suretiyle kullanılmıştır. Bu çalışmada, sekiz karışım grubu iki FA lü ve FA süz kategorilere bölünmüş ve her kategoride bir referans grubunu yanı sıra üç ayrı gurup yer almıştır. Bunlardan ikisi yalnız NS ya da CNT içerirken, üçüncü grup NS ve CNT lerin birlikte olduğu karışımları kapsamıştır.
Geçmişte yapılan çeşitli araştırmalara dayanarak en uygun yüzdeler NS, CNT ve FA için, sırasıyla %2, %0.08, ve %40 olarak belirlenmiştir. SCC karışımların taze özellikleri Slump-flow, V-Funnel ve L-Box deneyleri ile, sertleşmiş özellikleri ise, tek eksenli basınç ve eğilme deneyleri ile elde edilmiştir.
Super akışkanlaştırıcı ve su çimento oranının sabit tutulduğu karışımlarda, NS yüksek su ihtiyacına sebep olması sebebiyle, taze betonun işlenebilme özelliklerini kötü yönde etkilemiştir. Ancak, FA lü karışımlarda, NS işlenebilirlik özelliklerini anlamlı bir biçimde geliştirmiştir. %40 FA katılması durumunda şahit numunelere göre terleme ve ayrışma etkileri kaybolurken, bu katkıların yalnız ikili etkileri ele alındığında, CNT tüm durumlarda umut verici bir tesir sergilemiştir. Yüksek puzolanik reaktivitesinden dolayı, NS, SCC un hidratasyonunu hızlandırmış ve ikinci kategoride yüksek FA oranından kaynaklanan hidratasyondaki yavaşlamayı telafi etmiştir. CNT ün hidratasyonu dengeleyen etkisi FA içeren karışımlarda öne çıkmıştır. NS nın eğilme tokluk endeksleri üzerine, daha güçlü bir ara yüzey geçiş bölgesi ITZ ve daha iyi bir mikro yapı sağladığı, CNT ün tokluk endeksini %20 mertebesinde artırdığı görülmüştür.
Sonuç olarak, yapılan deneysel çalışmalar neticesinde, %2 NS, %0.02 CNT ve %40 FA içeren karışımların ele alınan teknik özellikler itibariyle en iyi SCC karışımı olduğu anlaşılmıştır. Elde edilen bütün teknik faydaların yanında, NS ve CNT ile desteklenmiş yüksek oranda FA kullanımı ile hem çevre dostu hem de mekanik açıdan gelişmiş özelliklerde betonlar imal edilebilmiştir. Ayrıca, CNT kullanımı ile enerji yutma kapasitesi daha yüksek, sünek betonların üretimi mümkün olmuştur.

2015, 143 sayfa

Anahtar Kelimeler: Kendiliğinden yerleşen beton, nanolif, nano silika, karbon nanotüp, uçucu kül

ABSTRACT

Master Thesis

THE SYNERGIC INFLUENCE OF NANOSILICA AND CARBON NANO TUBE ON FRESH AND HARDENED PROPERTIES OF HIGH VOLUME FLY ASH SELF-COMPACTING CONCRETES

Vahid JALILZADIAN NASL

Ataturk University
Graduate School of Natural and Applied Sciences
Department of Civil Engineering
Structural Division

Supervisor: Assoc Prof. Dr. Abdulkadir Cüneyt AYDIN

The influence of nano silica (NS), carbon nano tube (CNT) and fly ash (FA) as solo, binary or ternary compositions on fresh and hardened properties of self-compacting concretes were investigated in this study. All this material replaced with the portion of the cement at special replacement levels derived from available works. For the purpose of this investigation, the eight groups of mixes categorized into two categories with and without FA so that each category possessed a reference group and three other groups with only NS, CNT or both of them.

On the basis of different previous works, the optimum substitution percentages selected 2%. 0.08% and 40% for NS, CNT and FA, respectively. The investigated fresh properties were slump-flow, V-Funnel and L-Box tests. On the other hand, compressive strength and flexural toughness test studied and compared as hardened properties of SCC.

Test results illustrated that NS worsened the fresh state properties due to its higher water demand since the super plasticizer (SP) proportion and w/c ratio kept constant for all mix groups. Nonetheless, in presence of FA, NS improved these properties significantly and removed segregation and bleeding effects of 40% FA. While just the binary influence of these materials was remarkably improving, CNT showed a promising influence in all cases. According to its high reactivity, NS accelerated hydration of SCC and compensated the retardation caused by high volume of FA in second category whereas the balancing effect of CNT on mixtures including FA was interesting. Although NS demonstrated its role in improving flexural toughness indices by providing stronger interfacial transition zone (ITZ) and better microstructure for SCC, CNT give a 20% increase to toughness indices of SCC.

Finally, resulting from empirical tests, the mix with 2% NS, 0.02% CNT and 40% FA can be considered as the best SCC mix due to discussed specifications. Besides all convenient fresh properties, by support of NS and CNT, the inclusion of high volume of FA led to sustainable construction and production of a more environment friendly concrete with improved mechanical properties. Moreover, CNT resulted in more ductile concrete with higher energy absorbing capacity.

2015, 143 pages

Keywords: Self compacting concrete, nanofiber, nanosilica, carbon nanotube, fly ash

ACKNOWLEDGEMENTS

I would like to express my profound appreciation to my devoted and patient supervisor, honorable Assoc. Prof. Dr. Abdulkadir Cuneyt AYDIN, not only for his educational and technical advices throughout this study, but also for all his motivating guidance and discussions to follow the road of life as a follower of reality.

I would like to thank my dear friendS Ali Oz, Mahmut KILIÇ and Mahyar MAALI for their valuable helps in various stage of this study.

I wish to dedicate this work to all shining stars of the heaven of science through history like Omar Khayyam who protected the light of knowledge to lighten our minds despite wind chill of ignorance.

Finally, I hope my little daughter Deniz to continue their way.

November-2015
Vahid JALILZADIAN NASL

CONTENTS

SYMBOLS and ABBREVIATIONS LIST

$\delta 0$	: First crack deflection
ASR	: Alkali silica reaction
b	: Width or breadth of the section
BSE	: Backscattered electron
Bp	: Retained water ratio
CNT	: Carbon nano tube
CO_2	: Carbon dioxide
CPM	: Compressive packing model
CSF	: Condensed silica fume
C-S-H	: Calcium silica hydrate
D	: Particle size in µm
d	: Height or depth of the section
DSC	: Differential scanning analysis
DTA	: Differential thermal analysis
E	: Module of elasticity
Ep	: Deformation coefficient
F	: Total induced load
FA	: Fly ash
F'c	: Compressive Strength
FVS	: Fresh visual stability
GGBS	: Ground granulated blast furnace slag
H_1, H_2	: Depths of concrete
HP	: Hyperplasticizer
HPC	: High performance concrete
HRWR	: High range water reducer
HSHPC	: High strength high performance concrete
HVFA	: High volume fly ash
HVFC	: High volume fly ash concrete
I_N	: Flexural toughness index

ITZ	: Interfacial transition zone
k	: K-value/factor
L	: Distance between two lower supports of beam
LPDM	: Linear packing density model
LSP	: Limestone powder
M	: Metakaolin
MIP	: Mercury intrusion porosimetry
MWCNT	: Multi wall carbon nano carbon tube
NA	: Nano-Al2O
NC	: Nano-CuO
NF	: Nano-Fe2O3
nm	: Nano meter
NS	: Nano silica
NT	: Nano-TiO2
NVC	: Normally vibrated concrete
NZF	: Nano-ZnFe2O
NZr	: Nano-ZrO2
OPC	: Ordinary portland cement
P(D)	: Fraction of total solids smaller than D
PFBC	: Portland blast furnace cement
PC	: Portland cement
PCE	: Polycarboxylic ether
PCS	: Post-crack strength
PFA	: Pulverized fuel ash
PLSC	: Portland limestone cement
PSD	: Particle size distribution
P_v-δ	: Load versus deflection
q	: Distribution modulus
SCC	: Self-compacting concrete
SCM	: Supplementary cementitious materials
SEM	: Scanning electron microscopy

SF	: Silica fume
S-F	: Slump-flow test
SP	: Superplasticser
SSM	: Solid suspension model
TGA	: Thermogravimetric analysis
$t_{v\text{-}f}$	: Time of V-Funnel test
UHPC	: Ultra high performance concrete
V-F	: V-Funnel test
VMA	: Viscosity Modifying agent
w/b	: Water binder ratio
w/c	: Water cement ratio
wt	: Weight
xrd	: X-ray diffraction

LIST OF FIGURES

LIST OF TABLES

1. INTRODUCTION

Self-compacting concrete (SCC) must be considered as one of the most affecting achievements by which the construction industry has been able to develop significantly along with other fields of science and technology. SCC can be utilized to satisfy the all necessary conditions for an ideal design and implementation. In the other words, the higher compressive strength of SCC results in a better stability whereas self-compactibility makes its placement so easy with no need to manpower which means an economic concrete. The ability to pass narrow spaces provides more facilities to use more congested sections as well as thinner profiles which leads to more options to design and execute projects with more affective applications. The aesthetic aspect of the structures can be improved owing to better finishes of SCC. Moreover, durability of this kind of concrete is the most considerable advantage. These unique specifications of SCC depend on very special fresh and hardened properties of the concrete. Filling and passing ability together with resistance to segregation are the main characteristics of SCC in fresh state. On the other hand, refined pore structure, improved microstructure and homogenous matrix are governing factors of SCC which provide an improved mechanical properties and increased durability.

To achieve all mentioned above, a concise approach is needed in choosing and proportioning of cement, fillers, aggregates and admixtures of SCC to be include in a disciplined mix design methodology.

The intrinsic texture of SCC make it necessary to use supplementary cementitious materials as additions in SCC. Fly ash, ground granulated blast furnace (GGBS) and metakaolin are extremely fine materials with high pozzolanic reactivity which are mainly by-products of different industrial procedures. Their inclusion in mix not only helps SCC to gain stated valuable properties, but also provides the condition to a significant reduction in carbon dioxide emission to the atmosphere through replacement with cement.

On the other hand, nano technology is rapidly growing and encompassing the every single field of science and industry where construction is not an exception. Thus, the presence of nano particles should not be ignored. Owing to their extremely tiny dimensions, these particles play an outstanding role in improving various properties of normal vibrated and self-compacting concretes. They adjust particle size distribution of the mixture to make it more homogenous and cohesive which results in either enhanced flow ability of fresh state or decreased empty space of hardened state. Their higher reactivity due to their higher surface area causes stronger concretes. In addition, they trigger nucleation sites in microstructure of the concrete to produce denser texture beside the stronger interfacial transition zone. However, the percentage of inclusion has particular importance to avoid agglomeration and its disturbing consequences. Additionally, carbon nano tubes demonstrate a marvelous impacts on numerous properties of concrete mix because their completely special shape. These are tubular fiber shape materials in nano dimensions. They are capable of changing tensile and flexural strength of concrete significantly by bridging cracks and transferring and bearing the surplus stresses. Moreover, they restrain crack propagation in commence of cracks to help formation of not only a less permeable mixture but also more functional ITZ. The best result of their inclusion in the mixture could be a more ductile concrete.

In this thesis, previous related studies about self-compacting concretes, supplementary cimentitious materials, nanoparticles investigated. The most effective proportions for fly ash, nano silica and carbon nano tube determined and their solo, binary or ternary composition provided. For the purpose of this research, diverse influences of various combinations on different aspects of self-compacting concrete studied to see how they can remove the weak points of each other or boost their positive effects. The objective was to achieve a more environment friendly self-compacting concrete with high strength and better ductility.

2. LITERATURE REVIEW and BACKGROUND

2.1. Self-Compacting Concretes

As a relatively new type of concrete, SCC needs a closer focus on its fresh and hardened properties. Thus, it seems absolutely necessary to have detailed knowledge about the different aspects of SCC itself. For this purpose, this section is going to cover this matter.

2.1.1. General

Self-compacting concrete (SCC), also referred to as self-consolidating concrete is considered as one of the most significant developments and important achievements in building and construction industry (Brouwers and Radix, 2005). Owing to its unique properties, it has attracted attention of so many researchers from all over the world to focus on variety of methods to improve behaviors and widen fields of utilization of this kind of concrete.

First initiated in Japan in the mid-1980s as an underwater placement technology, SCC has been developed in recent years as a niche product and a problem solver (Gaimster and Dixon 2003).

Flow capacity of SCC assures complete filling of framework through dense reinforcement even in narrow sections with no compaction energy. At the same time, it shows neither segregation nor bleeding. Therefore, eliminating vibration labor and relevant defects like honeycombing, SCC shows its impact on concrete cost, time scale, working condition, health, strength and durability.

2.1.2. Definition and advantages

SCC is a highly flowable, yet stable concrete that can spread readily into place and fill the formwork without any consolidation and without undergoing any significant separation (Gaimster and Dixon 2003).

Eliminated vibration and difficulty of placement in congested reinforcement, SCC results in many advantages in different topics.

The ease of placement makes this possible to design slimmer elements (Gaimster and Dixon 2003) which results in more usable space for architects. Furthermore, as discussed in trials undertaken by RMC Technical Center, surface finish is one of the outstanding profits of SCC which provides fascinating architectural possibilities.

Slimmer elements also mean reduced self-weigh. On the other hand, there is so smaller need for energy consumption, skilled labor force and supervision in SCC than normally vibrated concrete (NVC) which results in reduction of costs.

Alongside the elimination of white finger syndrome, SCC contributes to reduction in noise level, required energy even consumed materials by avoiding spillage of materials and reduction in cement content, and consequently lesser CO_2 emission (Gaimster and Dixon 2003).

Additionally, SCC helps precast industry because of its ease of casting to inaccessible, complex and congested molds as well as less damage of formwork.

In this respect, the benefits of SCC can be summarized as below:

- More architectural possibilities
- Thinner concrete sections

- Improved durability
- Improved surface quality
- Lower costs and shorter time
- Improved and safer working environment
- More sustainable and clean technology
- Improved in situ quality in difficult conditions
- Reduction in site manpower
- Faster construction and easier placing

(EFNARC 2002; Gaimster and Dixon 2003)

2.1.3. Constituents and Design of the Mixture

Generally in comparison with conventional concretes, SCCs possess mix design characteristics such as lower coarse aggregate contents and w/c ratio whereas super plasticizer and paste content are increased alongside with possible use of viscosity modifying admixtures (The European Guidelines for Self-Compacting Concrete 2005).

There are two main requirements for SCC in both choosing and designing steps of the mix design:

- Highly mobile concrete, so low yield stress
- Highly resistant concrete to segregation, so high viscosity

Merely addition of water or super-plasticizer (SP) to decrease the yield stress will also lower the viscosity of the mix. Thus, the best way to increase viscosity can be either change in mix constituent or use of viscosity modifier agents (VMAs) and reaching to a balanced point between the shear rate and shear stress (Gaimster and Dixon 2003).

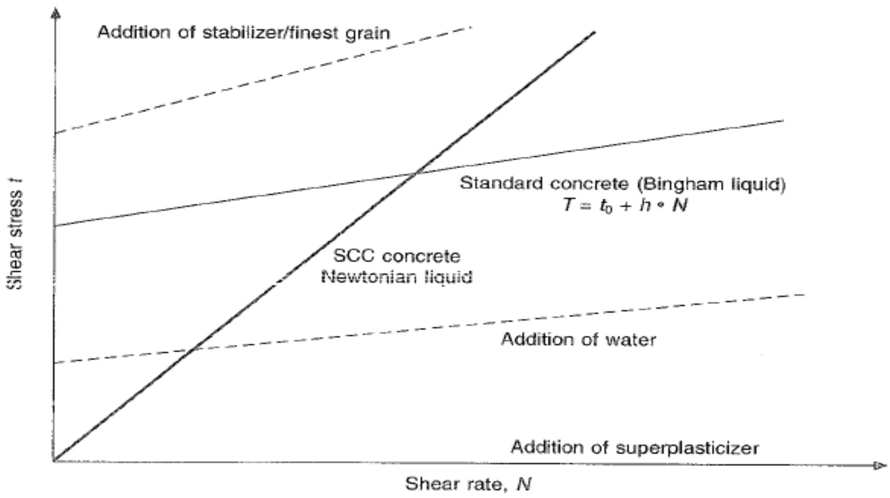

Figure 2.1. Rheological properties of concrete (Gaimster and Dixon 2003)

2.1.3.a. Cement and fine fillers

Similar to other constituents, cement of SCC is determined according to purposed application rather than specific requirements for SCC. As with other constituents again, the utilized cement must conform to EN 197-1 (The European Guidelines for Self-Compacting Concrete 2005)

Portland cement (PC) has been used as the main binder in the majority of researches. Other fine particle binders such as pulverized fuel ash (PFA) and GGBS introduced gradually to increase in workability and reducing PC content and heat of hydration (Gaimster and Dixon 2003).

These additions are classified as type I and II in accordance with their reactive capacity. Fresh properties such as cohesion or segregation establish their inclusion in mix (The European Guidelines for Self-Compacting Concrete 2005). However, their significant impact on hardened properties should not be ignored.

Although ultra-fine particles like condensed silica fume (CSF) can reduce workability and slump of the mix, some works used them together with SP in SCC.

Since the fines content of SCC is much higher than NVC regarding the required stability, cement content range can be higher between 450-500 kg/m^3. Offsetting this, the fine filler materials such as limestone has been accepted according to its economic feasibility (Gaimster and Dixon 2003).

There are many other works in this respect and in forthcoming chapter will be discussed sufficiently

2.1.3.b. Aggregates

Shape, particle size distribution, moisture content, grading, variation in fine content and source of aggregates are important factors in choice of aggregates. EN 12620 and EN 206-1 clarify the requirements in this regards (The European Guidelines for Self-Compacting Concrete 2005)

Having a major impact on workability and stability of SCC, sands with fineness moduli of 2.4-2.6 can be used as fine aggregates (Gaimster and Dixon 2003). Fine content is a function of both binder and fine aggregate as well as its grading. In terms of coarse aggregates, both gravels and crushed rocks can be used by maximum size of 20 mm.

2.1.3.c. Admixtures

Fineness, carbon content, alkalis and C_3A are some of different factors which can influence the performance of admixtures. Therefore, the main admixtures, super plasticizers and viscosity modifying admixtures, as well as other agents such as air entraining, accelerating or retarding admixtures should be conformed to suggested codes (The European Guidelines for Self-Compacting concrete 2005).

The development of SCC is significantly indebted to advances in admixture technology. Modern SPs based on polycarboxylic ether (PCE) retains the workability of the mix through the mechanism of electrostatic repulsion and steric hindrance.

The molecules of PCE super plasticizes carry –CO2Na groups which in water, dissociate into –CO2 and Na+. The -CO2 remains attached with a moderate negative charge used to be attached to the cement grain. The long polyether group orientate away from the cement surface but will resist becoming entangled with the polyether chains attached to an adjoining cement grain, thus keeping to the two grains apart (Dransfield 2003).

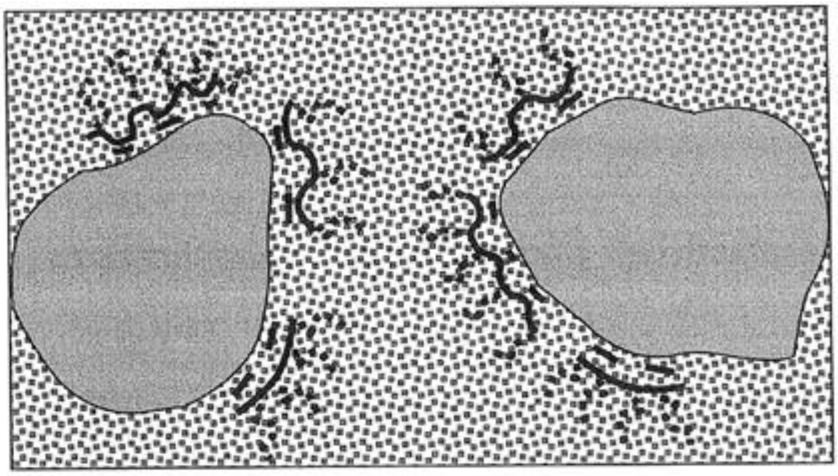

Figure 2.2. Main mechanism in PCE SP (Dransfield p. 4/15, 2003)

The other most effective admixtures for SCC are viscosity-modifying admixtures (VMAs). They can be considered to be beneficial for SCC as below:

- Less sensitive to variations in the moisture content of the aggregate
- The effects of small changes in the materials properties are minimized
- Lower powder content
- Reduces the level of production control
- Allows more fluid mixes to be used without the risk of segregation

- Improving placing rate
- Reduced risk of segregation and bleeding
- Reduced formwork pressure by thixotropic effect
- Better surface appearance (Guidelines for Viscosity Modifying Admixtures for Concrete 2006)

They are typically high molecular weight soluble polymer. Their interaction with water increases viscosity to increase viscosity to avoid segregation (Gaimster and Dixon 2003). Some other types of VMA can be listed as:

- Welan gum a very expensive natural polysaccharide,
- Glucose-based VMA,
- Cellulose ether-based VMA,
- Alginate and
- Polyethylene oxide which increase the viscosity by interacting through hydrogen bonding of H_2O.

2.1.3.d. Mix design

The all variety of mix designs for SCC recognizes two separate phases for it:

1. Continuous: water, admixture, cement and fillers of particle size < 0.1 mm.
2. Particle: coarse and fine aggregates.

The outline of the mix design can be generally summarized as below:

- evaluate the water demand and optimize the flow and stability of the paste
- determine the proportion of sand and the dose of admixture to give the required robustness
- test the sensitivity for small variations in quantities (the robustness)

- add an appropriate amount of coarse aggregate
- produce the fresh SCC in the laboratory mixer, perform the required tests
- test the properties of the SCC in the hardened state
- produce trial mixes in the plant mixer (The European Guidelines for Self-Compacting concrete 2005).

Since the first developed model in 1988 used the constituent materials of NVC, there have been many other works which leads to three fundamental governing factors:

1. Fresh properties
2. Volume of coarse aggregates
3. Use of SP

Domone *et al.* introduced two factors for showing the suitability of binder used in SCC:

1. B_p= retained water ratio: absorbed and void filling water for powder
2. E_p= deformation coefficient: water changes sensitivity

Characteristics of the mortar depend on sand content (approximately 40%) and paste characteristics. However the coarse aggregates has vital role in both fresh and hardened properties of SCC. High coarse aggregate content not only can reduce the segregation resistance of the mix, but also may cause blockage of the flow. The frequency of collisions and contact between aggregate particles can increase as the relative distance reduces leading to a higher internal stress. For this reason, the coarse aggregate should be limited to 50%. There is no unique method for design because of wide variety of used material, but here, there is a basic summary from different researchers:

a. W/b < 50
b. Lower coarse aggregate content than NVC
c. Higher paste content than NVC

d. Introducing admixtures and additions to increase workability and resistance to segregation.

e. Trial mixes by SP and VMA

Some of the most highlighted methods can be synopsized as bellow:

A rational mix design method founded on four steps:

i. Coarse aggregate content 50% of solid volume
ii. Fine aggregate content 40% of the mortar volume
iii. W/b 0.9-1.0% by volume
iv. SP dosage and final w/b determined by self-compactability

Since w/b in SCC is low enough, it impacts workability rather than compressive strength.

A rational method developed to linear optimization mix proportioning by mathematical approach considering nine steps. Some limitations are delivered in Table 2.1.

Table 2.1. Limiting mix properties for successful self-compacting concretes (Gaimster and Dixon 2003)

	Maximum aggregate size 20 mm	Maximum aggregate size 10 mm
Coarse aggregate Content (kg/m^{3+})	0.5 ×dry rodded unit weight	0.5-0.54 ×dry rodded unit weight
Max water content	200	
Water/powder ratio by wt (w/p)	0.28-0.40	0.28-0.50
Water/(powder+fine aggregate) ratio by wt	0.12-0.14	0.12-0.17
Paste volume (m^3/m^3 concrete)	0.38-0.42	

In another suggested model for self-compacting concrete the strength and durability requirements considered and these stages were followed:

1. The void content is measured to find the minimum paste volume to fill voids of aggregates according to ASTM C 29/C29M.
2. Consideration of blocking criteria which is based on the mechanism of mortar flow.
3. Adjusting the w/b, SP, VMA and sand content.
4. Determination of concrete proportions.

Another introduced model for mix design is solid suspension model mix design. Following nine steps, this method is based on that part of water which fills the voids of binder and coarse aggregates whereas the reminder controls the workability of the mix (Gaimster and Dixon 2003).

Brouwers and Radix (2005) through series of tests about mechanical properties and durability concluded that the packing theory of Andreasen and Andersen and its modification by Funk and Dinger can be the best way to produce an inexpensive SCC meeting standards and requirements. This is consistent with works conducted by many researches on various topics of SCC who selected this method for mix design in their experiments (Yu *et al.* 2014).

It should be mentioned that there are recently described methodologies which are considering SCC with different additions regarding this fact that SCC encompass a various range of particles. For instance, Dinakar and Manu (2014) suggested a new method for high strength high performance concrete (HSHPC) and SCC using metakaolin.

2.1.4. Fresh SCC

Plastic properties of SCC are the main characteristics by which SCC has been a unique type of concrete in construction industry. Hardened properties, on the other hand, are firmly depended on fresh features. In other words, it is the plastic specifications which governs significantly the hardened advantage or disadvantages. Therefore, influencing factors of fresh state SCC and related test methods are of enormous interest.

There are three main parameters for plastic state of SCC affecting all fresh properties.

1. Filling ability
2. Resistance to segregation
3. Passing ability

Using EFNARC and The European Guidelines for Self-compacting concrete (2005), as the most credible references and other works, these principles together with the requirements, test methods and other profitable information are concisely discussed here.

2.1.4.a. Filling ability

Filling ability relates to mobility and can also be known as unconfined flowability. This is the ability of SCC to change shape and flow into and fill completely all spaces within formwork under its own weight. To reach these properties, it is necessary to reduce the interparticle friction using two ways:

1. Using SP to reduce surface tension
2. Inclusion of fillers, consequently optimizing the packing of fine particles.

Regarding concrete as a Bingham fluid, a lower shear yield stress and a limited plastic viscosity value should be ensured by test methods such as: slump flow, T_{50}, V-funnel and Orimet.

2.1.4.b. Resistance to segregation

Besides the mobility, SCC should be stable under moving condition and maintains the homogeneity which can be achieved by:

1. Using SP to cause water demand reduction to avoid bleeding as well as minimizing segregation a well-graded concrete.
2. Introducing VMA together with more fine content to protect viscosity of the liquid phase and suspension states of particles.

GTM and V-funnel at $T_{5\ min}$ are the two test methods to investigate this parameters.

2.1.4.c. Passing ability

This is the ability of concrete to pass through immovable objects in the frame formwork and tight openings such as congested confinement gaps. To reach this goal a higher volume paste is required. Measurement can be carry out via U/L/Fill-Box or J-ring teats methods

Table 2.2 includes the accepted ranges of the results for tests by EFNARC whereas EN 206 requirements all are necessary.

Table 2.2. Conformity criteria for the properties of SCC (The European Guidelines for Self-Compacting concrete 2005)

Property	Criteria
Slump-flow class SF1	≥ 520mm, ≤ 700mm
Slump-flow class SF2	≥ 640mm, ≤ 800mm
Slump-flow class SF3	≥ 740mm, ≤ 900mm
Slump-flow class specified as a target value	± 80mm of target value
V-funnel class VF1	≤ 10s
V-funnel class VF2	≥ 7s, ≤ 27s
V-funnel specified as a target value	± 3s
L-box class PA1	≥ 0,75
L-box class PA2	≥ 0,75
L-box specified as a target value	Not more than 0,05 below the target value
Sieve segregation resistance class SR1	≤ 23
Sieve segregation resistance class SR2	≤ 18

2.1.4.d. Test methods of the plastic state

Since SCC is considered almost a new type of concrete mixture, there is a number of tests which are specially designed for evaluating fresh properties of this kind of concretes. This section is going to explain these methods briefly.

- Slump flow test (1) and T50cm test (2)

This is applied to assess the horizontal free flow of the SCC in absence of any obstruction. Test measures the mobility/deformity under a low rate of shear of self-weight. Thus, the greater values direct higher ability of self-filling.

The T_{500} is further evaluation by which the filling capacity assessment is more completely made. The lower the time, the better flowability (EFNARC 2002).

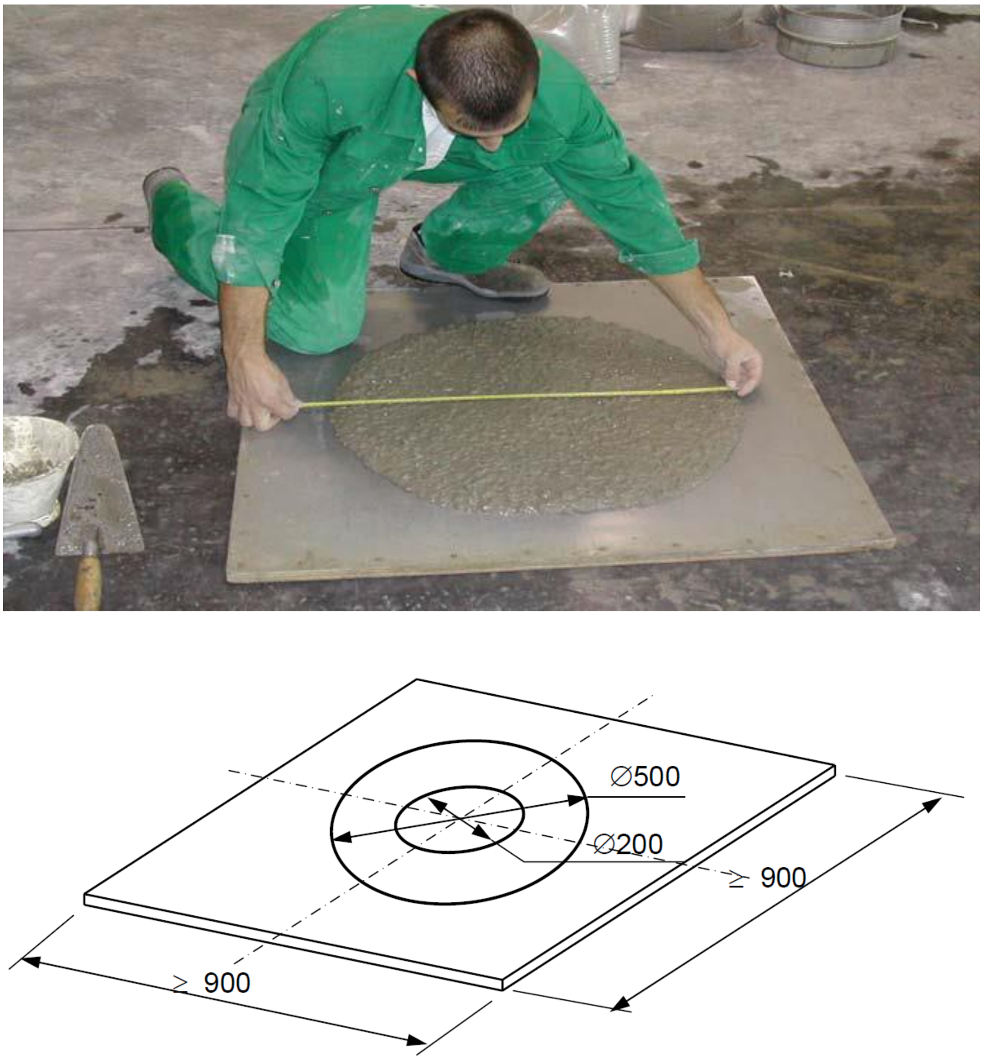

Figure 2.3. Slump-flow and T500 time for self-compacting concrete (The European Guidelines for Self-Compacting concrete 2005)

- J-Ring test (3)

This targets the passing ability of the SCC indicating the degree of restricted passage through bars. J-ring test can be performed in conjunction with slump flow test (EFNARC 2002).

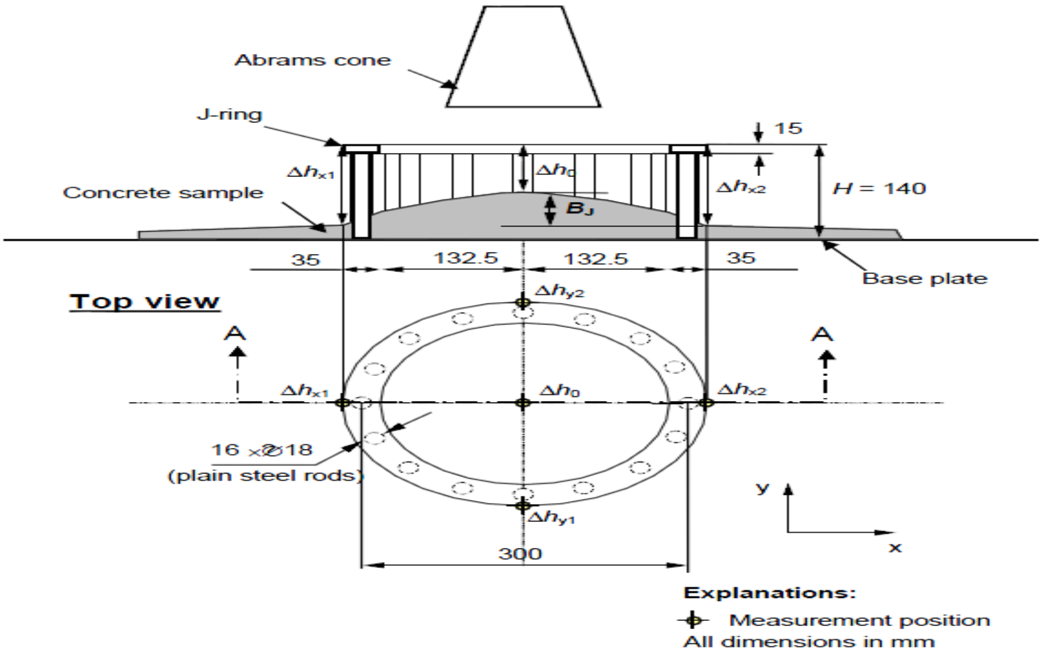

Figure 2.4. J-ring used in conjunction with the slump flow (TESTING-SCC 2005)

- V funnel test (4) and T_{5min} (5)

Although this test has been designed to measure the filling ability of SCC with a maximum size of 20 mm, the result can be affected by factors other than flow like too much coarse aggregates. Because the inverted cone shape can be cause the mix to block reflecting in the results. High flow time can also be associated with low deformability due to a high paste viscosity, and with high inter-particle friction. After 5 minutes of settling, segregation of concrete will show a less continuous flow with an increase in flow time (EFNARC 2002).

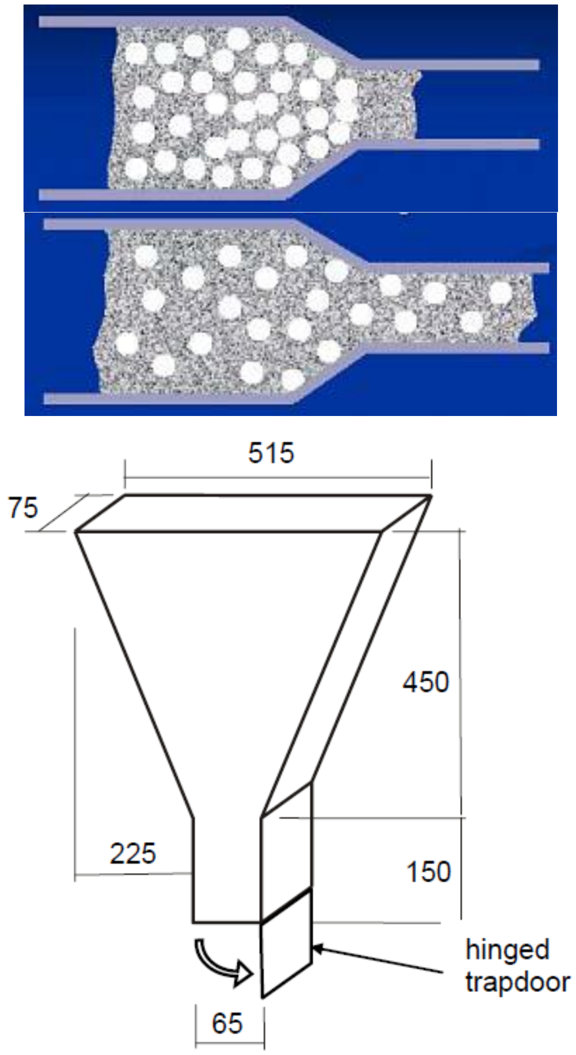

Figure 2.5. V-funnel test equipment (The European Guidelines for Self-Compacting Concrete 2005)

- L Box test method (6)

Different parameters such as mobility, flow speed and passing ability can be assessed by this method. Furthermore, segregation and leveling may visually be investigated. Otherwise, a section of concrete can be sawed from the horizontal section and be inspected. Anyhow, $H_2/H_1=1$ indicates a water like flow. The nearer the blocking ratio to unity, the better is the flow of SCC. T_{200mm} and T_{400mm} indicate the ease of flow as well (EFNARC 2002).

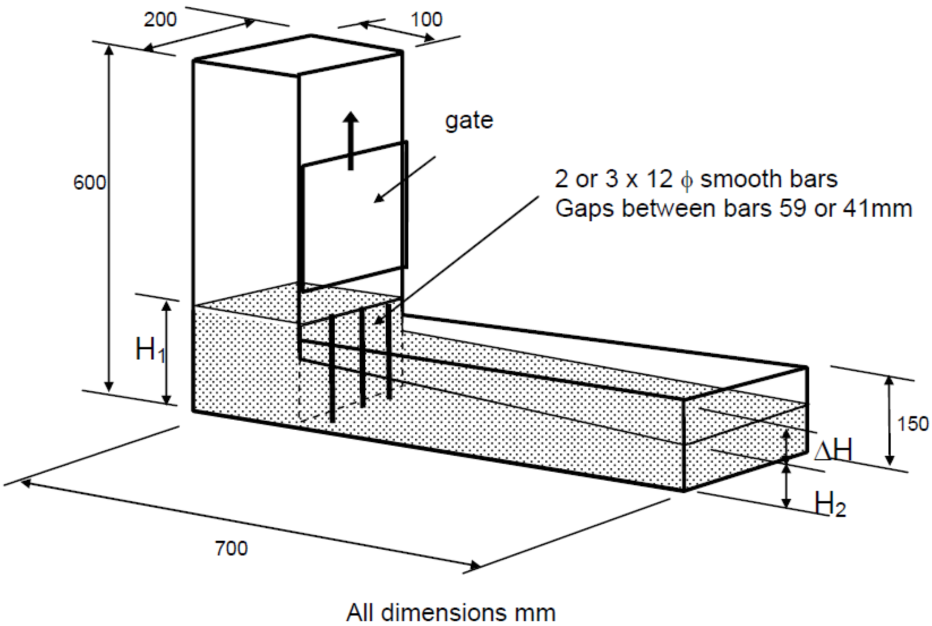

Figure 2.6. L-box test (The European Guidelines for Self-Compacting Concrete 2005)

- U Box test method (7)

In this test what literally concrete has to do is assessed and the filling ability is directly observed. Therefore, the nearer the H_2-H_1, the "filling height" is to zero, the better the flow and passing ability of the concrete (EFNARC 2002).

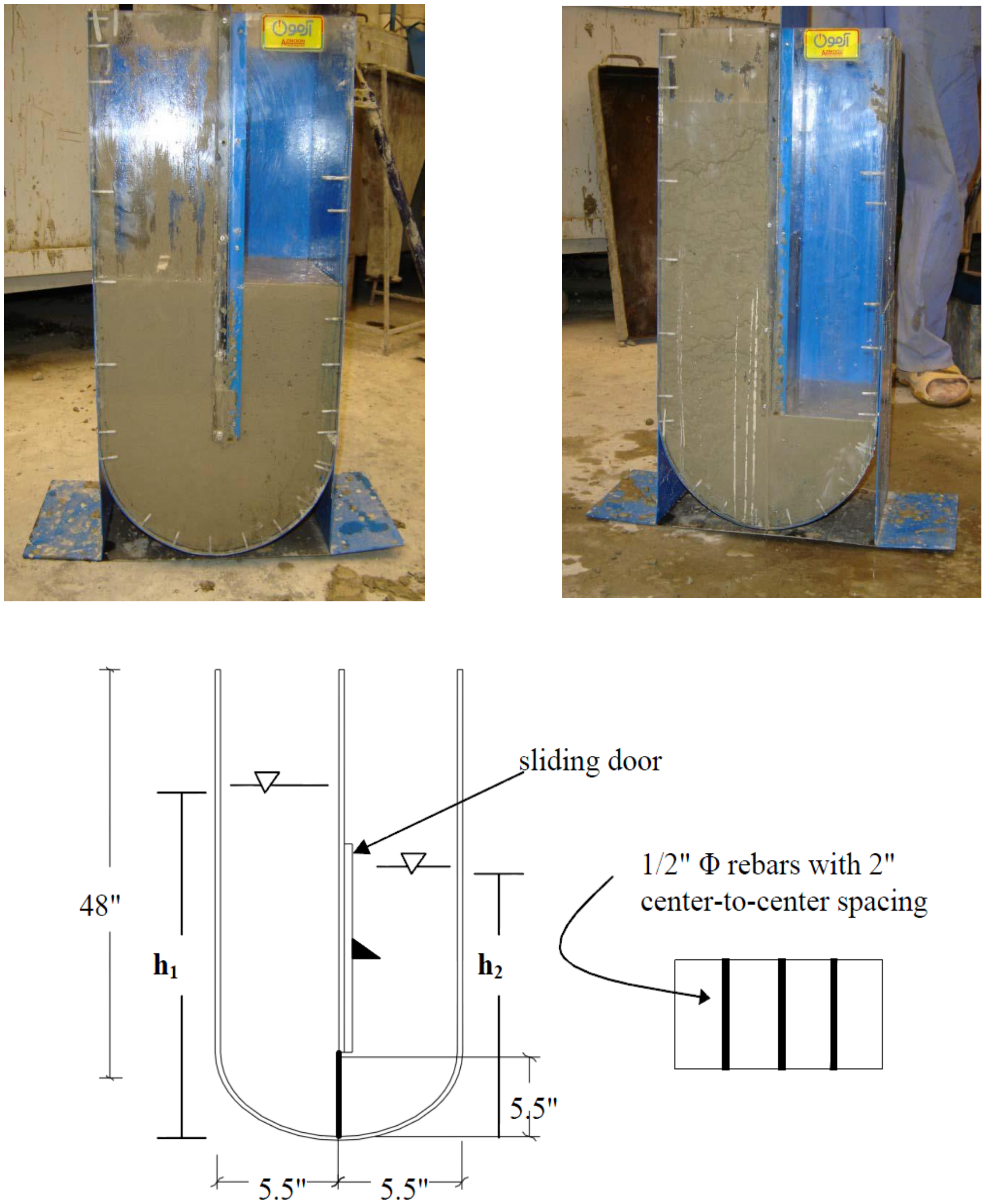

Figure 2.7. U-box apparatus

- Fill Box test method (8)

Although the test is designed to assess the filling ability of the mix with maximum aggregate size of 20 mm, the poor segregation resistance or passing ability can be detected for concrete with an even high filling ability. Thus, it gives a good impression of self-compacting characteristics of SCC. Performing the whole test within eight minutes, the average filling percentage is calculated as:

$$F= \{(h1+h2)/ 2\times h1\} \times 100\%$$

(EFNARC 2002).

Figure 2.8. Filling-box apparatus

- GTM screen stability test method (9)

The test is a very effective way of assessing the stability of SCC. Empirical observations suggest that if the percentage of mortar which has passed through the sieve, the segregation ratio, is between 5 and 15% of the weight of the sample, the segregation resistance is considered satisfactory. Below 5% is excessive and likely to affect the surface finish. Above 15%, and particularly 30%, there is strong likelihood of segregation (EFNARC 2002).

- Orimet test (10)

This test measures the ease of flow of the concrete. Shorter flow times indicates -greater flowability. For SCC a flow time of 5 seconds or less is considered appropriate. The inverted cone shape orifice restricts flow, and prolonged flow times may give some indication of the susceptibility of the mix to blocking and/or segregation (EFNARC 2002).

Figure 2.9. Orimet test apparatus

2.1.5. Hardened SCC

SCC not only possess so many unique properties in plastic state to be considered as a solution for an abundant of construction problems, but also shows many advantageous in its hardened state, particularly when some special powders, nanoparticles and fibers are included. Since the matter of interest of this work is also hardened properties of SCC associated with such materials, here, the mechanical properties of hardened SCC will discussed very briefly and general information about the mechanical properties and durability of SCC and related test methods will be provided. The main focus of the paper will be presented at next chapters.

2.1.5.a. Mechanical properties of hardened SCC

Owing to its lesser w/b ratio, SCC should present a better compressive strength than NVC. Moreover, vibration of NVC makes the water of the mix to have a tendency to migrate to surface causing more porous microstructure and weaker interfacial transition zone (ITZ) development. However, SCC has a more homogeneous matrix with minimal ITZ developed between coarse aggregates and mortar paste.

Cores taken from an in situ work cleared that compressive strength of SCC is closer to the standard cubes. Additionally, less reduction of compressive strength in higher sections of columns was observed which are proof for the better homogeneity of SCC (Gaimster and Dixon 2003).

Tensile strength of SCC can be safely assumed to be similar to NVC for a given compressive strength because the higher volume of the paste in SCC has no significant effect on tensile strength.

In terms of module of elasticity (E), according to this fact that the bulk volume of the mix is aggregate, the amount and type of aggregates, consequently the module of elasticity of them have the most influence in this regards. Hence, the increased paste content of SCC is expected to result in a reduction in elasticity module.

Creep is influenced by porosity which is related to w/c ratio. Taking place in paste and restricted by aggregate, creep is influenced by content and elasticity module of aggregates. As a result of higher paste volume and lower E, the creep of SCC can believed to be reduced.

SCC possesses a lower w/c besides a higher compressive strength. As the drying shrinkage happens by loss of water from paste and aggregate to the atmosphere despite the autogenous shrinkage which occurs by consumption of internal water during hydration, the previous one is less affected than the latter one.

SCC fluidity and cohesion minimize the bleeding and segregation of mix during placement which is the main cause to failure of concrete to encompass completely the bars. Therefore, bond of SCC to reinforcement is more robust particularly for top bars in deep sections (The European Guidelines for Self-Compacting concrete 2005).

2.1.5.b. Durability of hardened SCC

Durability is related primarily to its permeability and diffusion to liquids and gases and its penetrability. Surface layer should limit the ingress of deleterious substances such as carbon dioxide, chloride, sulfate, water, oxygen, alkali and acids in aggressive environments. The main reason for development of SCC was to compensate the lack of compaction of the surface layer and congested reinforcement due to vibration difficulties. During internal or external vibration procedure, the influenced area does not receive the same compaction energy resulting in heterogeneous structure with different permeability area. Therefore, negative effects like honeycombing, segregation and bleeding occur. Due to being free from these shortcomings, SCC possesses a reliable low and uniform permeability and subsequent better durability (The European Guidelines for Self-Compacting concrete 2005)

2.1.5.c. Test methods of hardened SCC

The test methods of SCC in hardened state are the same as normally vibrated concretes test procedures. Therefore, the only most important considerations of these test methods has been pointed out in this section.

- Uniaxial compressing testing

There are variety of standards to study the compressive strength of concretes. However, the point is to avoid deviation from the standard procedures of curing, testing and handling apparatus. The main faults can be appear by sampling error, failure to remix sample, distorted mold, lack of mold oil, incomplete compaction (not relevant to SCC), incorrect curing temperature, discontinuous moist cure, faulty sample location or faulty testing machine. Figure 2.10 illustrates abnormalities of sample failures.

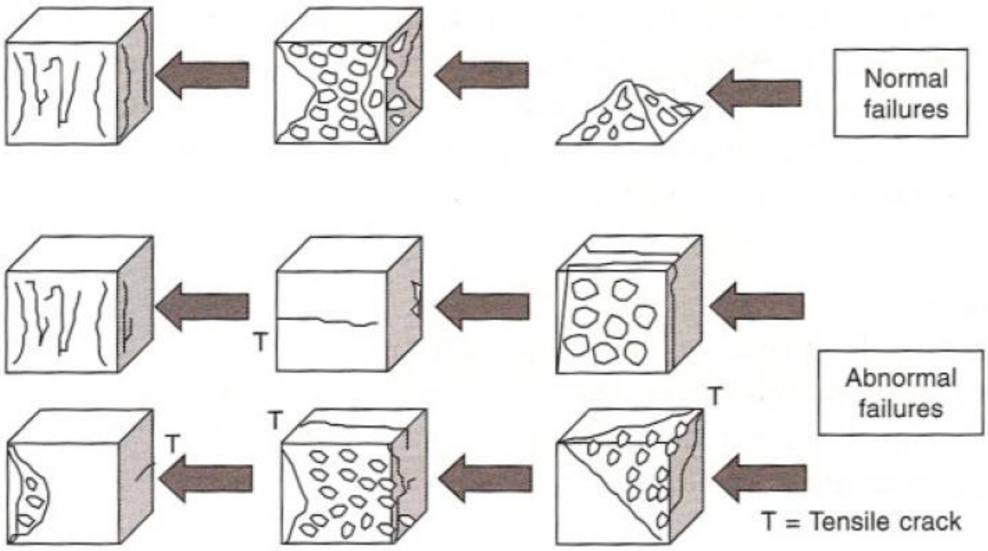

Figure 2.10. Normal and abnormal sample failures (Newman 2003)

The meaningful difference between actual and assumed force system due to fixing problems is illustrated in Figure 2.11.

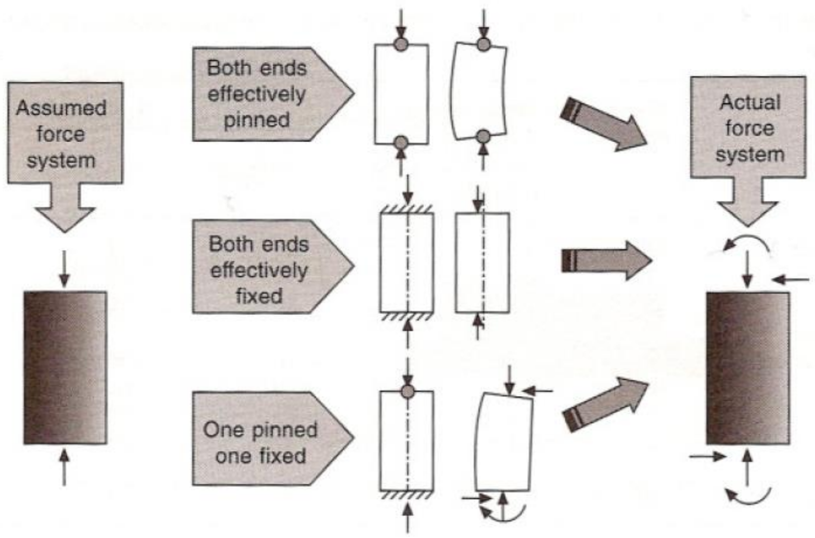

Figure 2.11. Problems with force transfer to specimens (Newman 2003)

Errors in locating centrally can lead the samples to one-sided bending mode of failure which could be able to reduce the compressive strength dramatically.

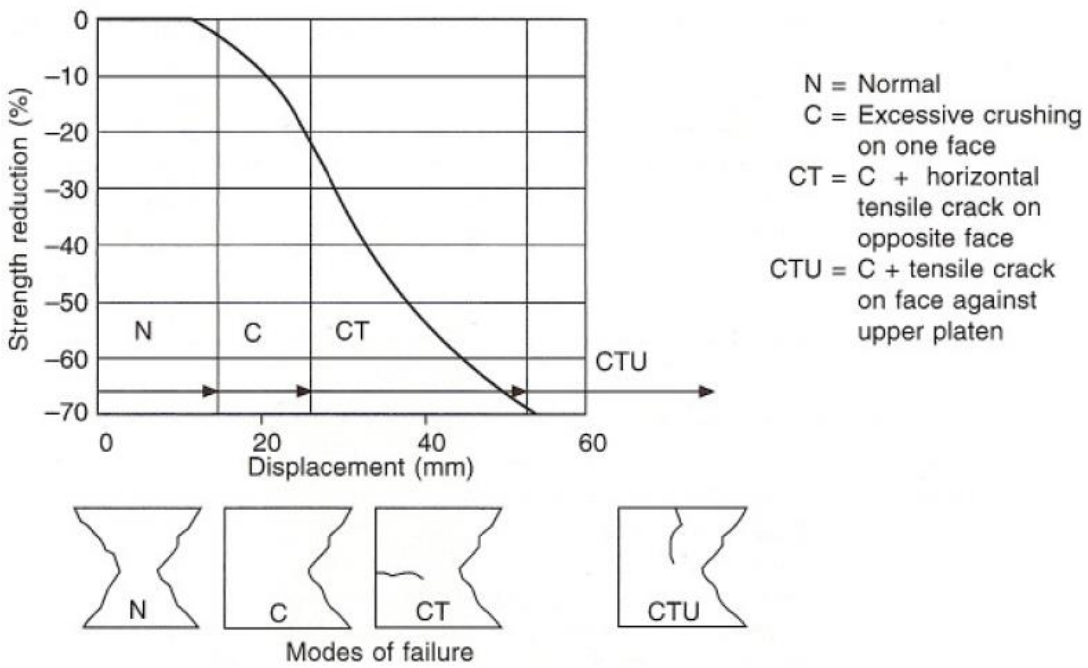

Figure 2.12. Strength reduction due to eccentric location (Newman 2003)

- Tensile strength testing

There are two types of tensile strength testing methods named Direct Tension Testing and Indirect Tension Testing. Figure 2.13 shows the related equipment of the first. For various search purposes, this machine is used to apply force through lazy tong grips using bonded end plates in a relatively complex procedure.

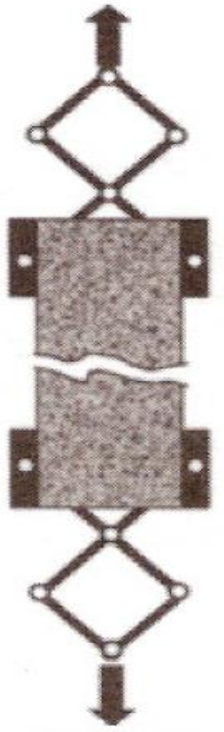

Figure 2.13. Direct tensile testing device (Newman 2003)

In indirect tensile testing which is also referred to as splitting test or Brazilian test, the cylinder is located horizontally between two plates of a standard compressing machine. Figure below is the schematic demonstration of the procedure.

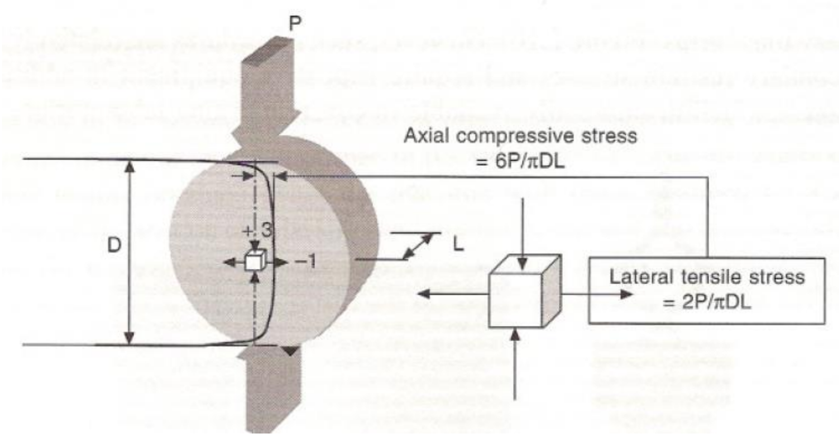

Figure 2.14. Indirect tensile testing (Newman 2003)

- Flexural strength testing

In this method, two steel roller bearings support the prismatic concrete beam at the ends. A compressing machine is used to load system through to other steel roller bearings at the third points on the top of the sample. Therefore, a constant bending moment zone is produced between to upper roller bearings to induce a symmetrical stress distribution of stress along vertical profile of prism. Naturally, the stress is compressive above the neutral axis and tensile below it. The flexural strength can be measured as:

$$FL/b\mathrm{d}^2$$

Where:

F= Total induced load
L= Distance between two lower supports of the beam
b= Width or breadth of the section
d= Height or depth of the section

In the case of just center-point loading the flexural strength is calculated by:

$$3FL/2b\mathrm{d}^2$$

- Flexural toughness testing

According to ASTM C 1018, the prismatic sample is tested by a similar equipment stated in previous flexural strength test. Drawing load versus displacement diagrams for sample, the area under the curve could be calculated. These areas at each point of the curve are the integration of load multiplied by displacement which gives the energy absorbed up to that certain point to cause the relative deflection. First of all, A_1, the area showing the absorbed energy of first crack deflection or δ_0 is calculated. As a consequence, the areas of energy related to $3\delta_0$, $5.5\ \delta_0$, $10.5\ \delta_0$ and $15.5\ \delta_0$ is calculated and divided by A_1Type equation here. to achieve I_5, I_{10}, I_{20} and I_{30}, respectively. These indices are flexural toughness indices which are used to an accurate analogy of energy absorption capacity, elasto-plasticity or ductility of the specimens. The more the value of I_N is close to N, the better elasto-plastic material the specimen is. Figure 2.15 and 2.16 demonstrates the details.

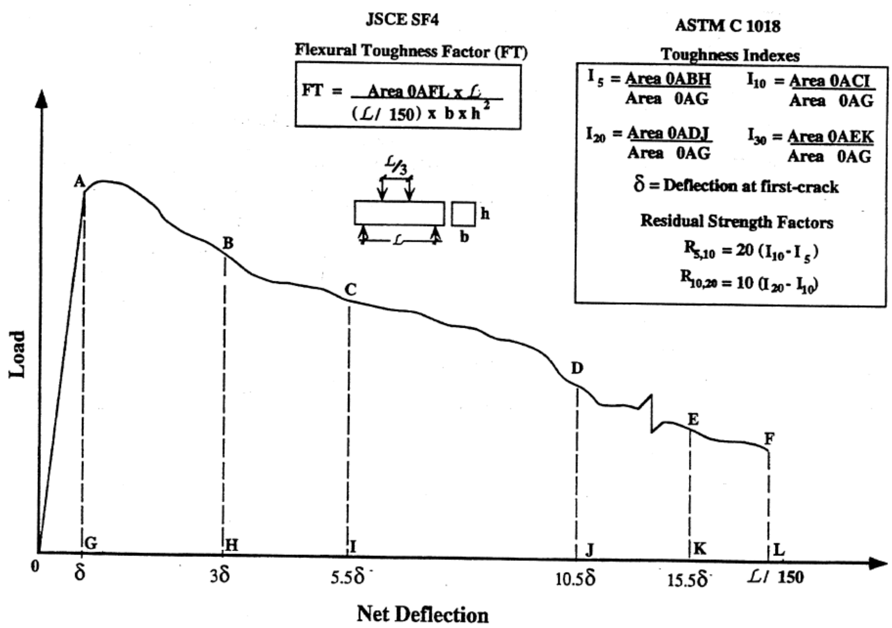

Figure 2.15. ASTM C 1018 and JSCE SF-4 techniques toughness characterization (Banthia 1995)

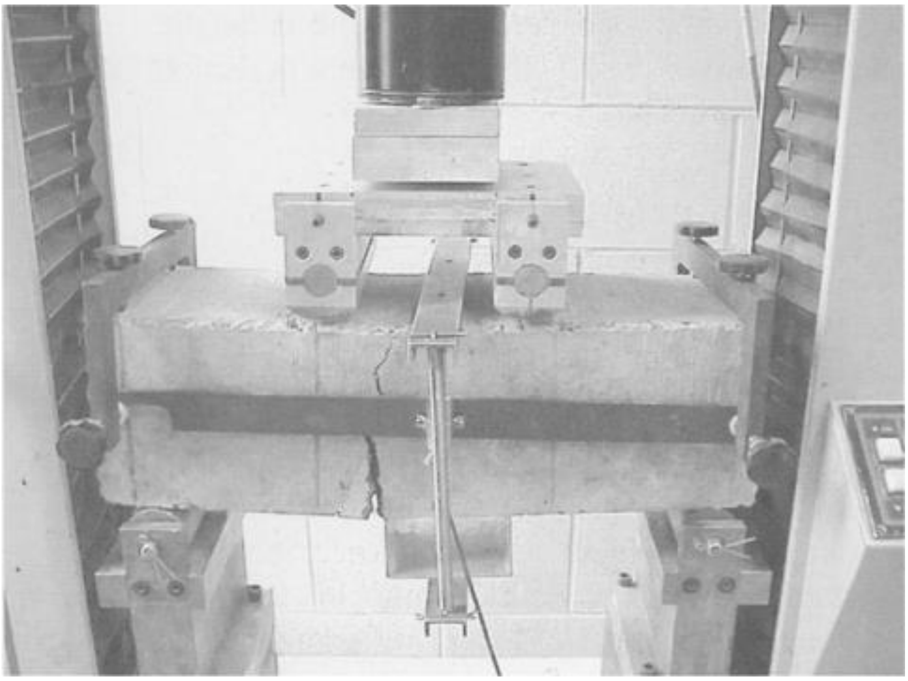

Figure 2.16. Set-up for flexural toghness (Banthia 2004)

- TGA or Thermogravimetric Analysis

Thermogravimetric analysis (TGA) is an analytical technique used to determine the thermal stability of a material and its fraction of volatile components by monitoring the weight change that occurs as the specimen is heated. The measurement is normally carried out in air or in an inert atmosphere, such as Helium and Argon, and the weight is recorded as a function of increasing temperature. In addition to weight changes, some instruments also record the temperature difference between the specimen and one or more reference pans (differential thermal analysis, or DTA) or the heat flow into the specimen pan compared to that of the reference pan (differential scanning calorimetry, or DSC).

There are two types of TGA instruments: vertical and horizontal balance.

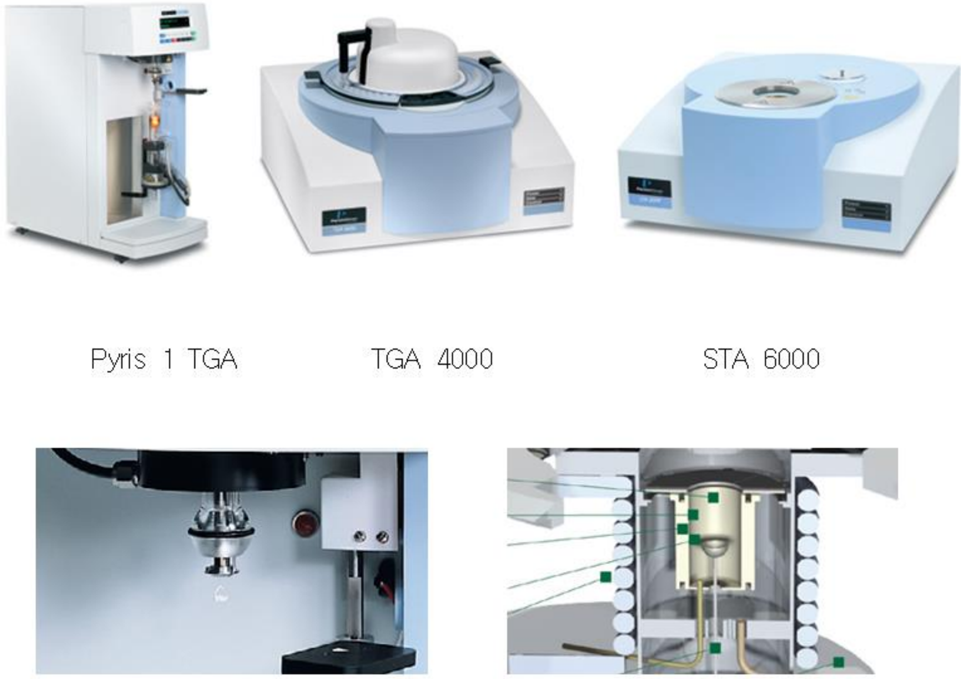

Figure 2.17. TGA apparatus (PerkinElmer Inc 2010)

In most cases, TGA test is performed in an oxidative atmosphere with a linear temperature ramp. The maximum temperature is selected so that the specimen weight is stable at the end of the experiment, implying that all the chemical reactions are ended. This approach provides two important numerical pieces of information: ash content (residual mass, Mres) and oxidation temperature (T0).

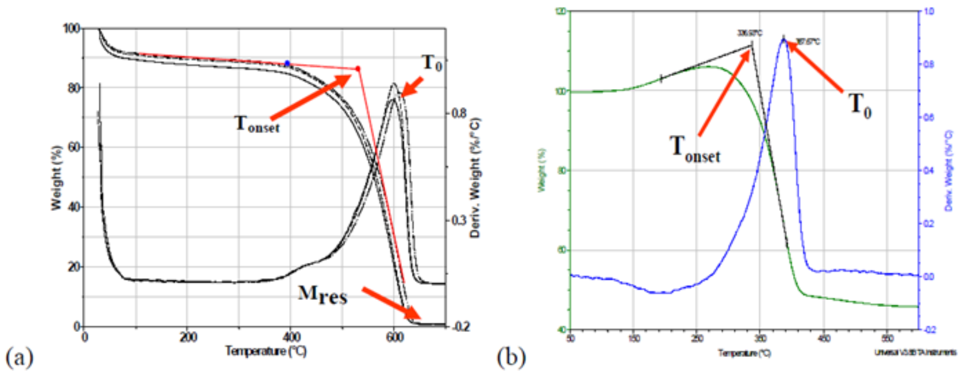

Figure 2.18. Ash content and oxidation temperature (Anderson materials evaluation Inc 2014)

In tests related to the concrete, this method is used to record the weight loss of the samples as they are heated up to 950°C with a constant rate such as 10°C/min. Free lime and calcium carbonate decompose at 450-500°C and 700-900 °C, respectively. The loss of $Ca(OH)_2$ shows its amount at a particular age which is itself indicating the degree of hydration of the mix (Anderson materials evaluation Inc 2014).

-MIP or Mercury Intrusion Porosimetry

Mercury porosimetry is an extremely useful characterization technique for porous materials by which pores between about 500 µm and 3.5 nm can be investigated, whereas a complete analysis may take as little as half an hour analysis time. Mercury porosimetry can provide a wide range of information, e.g. the pore size distribution, the total pore volume or porosity, the skeletal and apparent porosity, and the specific surface area of a sample. A key assumption in MIP is the pore shape:

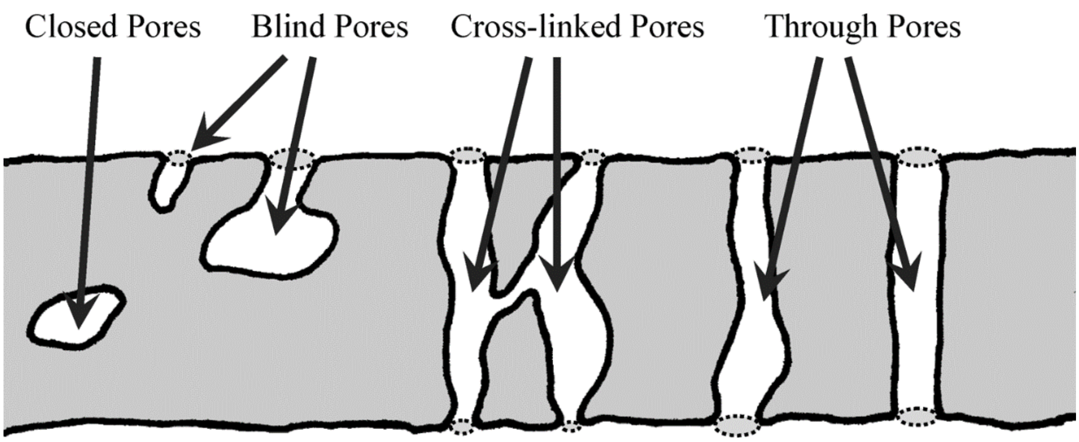

Figure 2.19. Pore types illustration (Giesche 2006)

Since mercury does not wet the most substances and will not spontaneously penetrate pores by capillary action, it must be forced to the pores by application of a stringently controlled external pressure which is inversely proportional to the size of the pores. From the pressure versus intrusion data, the instrument generates volume and size distributions using the Washburn equation. It is the non-wetting property of mercury combined with its high surface tension that almost uniquely qualifies it for using in probing pore space. At each surface interface with a liquid, there is tension which acts tangentially to the interface. This is termed “surface tension” and acts like an elastic membrane contacting the surface until the surface forces are in equilibrium with the forces tending to increase the surface area of the interface (Giesche 2006).

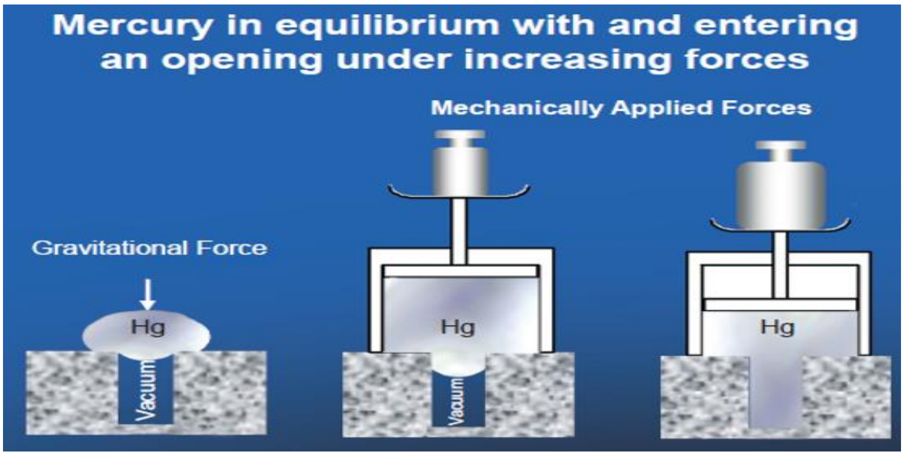

Figure 2.20. Mercury does not spontaneously penetrate (Micromeritics Inc 2014)

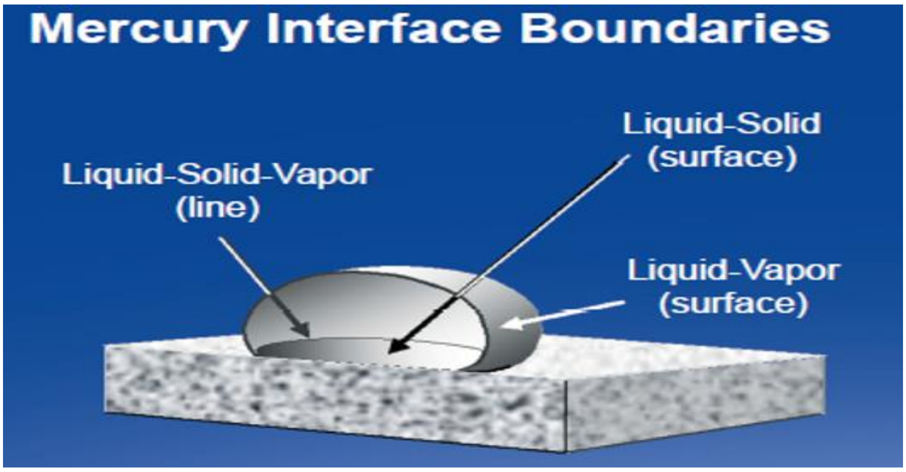

Figure 2.21. Mercury interface boundary (Micromeritics Inc 2014)

Surface tension, then, can be defined as the force per unit length acting along the surface of liquid at right angle to a line that separate the two phases. If mercury is placed in contact with a pore opening, the surface tension of mercury acts along the line of contact with the opening equal in length to the perimeter of the opening and creating a force-resisting entry. Therefore, at any pressure, the pores into which mercury intrude have diameter greater than:

$$D = -4\gamma \cos \emptyset / P$$

By measuring the volume of the mercury that intrudes into the sample material with each pressure change, the volume of pore in the corresponding size is known. The volume of mercury that enters pores is measured by a mercury penetrometer (an electrical capacitance dilatometer). These devices are very sensitive and can detect a change in mercury volume of under 0.1 μL (Micromeritics Inc 2014).

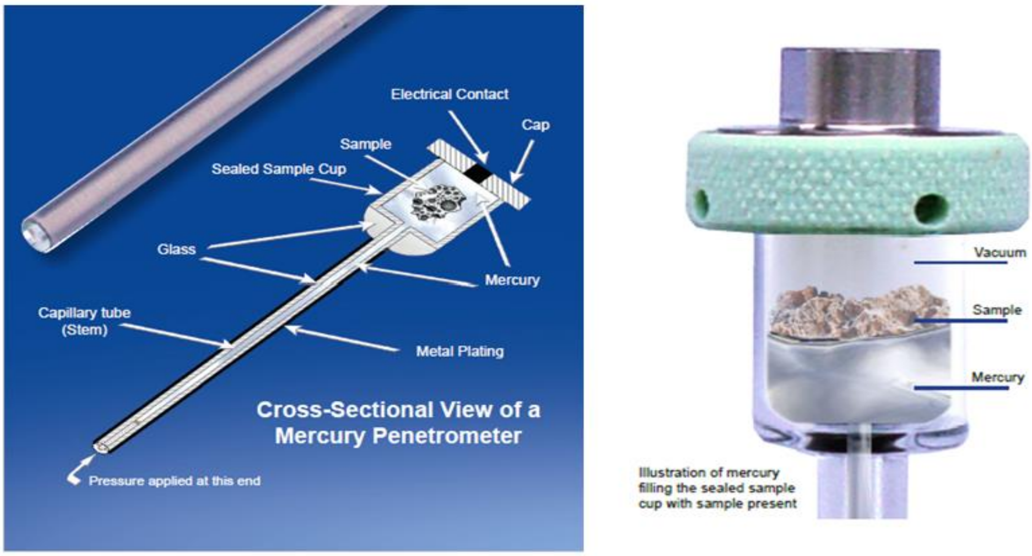

Figure 2.22. Penetrometer (Micromeritics Inc 2014)

- SEM Scanning Electron Microscopy

The microscope column, specimen chamber and vacuum system are on the left; the computer, monitor and many of the instrument controls are on the right.

Figure 2.23. SEM (Hafner 2007)

The black box (microscope column and specimen chamber) can be simplified as:

- Electron gun: a source of the electron beam which is accelerated down the column.
- Condenser and objective lenses: a series of lenses which act to control the diameter of the beam as well as to focus the beam on the specimen.
- Apertures: a series of holes in micron scale in metal film which the beam passes through and which affect properties of that beam.
- Specimen position: controls for x, y, z-height and orientation (tilt, rotation)
- Beam/specimen interaction: an area that generates several types of signals which can be detected and processed to produce an image or spectra.
- All the above mentioned at high vacuum levels.

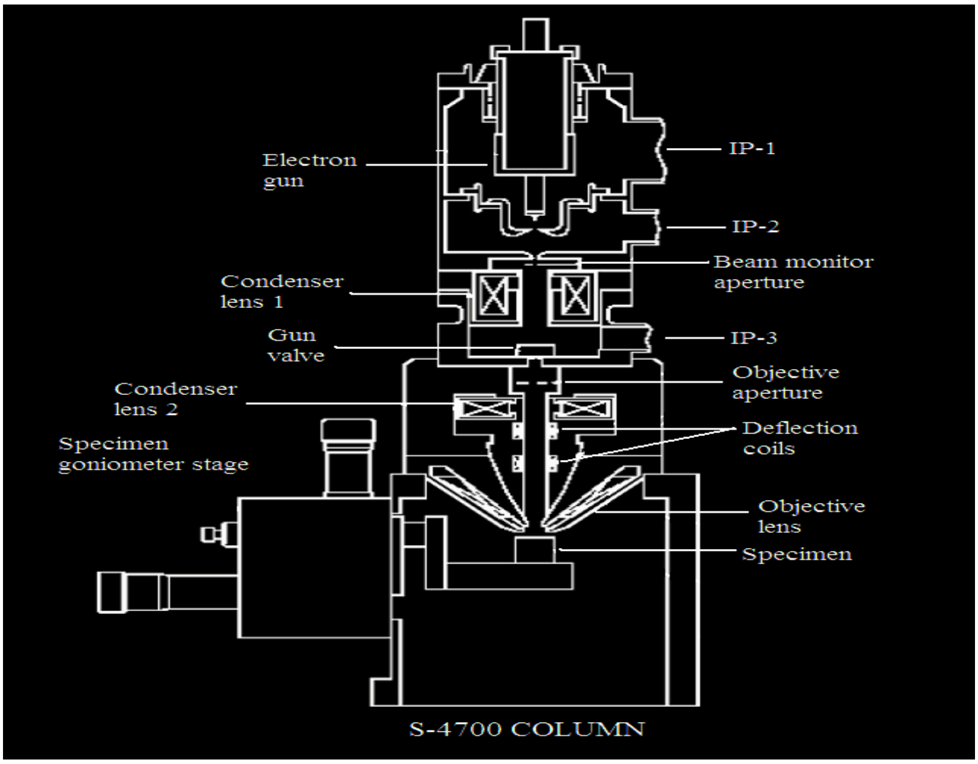

Figure 2.24. SEM section (Hafner 2007)

By taking a closer look, we can see the objective lens which focuses the beam on the specimen. Also a pair of deflector coils responsible of rastering. The monitor image is a two dimensional rastered pattern of grayscale values. Magnification is the area scanned on the monitor over area scanned on the specimen (Hafner 2007).

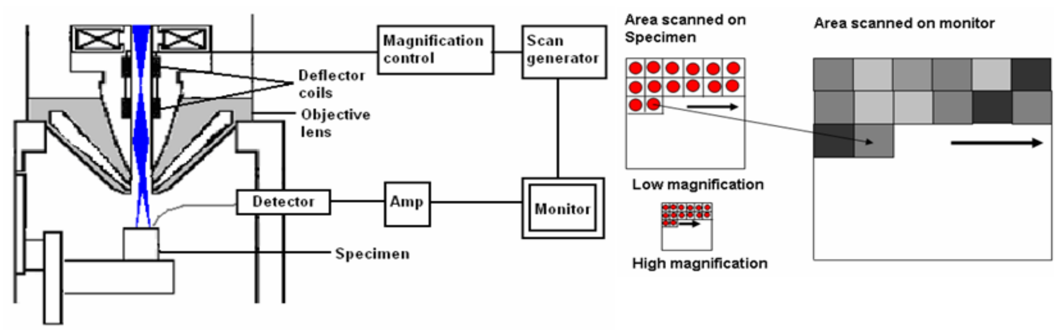

Figure 2.25. Magnification system (Hafner 2007)

- **Water Penetration Depth**

The method, EN 12390-8, concerns the determination of the depth of penetration of water under pressure. The test is performed by clamping a concrete prism 200×200×120 mm or 150 mm cube between two flanges with special circular gaskets. The water, under controlled pressure is then applied to the surface of concrete specimen. The penetration of water is measured after the testing period by breaking the specimen or taking the readings through the graduated glass burettes. Figure 2.19 is schematic illustration of penetration test apparatus.

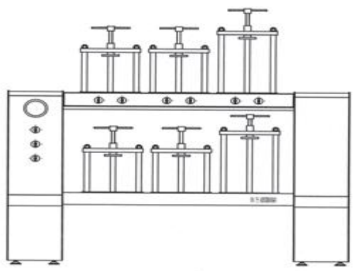

Figure 2.26. Penetration apparatus (Controls-Group 2014)

- **Water Sorptivity**

This test method, ASTM C 1585-04, is used to determine the rate of absorption (sorptivity) of water by hydraulic cement concrete by measuring the increase in the mass of specimen resulting from absorption of water as a function of time when only one surface of specimen is exposed to water. The exposed surface of the specimen is immersed in water. Water ingress of unsaturated concrete dominated by capillary suction during initial contact with water. The performance of the concrete subjected to many aggressive environment is a function, to the large extent, of the penetrability of pore system. This method is used for both interior and exterior samples which usually demonstrate different rates (ASTM C1585-04 2007).

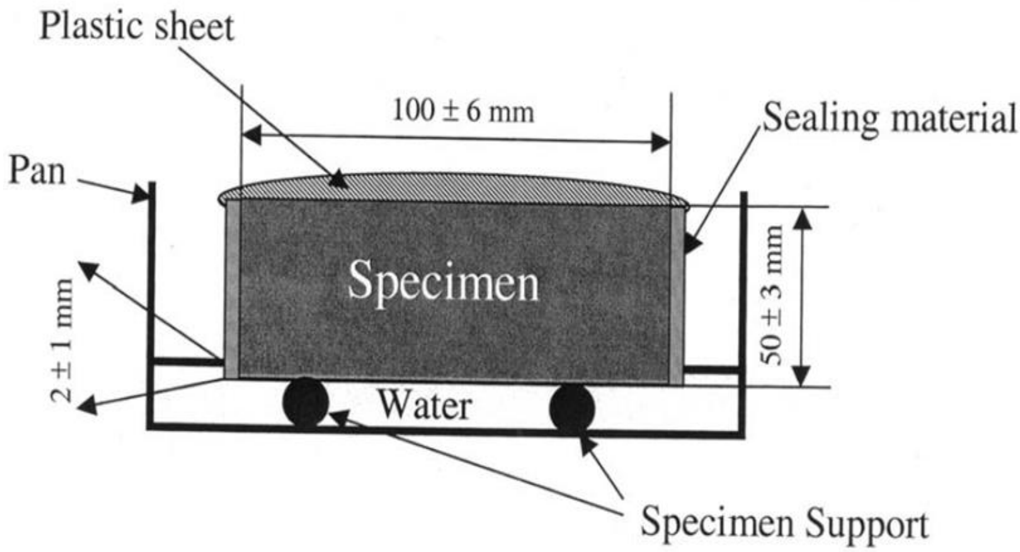

Figure 2.27. Schematic procedure of water sorptivity (ASTM C1585-04 2007)

- **Chloride Migration Coefficient**

Diffusion is the movement of molecules or ions under a concentration gradient or, more strictly, chemical potential, from a high concentration zone to a low concentration zone.

This procedure, NT BUILD 492, is for determination of chloride migration coefficient in concrete by measuring the concrete resistance to chloride penetration. The method requires cylindrical specimens with a diameter of 100 mm and a thickness of 50 mm. This non-steady-state migration coefficient cannot be directly compared with chloride diffusion coefficient obtained from other tests. Migration is the movement of ions under the action of an external electrical field. An external electrical potential is applied axially across the specimen and forces the chloride ions outside to migrate into the specimen. After a certain test duration, the specimen is axially split and a silver nitrate solution is sprayed on to one of the freshly split sections. The chloride penetration depth can then be measured from the visible white silver chloride precipitation (NT BUILD 492 1999).

- **Freeze-thaw Resistance**

This test method, ASTM C666, covers the determination of the resistance of concrete specimens to rapidly repeated cycles of freezing and thawing in laboratory by two different procedures:

a) Rapid freezing and thawing in water
b) Rapid freezing in air and thawing in water

Neither procedure is intended to provide a quantitative measure of the length of service that may expected from a specific type of concrete. Molded beam specimens shall be cured for 14 days prior to testing unless otherwise specified. Beam specimens sawed from hardened concrete shall be moisture-conditioned by immersing in saturated lime water at 32°C±2°C for 48 hours prior to testing. Immediately after curing or conditioning period, bring the specimens to a temperature within -1°C and +2°C of the target thaw temperature that will be used in the freeze thaw cycle and test for fundamental transverse frequency. Determine the mass and average length and cross section dimensions of the concrete specimen within the tolerance required. Start test by placing the specimens in the thawing water at the beginning of the thawing phase of the cycle. Remove the specimen from the apparatus, in a thawed condition at intervals not exceeding 36 cycle exposure to freezing-and thawing cycles, test for the fundamental transverse frequency and measure length change. Determine the mass of each specimen and return them to the apparatus. Continue each specimen in the test until it has been subjected to 300 cycles or until its relative dynamic modulus of elasticity reaches 60% of the initial modulus, whichever occurs first, unless other limits are specified (ASTM C 666/C 666M–03 2008).

2.2. Supplementary Cementitious Materials (SCMs)

An analysis of eleven years of case studies on SCC showed that approximately in all of them one or more additions had been used blended with PC. The most often used powder was limestone powder. However, there were ternary, even quaternary mixtures. In above 50% of the cases powder contained more than 30% addition. Reduction in hydration temperature as well as PC content were the dominant reasons for use of SCM in most of the cases (Domone 2005).

Table 2.3. Components of powder (Domone 2005)

Powder components	Number of cases
PC	2
PC + LSP	19
sr PC +LSP	1
PLSC +LSP	3
PC + GGBS	8
PBFC	2
PC + CSF	5
PBFC + PFA	9
PBFC + LSP	1
PC + PFA	4
PC + PFA + CSF	3
PC + PFA +GGBS	1
PLSC + PFA	3
PLSC + LSP + PFA	1
PC + GGBS + CSF	1
PFAC + LSP + CSF	1
PBSC + PFA +LSP	2
No information	2

Introduction of principal SCMs such as fly ash (FA), ground granulated blast furnace slag, silica fume (SF) and metakaolin (M) as well as fillers like limestone powder in either partial cement replacement or mineral additives to concrete, has great effects on both fresh and hardened properties of concrete (Sfikas *et al.* 2014). It could be achieved due to physical action like improved grain-size distribution and particle packing or chemical action such as increased particle packing gained from high pozzolanic reactivity.

But far from the technical or economic advantages of using such materials, there is another shocking fact which makes the interest of application of SCMs paramount. The production of one tone of PC, the main ingredient of our miraculous inexpensive durable construction material, is responsible for release of one tone of carbon dioxide to the atmosphere of the earth, where is the only inhabitable home planet for life (Sfikas *et al.* 2014). Hence, incorporation of different SCMs not only improves various properties of SCC, but also supports the concept of sustainable construction.

In this stage, it is better to present the general definition and characteristics of SCMs themselves, summarized from various resources, before considering their effects on SCC.

2.2.1. General Information

Defined as a natural or artificial material containing silica in a reactive form, a pozzolana can chemically react with alkalis to produce cementitious products, provided that it is finely divided to high surface area together with the presence of moisture. Moreover, the silica should be amorphous or glassy (Lewis *et al.* 2003).

EN206-1 has classified such additions in two groups:

- Type I: inert additions like limestone
- Type II: pozzolanic or latent hydraulic additions

Although there are some footprints of contribution of limestone powder in hydration process, it is generally considered as an inert filler in concrete particularly for SCC to increase the cohesiveness in fresh state. On the other hand, for type II additions, the k-value concept is applied to show cementing efficiency factor of SCMs for mix design. However, this can be applied for other parameters like compressive strength, durability, etc.

2.2.1.a. Fly ash

Fly ash can be used to either reduce the sensitivity of SCC mix to the changes in water content or increase cohesion of mix provided that its amount remains below the point after which the high cohesive SCC mix is resistant to flow (The European Guidelines for Self-Compacting Concrete 2005).

As coals burns between 1250-1600°C in a power station all incombustible materials merge to form spherical glassy droplets of silica, alumina and iron oxide. The silica of FA reacts with calcium hydroxide, the by-product of OPC hydration, to fill interstitial pores resulting in less permeability and high durability due to produced finer pore structure. Meanwhile, it is helpful for dispersion of PC particles.

$$3\ Ca(OH)_2 + SiO_2 = 3CaO.SiO_2 + 3H_2O$$

The lime etches the surface of glassy SiO_2 and decrease the Ca/Si ratio. Although FA retards the reaction of alite at early ages, due to the provision of nucleation sites on the surface of FA, it accelerates the production of alite at middle ages. Other parameters are involved as well. If there is adequate amount of water, the later the age, the more contribution to strength gain. The higher the temperature, the greater the reaction rate or the finer the FA, the greater surface for reaction.

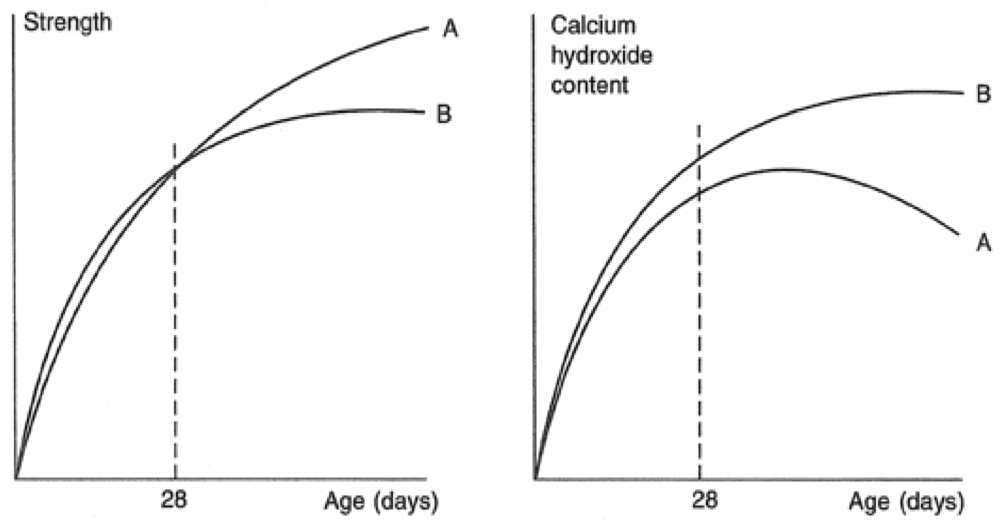

Figure 2.28. Influence of calcium hydroxide on strength development [A with FA] (Lewis *et al.* 2003).

Generally spherical less than 50µm particles of FA confer fluidity by optimizing packing which results in lesser water demand and more cohesiveness. These can reduce the bleeding and shrinkage of the mix. Furthermore, the lower particle density of FA (2300 kg/m^3) in comparison with PC (3120 kg/m^3), in terms of mass substitution, leads to more fine cementitious material and subsequently less water demand. So, there is a higher strength and better quality of surface finishes (Lewis *et al.* 2003).

2.2.1.b. Ground granulated blast furnace slag

After reduction and separation of the iron from the ore, the remained siliceous and aluminous residue fuses with a limestone flux and ash from coke to produce the slag as a by-product. The two methods for qualifying this to suitable GGBS are granulation and pelletization in both of which it is necessary to cool the slag rapidly. Otherwise, it would crystallized to a well-ordered, stable, non-reactive but not glassy structure (Lewis *et al.* 2003).

The major oxides of GGBS are presented in table below compared to PC.

Table 2.4. Typical oxide composition of UK PC and GGBS (Lewis *et al.* 2003)

Oxide	Composition (%)	
	PC	GGBS
CaO	64	40
SiO_2	21	36
Al_2O_3	6	10
Fe_2O_3	3	0.5
SO_3	2	0.2
K_2O	0.8	0.7
Na_2O	0.5	0.4

The latent hydraulicity of GGBS which is locked in its glassy structure, needs to be disturbed via activation. The sulfates and alkalis in PC can increase the PH of system in this regard. In primary reactions OPC reacts with water whereas GGBS with water and the hydration products of GGBS. In secondary reactions the OPC hydration products combine with GGBS as well as the GGBS primary reaction products. The rate of reactions depends on the PC content, temperature, chemical composition and fineness. The table below summarizes the various hydraulic indices in which the CaO and MgO show improvement but SiO_2 shows reduction.

Table 2.5. Limits for GGBS (Lewis *et al.* 2003)

Property	Limit
Chemical modulus/Reactivity index $\frac{CaO+MgO}{\mathrm{SiO2}}$	≥ 1.0
Lime-silica ratio $\frac{CaO}{SiO2}$	≤ 1.4
Glass count XRD	$\geq 67\%$
Fineness	> 275 m^2/kg
Moisture content	$\leq 1.0\%$

Table 2.6. Other properties of typical UK PC and GGBS (Lewis *et al.* 2003)

Property	PC	GGBS
Shape	Angular	Angular
RD	3.15	2.90
Color	Grey	W

Due to its smoother surface texture and delay in chemical reaction, GGBS causes a lesser water demand for mixes with equal slump. Moreover, slow reactivity of GGBS results in less heat of hydration and longer setting time as a benefit in large pours with less thermal cracking.

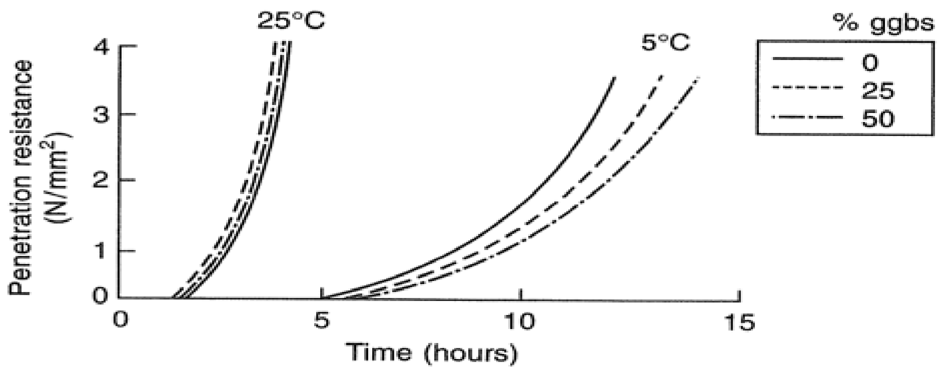

Figure 2.29. Influence of slag content and temperature on setting (Lewis *et al.* 2003)

2.2.1.c. Silica fume

First obtained in Norway, 1947, during environmental concerns, silica fume (SF) is a by-product of silicon, ferrosilicon and other metal alloy smelting furnace which is extracted from the exhausted gases. This filtered fume is very fine powder mainly composed of high percentage of silicon dioxide SF is produced using high-temperature reduction of quartz in an electric arc. This normally grey ultrafine powder contains at least 85% SiO_2 with the mean particle size of 0.1-0.2 micron. The spherical shape particles possess minimum specific surface of 15 000 m^2/kg.

Table 2.7. Comparison of cementitious materials available in the UK (Lewis *et al.* 2003)

	PC	PFA	GGBS	Microsilica
Physical data for cementitious materials				
Surface area (m^2/kg)	350-500	300-600	300-500	15 000-20 000
Bulk density (kg/m^3)	1300-1400	1000	1000-1200	200-300
Specific gravity	3.12	2.30	2.90	2.2
Chemical data for cementitious materials				
SiO_2	20	50	38	92
Fe_2O3	3.5	10.4	0.3	1.2
Al_2O_3	5.0	28	11	0.7
CaO	65	3	40	0.2
MgO	0.1	2	7.5	0.2
$Na_2O + K_2O$	0.8	3.2	1.2	2.0

There are different forms of SF to accommodate transportation, storage and dispensing difficulties because the powder is a hundred times finer than OPC. Namely:

- Undesified form for grouts, mortars and repairs,
- Densified form for precast and readymix,
- Micropelletized form for composite cements and
- Slurry form for semi-dry precast and SCC.

According to the fact that the inclusion of a typical dosage between 8 and 10% by cement weight adds between 50 000 and 100 000 microsphere per cement particle to the mix, there is significant effects in mix properties. Cohesiveness increases while slump decreases, however the increased water demand should be negated using plasticizers or even super plasticizers or reduction in sand content. Acting like ball bearings this ultrafine particles aid pumping, vibrating and tamping of concrete. Less segregation besides less bleeding are the other characteristics of SF concretes. Although, it should be considered that gelling does not necessarily means rapid set. Being a pozzolana, SF needs calcium hydroxide for activation. Here, it is better to point out that the fine filler effect of SF with a bulk density equal to one fifth of cement has to be taken to account in mix design.

Pozzolanic reaction takes over from physical effects during setting and hardening of concrete. Reacting with liberated $Ca(OH)_2$ and producing calcium silicate and aluminate hydrates, it increases the strength and reduces the permeability of mix due to the densified matrix. Because of greater surface area and higher silicon dioxide content, SF is much more reactive than before mentioned SCMs with a 4-5 times greater cementing efficiency than PC. However, researches shows that there is no concerns about pH level reduction because it is yet above the level which is necessary to avoid carbonation or protect steel passivity. In contrast, it can be beneficial to reduce alkalinity by binding K^+ and Na^+ to diminish the risk of ASR. Additionally, thanks to produced C-S-H, the voids are better filled, the gaps between cement grains and aggregate particles are sufficiently bridged and all these coupling with physical filling effect results in more homogeneous matrix (Lewis *et al.* 2003).

2.2.1.d. Metakaolin

Metakaolin (M) is produced from dehydroxylation of kaolin, a natural decomposition of feldspar used in porcelain, china and paper industry, at 450°C and formed in kiln when heated between 700-800°C. The calcined, cooled rapidly and ground product possesses a highly disorganized structure. Particle density of m is 2.4, lower than that of PC (3.1). Thus, in terms of replacement, it increases the cementitious material content and cohesiveness of the mix resulting in improved workability, bleeding and surface finishes (Lewis *et al.* 2003).

2.2.2. The effects of SCMs on hardened properties of concrete

2.2.2.a. Fly ash

Fly ash concretes has slightly better module of elasticity than equivalent grade of OPC concrete. Owing to its greater long-term compressive strength, the creep of concrete is decreased particularly under the condition of no moisture. Moreover, the tensile strain capacity is marginally lower than normal concrete and a greater risk of early thermal cracking partially offsets the benefits of lower hydration heat. Considering to its slower rate of hydration, curing should be fallowed precisely. Graphs below present some mentioned properties.

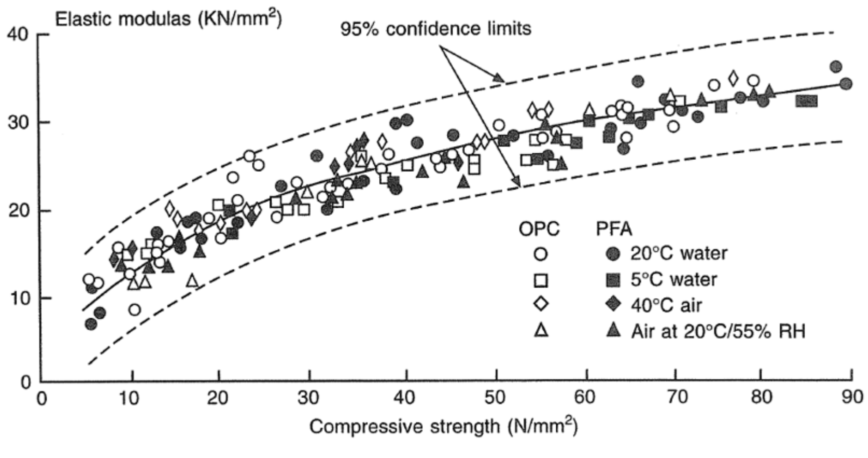

Figure 2.30. Relationship between the E and strength for FA and PC concrete (Lewis *et al.* 2003)

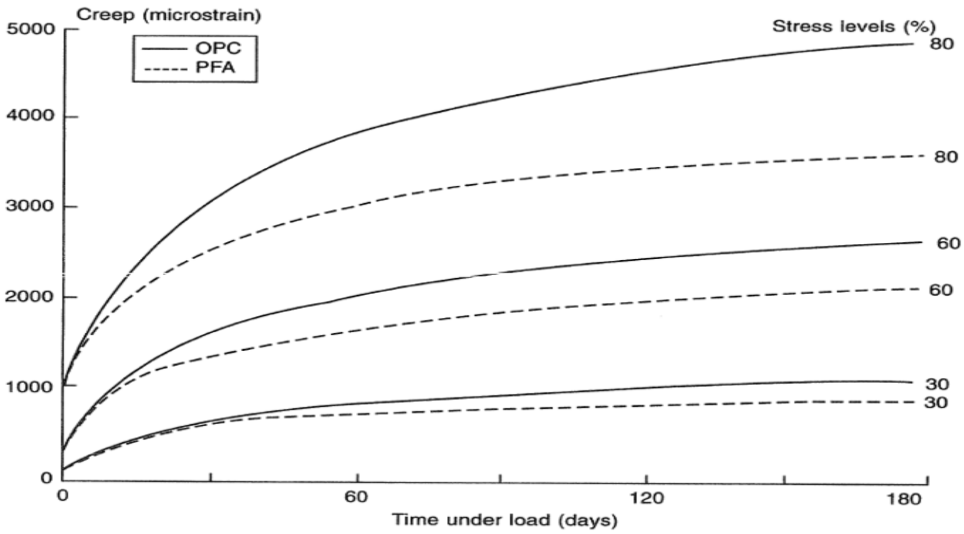

Figure 2.31. Creep of fly ash and PC concrete loaded to different stress levels (Lewis *et al.* 2003)

2.2.2.b. Ground granulated blast furnace slag

Since the GGBS has a slower hydration rate, the more the percentage of GGBS, the lesser the early age strength of the concrete. This concrete is more sensitive to temperature change because of possessing a higher activation energy. In the other words, the rate of strength gain increases with increasing temperature and vice versa. Furthermore, its tensile strength capacity as well as module of elasticity is a little higher than normal concrete. Due to its greater strength gain at later ages, rise of GGBS content results in drop of creep. The GGBS has also very little if any influence on the drying shrinkage. Graphs below conveys some of discussed matters.

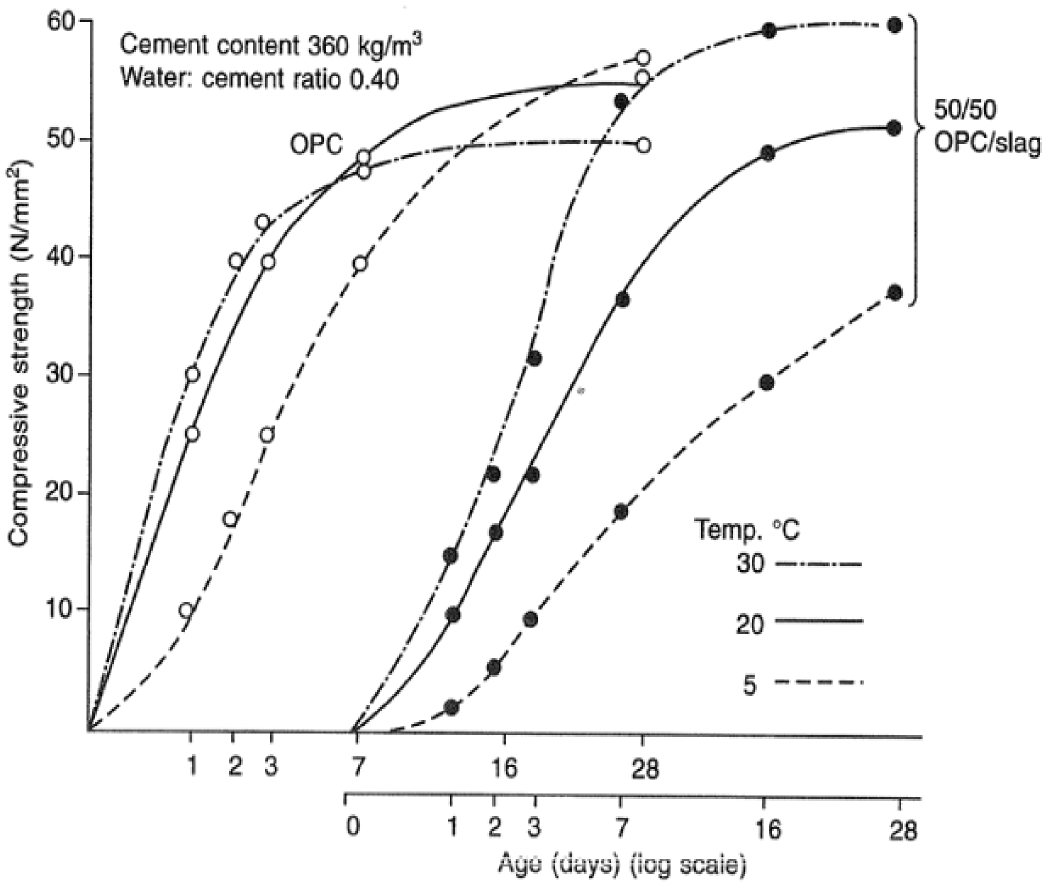

Figure 2.32. Influence of temperature on strength development for concrete with and without slag (Lewis *et al.* 2003)

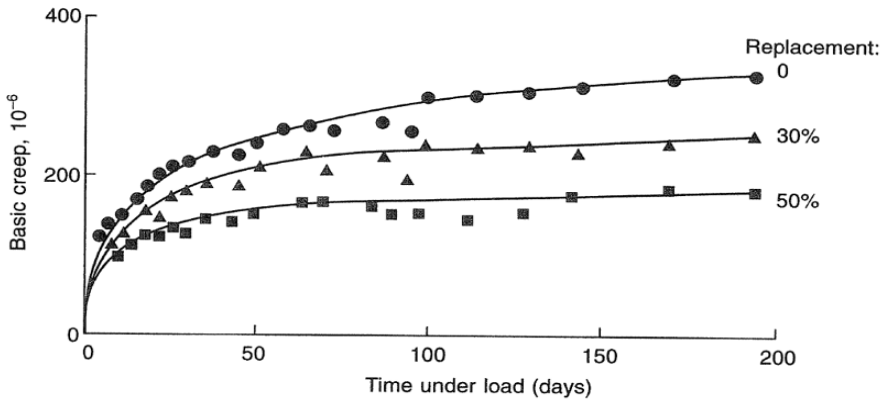

Figure 2.33. Effect of GGBS on basic creep in water at 22°C (Lewis *et al.* 2003)

2.2.2.c. Silica fume

Silica fume can increase the strength of concrete between 30 to 100%. The tensile and flexural strength fallow the same pattern. The higher compressive strength leads to a more brittle concrete as a general rule, however, the module of elasticity does not fallow the same model of tensile strength and increase just slightly. An improvement in bonding to substrates, old concrete, reinforcement, fibers and aggregates is resulted from much finer paste phase. If there is no compensator the creep will be increased.

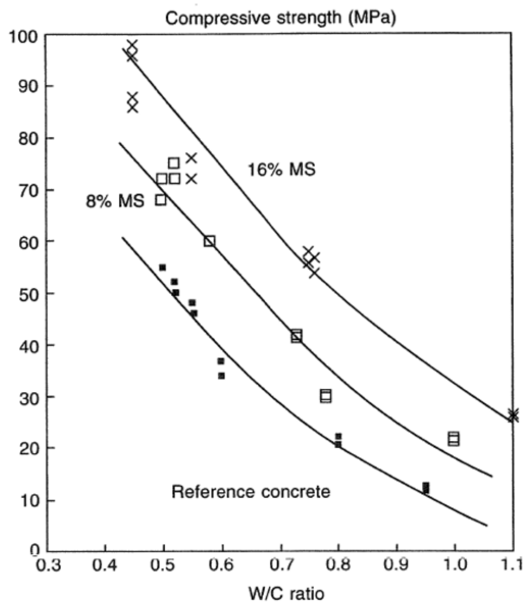

Figure 2.34. Strength versus w/c (Lewis *et al.* 2003)

2.2.2.d. Metakaolin

Metakaolin increases the compressive strength significantly if its inclusion be limited between 5-10% but higher contents has no effect on this matter. The elastic module of elasticity and tensile strength are similar to those of normal concrete but the latter is accelerated significantly with metakaolin at early ages. There is a similar creep in this kind of concrete, whereas, drying shrinkage decrease because of decreased porosity and permeability and subsequent lesser water loss from concrete (Lewis *et al.* 2003).

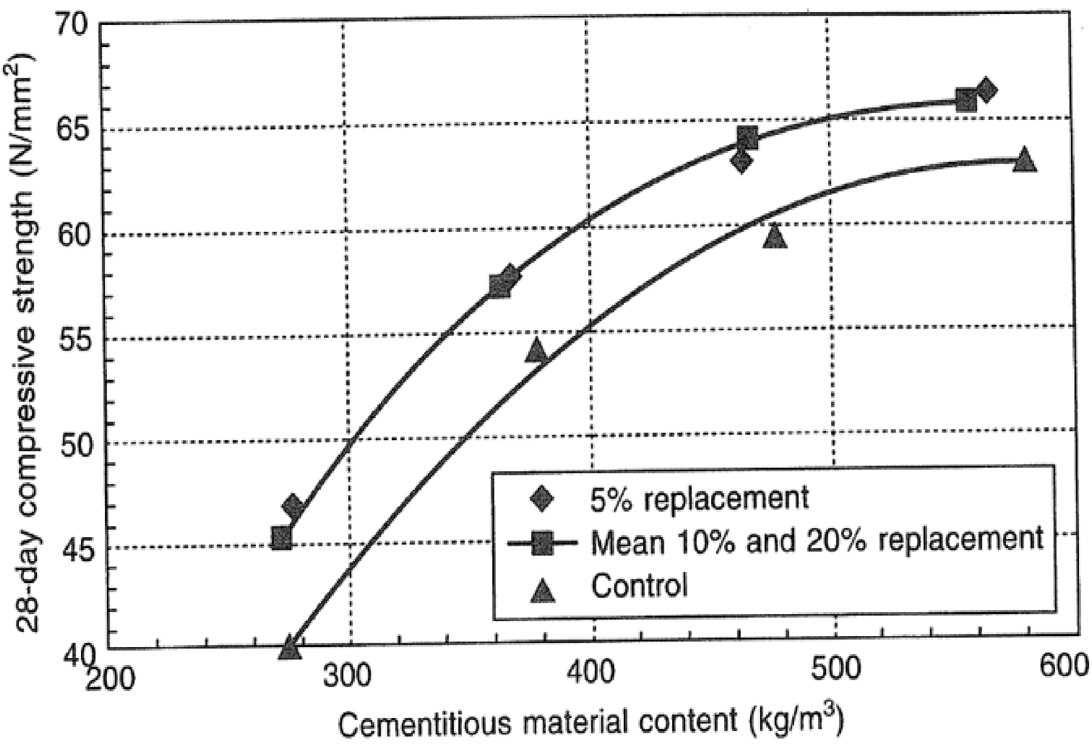

Figure 2.35. Effect of metakaolin on compressive strength of concrete (Lewis *et al.* 2003)

2.2.3. The effects of SCMs on durability of concrete

2.2.3.a. Fly ash

Alkali silica reaction (ASR):

ASR is process in which the alkalis such as sodium and potassium hydroxide react with available silica in the aggregates and produce a highly water absorbing gel. This gel is capable of absorbing pore solution water. This results in an expansion which disturbs the concrete structure. Fortunately, only 16-20% of alkalis of FA are soluble in water and therefore, FA can prevent ASR to the point that 25% inclusion of FA is required to avoid ASR according to BSI 5328.

Carbonation:

Since carbonation is a function of permeability and lime availability, although, FA reacts with lime decreasing the pH of the pore solution the alkaline environment is enough for passivity and together with lesser permeability the carbonation is similar to that of plain concrete.

Seawater and chloride attack

The main sources of chloride is external sources including seawater and de-icing salts. FA not only contains some oxides of alumina to act like C_3A and C_4AF of OPC by chloride ions to slow their movement, but also reduces chloride ions ingress effectively due to significant reduction in permeability.

Freeze-thaw damage

Less porosity and low permeability are the two principal characteristics of FA concretes. Thus, there is not suitable space in such concretes to relieve the pressure produced through expansion of freezing water. As a result, FA concretes possess lesser freeze-thaw resistance than that of OPC concrete unless air entraining agents be used.

Sulfate attack

Sulfate ions react with hydration products of concrete to form secondary gypsum and ettringnite. This originates a deteriorative pressure in concrete structure. FA reduces the pore size which slows the penetration of sulfate ions as well as the volume of formed ettringnite. Moreover, it drops the amount of available $Ca(OH)_2$ necessary to formation of gypsum. FA also diluted C_3A, the most prone product to attack, through reacting with a proportion of it at early ages. Therefore, FA increases the resistance to sulfate attack particularly where its content is in a range between 25-40%.

The other form of sulfate attack leads to formation of thaumasite with a very similar crystal to that of ettringnite:

- Ettringnite: $C_3A.3CaSO_4.32H_2O$
- Thaumasite: $CaCO_{3.}CaSO_4.CaAiO_3.15H_2O$

The volume expansion of thaumasite is about 45% of ettringnite make this kind of attack more difficult to be distinguish. FA is believed to be beneficial in this matter via reducing the permeability and subsequent ingress of sulfate ions (Lewis *et al.* 2003).

2.2.3.b. Ground granulated blast furnace slag

Thanks to properties like continued hydration and finer pore structure, GGBS concretes are less permeable than OPC ones. Therefore, they show better durability against harsh environmental conditions.

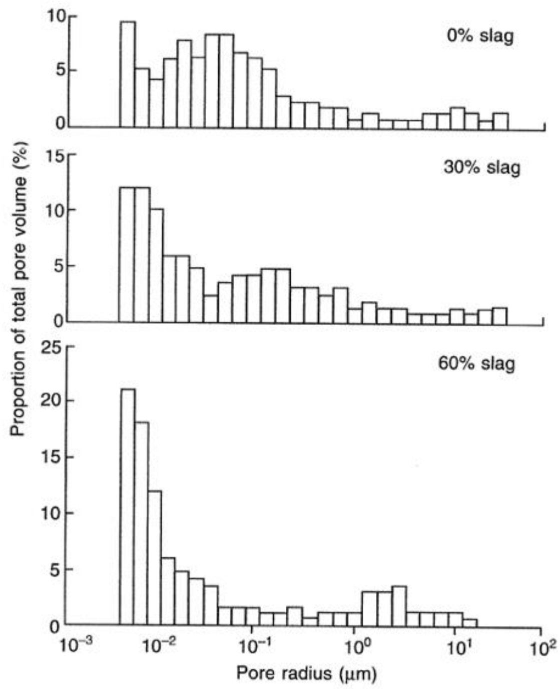

Figure 2.36. Influence of slag content on pore size distribution of pastes (Lewis *et al.* 2003)

Due to lower solubility of alkalis in GGBS, it can reduce the reaction between alkaline pore fluid and siliceous minerals found in aggregates. Therefore, slag concretes are less vulnerable to disruptive impacts of resulted expansion in *ASR*.

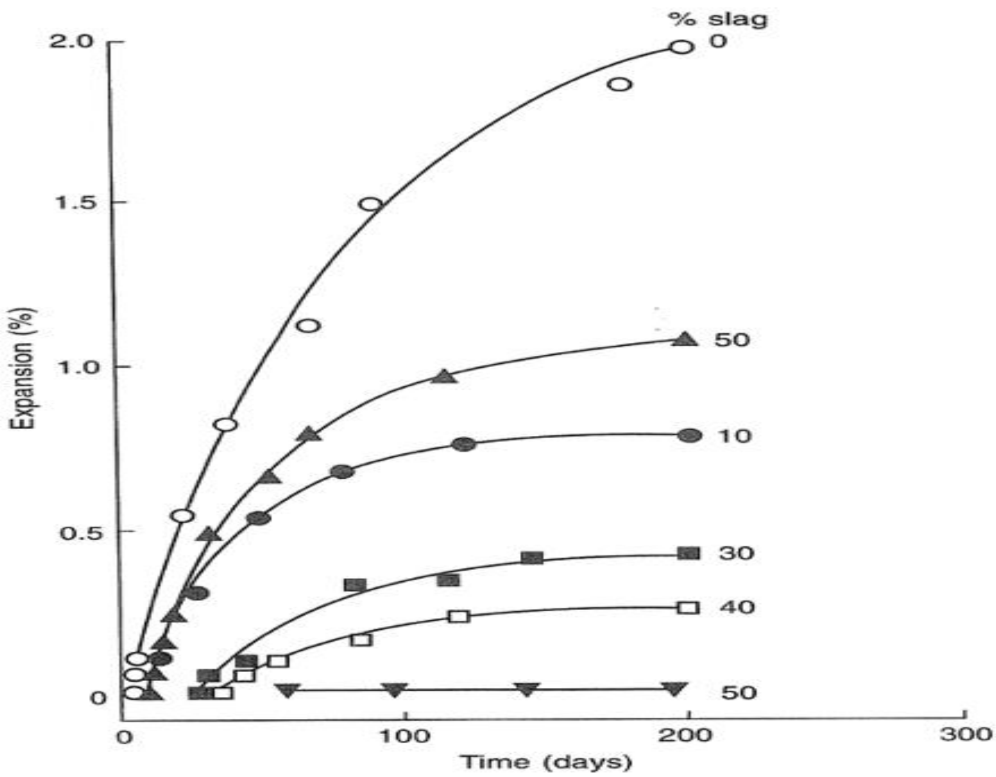

Figure 2.37. Influence of slag content on expansion due to ASR (Lewis *et al.* 2003).

In terms of *carbonation*, there is disputable opinions. Although there is a marginal increase in carbonation depth for slag concretes, in higher compressive strength and early ages no significant difference has been recorded.

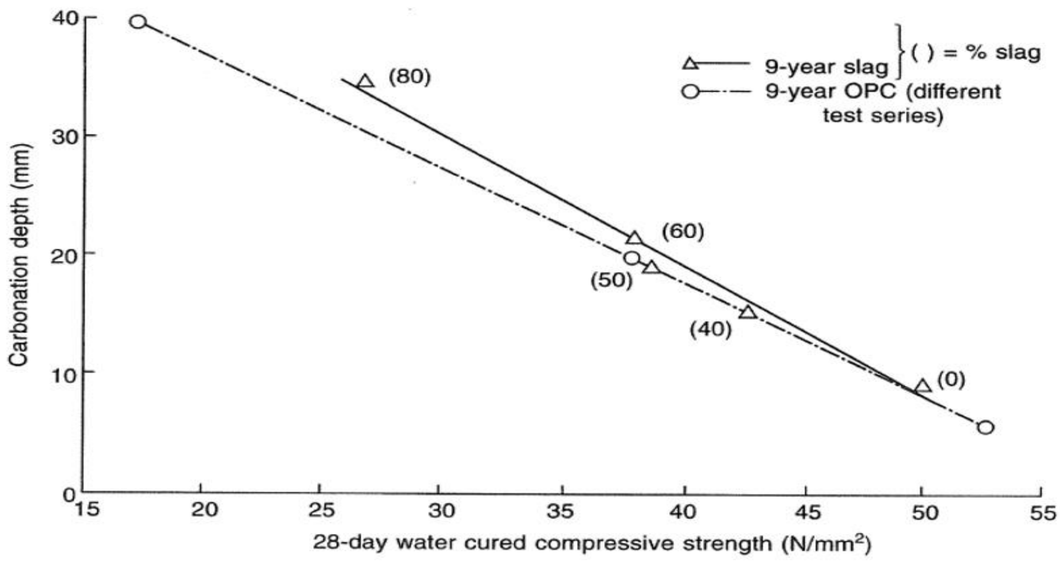

Figure 2.38. Influence of slag on relationship between carbonation depth and strength (Lewis *et al.* 2003)

Also it is noticeable that the secondary reactions of GGBS causes the pH level to remain in a protective level of steel passivity.

GGBS hydrates are capable of reaction with chloride ions. Coupling this fact with the inherent lesser permeability makes the movement of this ions slower. Thus, GGBS shows a significant improvement in chloride resistance of concrete.

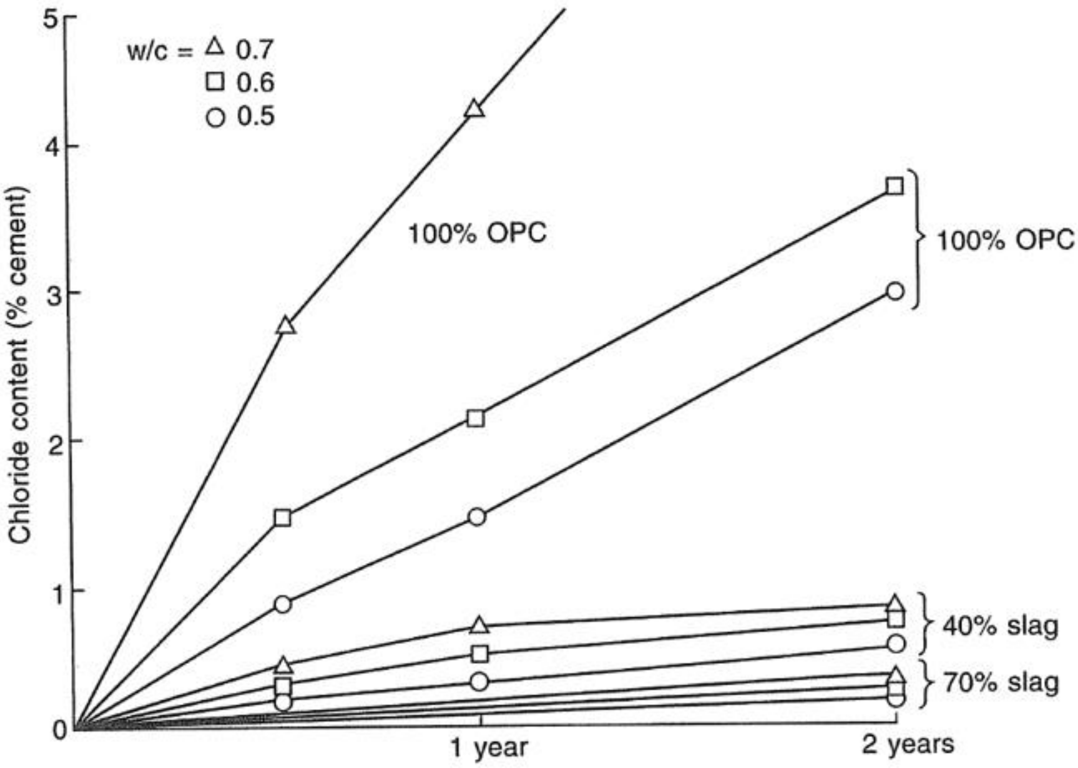

Figure 2.39. Influence of slag content on chloride diffusion (Lewis *et al.* 2003)

To increase the *freeze-thaw* resistance, the air entrainment is necessary because in concretes with higher amount of GGBS an inferior resistance has been recorded. In contrast, reduced permeability makes slag concrete pretty more resistance to *sulfate attack* (Lewis *et al.* 2003).

2.2.3.c. Silica fume

According to studies using drying methods in which the weight loss of concrete is measured after drying, the efficiency factor for SF was between 6 and 8. This indicates the greater effect of SF on permeability than on compressive strength. In active testing which exposes the concrete to aggressive substances and measures the depth of penetration, SF was revealed to be very impermeable. It is contributed to the dense microstructure and robust ITZ of SF concretes.

Silica fume reacts with calcium hydroxide and reduces the pH eliminating the first necessary factor of *ASR*. K^+ and Na^+ ions are bound through formation of calcium silicate hydrates. Therefore, potentially siliceous aggregates, the second factor for ASR, cannot react with them. The third parameter of ASR, water availability, is reduced due to refined pore structure and lower permeability.

Carbonation of SF concrete is an arguable matter but for concretes with compressive strength above 40 MPa, it seems to be reduced.

Although the reduced pH lowers the threshold limit of depassivation of the steel, but much lower chloride penetration coefficient negates this effect of SF in concrete.

In the matter of frost resistance, air entrainment into SF concrete is a very difficult issue. It may be due to this fact that both of them compete for the same space in matrix. Therefore, it is strongly recommended to use air entraining agents besides the super plasticizers.

Owing to less calcium hydroxide content, lower available alumina for ettringnite formation (more incorporated to SF) and reduced permeability due to refine pore structure, SF concretes resistance to sulfate attack can be considered similar to that of concretes made using sulfate-resistant cements. In conjunction with GGBS or PFA the performance is even higher than them (Lewis *et al.* 2003).

2.2.3.d. Metakaolin

It is well established that m is able to prevent the expansion of concrete through *ASR*. M reduces the $Ca(OH)_2$ to a such a low degree the ASR is suppressed as result of unavailability of swelling gel.

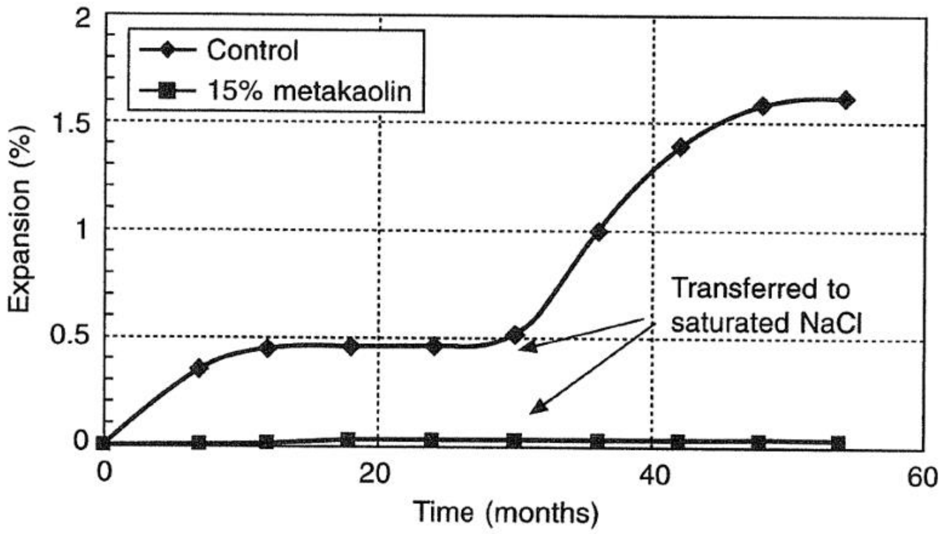

Figure 2.40. Effect of metakaolin on expansion due to ASR and immersion in NaCl (Lewis *et al.* 2003)

Different tests has confirmed that the m concretes are considerably resistant against *chloride penetration* and the reduction of the rate of diffusion of chloride is by an order of magnitude.

Table 2.8. Results of chloride penetration tests (Lewis *et al.* 2003)

Research Reference	Mix	Cementitious material content (kg/m^3)	Results of ASTM test (coulombs)		
			28 days	56 days	90 days
Calderone	Control	385	-	4832	-
	15% M	385	-	754	-
Martin	Control	385	3175	-	1875
	15% M	385	390	-	300
Ryle	15% M	400	625	395	310

Table 2.9. Effect of metakaolin on chloride ion diffusion coefficient (Lewis *et al.* 2003)

Sample type	w/c	M replacement %	Chloride ion diffusion coefficient $(cm^2s^{-1}) \times 10^{-9}$
Paste	0.5	0	90
	0.5	15	9
Mortar	0.6	0	220
	0.6	15	18
Mortar	0.7	0	680
	0.7	15	8
Mortar	-	0	597
	-	20	10

Although the *frost resistance* of concrete depends on factors such as strength, creep, extensibility and saturation, the main effective factor is the pore system. The inclusion of M correct this parameter to such a degree that M concretes show an excellent performance against cycles of freeze and thaw.

It is established that M concretes can show a better performance against *sulfate attack, acidic attacks* and *efflorescence* (Lewis *et al.* 2003).

2.3. Nanoparticles and Nanotubes

In this chapter the main concepts of the usage of nanotechnology and related products in concrete industry has been summarized very briefly as a preparation for the main research as in previous chapters.

2.3.1. Nanotechnology of concrete

As a definition, nanotechnology encompasses nanoscale science, engineering and technology that involve imaging, measuring, modeling and manipulating matter at the scale of one billionth of meter. Since a sheet of paper is approximately 100 000 nm, it is imaginable how small is nanoscale and how its utilization can influence the properties of concrete in different respects. Figure below represents the two main approaches of nanotechnology, top down and bottom-up, whereas the latter is the used approach for the purpose of modification (Birgisson *et al.* 2013).

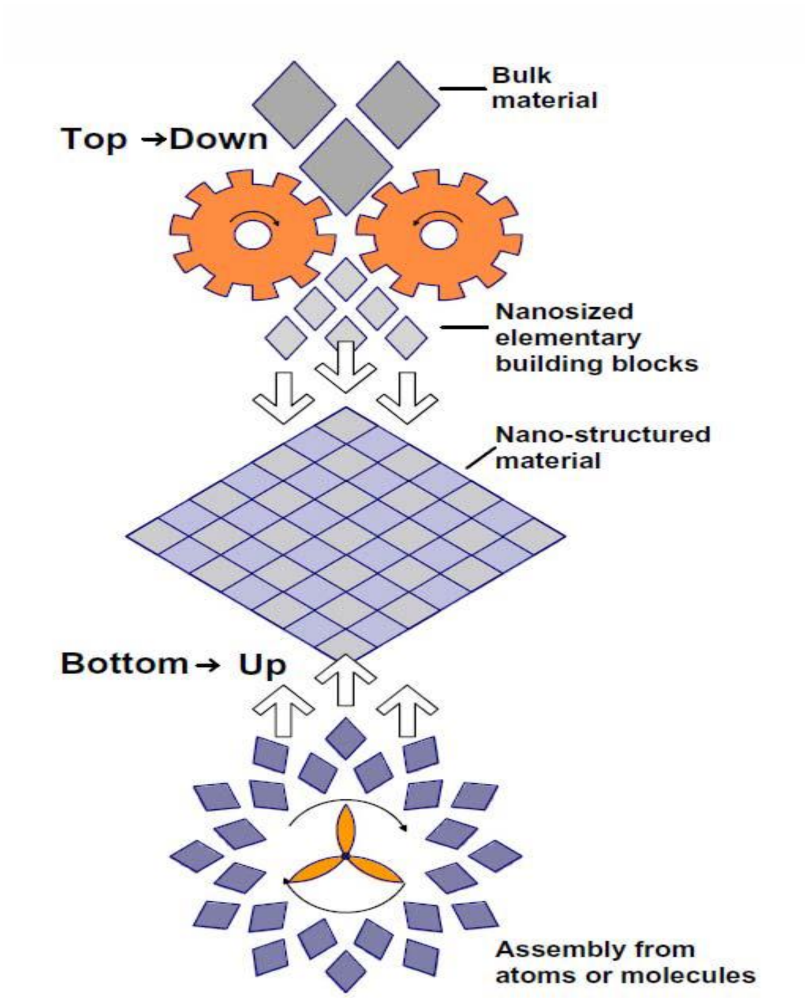

Figure 2.41. Top-down and bottom-up in nanotechnology (Birgisson *et al.* 2013)

Being composed of an amorphous phase, nanometer-to micrometer-size crystals, and bound water, the mechanical, durability, and sustainability properties of concrete can be affected to a high degree through exerted modifications in this scale.

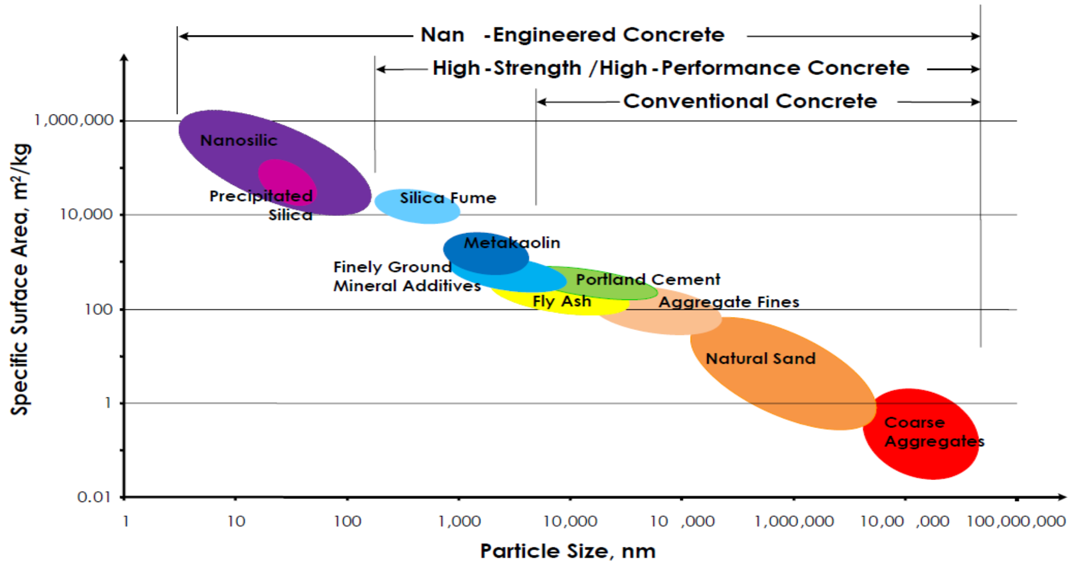

Figure 2.42. Particle size and specific surface area related to concrete materials (Birgisson *et al.* 2013)

The main component of the concrete, C-S-H, is a few nm size and has a great role on mix behavior by itself and the pore system which governs the water movement affecting shrinkage, cracking, etc. Thus, nanotechnology has a capacity to has a revolutionary impact on concrete industry by developing high-performance, sustainable and even intelligent concretes (Birgisson *et al.* 2013).

2.3.2. Mechanical effects of nanoparticles

Due to their greater surface area and higher reactivity, different nanoparticles show significant impacts on mechanical properties of concrete from various aspects. For instance, nanosilica accelerates cement hydration and formation of C-S-H because of creating nucleation sites duo to its higher surface energy. Filling very fine pores and reacting with $Ca(OH)_2$ to produce more gels, it can produce a stronger ITZ and a denser microstructure. Nanoindentation studies revealed that a stiffer C-S-H gel is produced besides all above. Together with nanosilica (NS), other nanoparticles such as nano-TiO2 (NT), nano-Fe_2O_3 (NF), nano-Al_2O_3(NA), nano-ZrO_2 (NZr) and nano-$ZnFe_2O_4$(NZF) improve properties like compressive and flexural strength, ITZ and porosity and many other mechanical behaviors (Birgisson *et al.* 2013).

2.3.3. Durability effects of nanoparticles

Various nanoparticles applied in concrete has improved durability characteristics of the mix in various aspects. Lower permeability, water penetration and diffusion depth, or capillary pores refinement and obstruction besides pore volume reduction, are some effects of the inclusion of nanoparticles due to their characteristics such as higher reactivity, finer filling size, electro-kinetically transformability and acting as nucleation sites to form a stiffer calcium silicate hydroxide. The latter which is tested by nanoindentation, has a great impact, not only in compressive strength development, but also significantly affects many aspects of durability. Moreover, improved ASR condition and shrinkage properties as well as lesser calcium leaching could be added to mentioned modifications (Birgisson *et al.* 2013).

In addition to improvements that nanoparticles can induce in resistance against environmental attacks like corrosion, sulfate and ASR, they, i.e. NS and NT, increase the abrasion resistance of concretes used in pavements. The better performance of concrete in flexural fatigue can be considered another positive effect of them.

2.3.4. Sustainability effects of nanoparticles

Addition of nanoparticles plays its role to help to production of sustainable construction materials. One way is to overcome the drawbacks of belite concretes and high-volume fly ash (HVFC) (Birgisson *et al.* 2013).

Although these types of concrete are environment friendly through less emission of carbon dioxide and energy consumption, they show a disadvantage with respect to early age strength. Inclusion of nanoparticles like $CaCO_3$ compensate this problem alongside a reduction in heat of hydration (Raki *et al.* 2010).

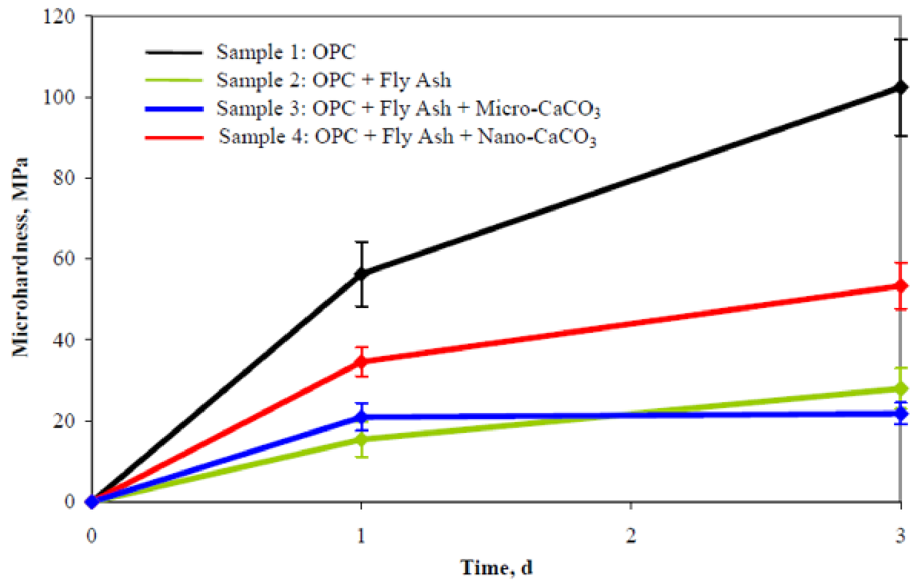

Figure 2.43. Microhardness measurement for the hydration of one day and three days (Raky *et al.* 2010)

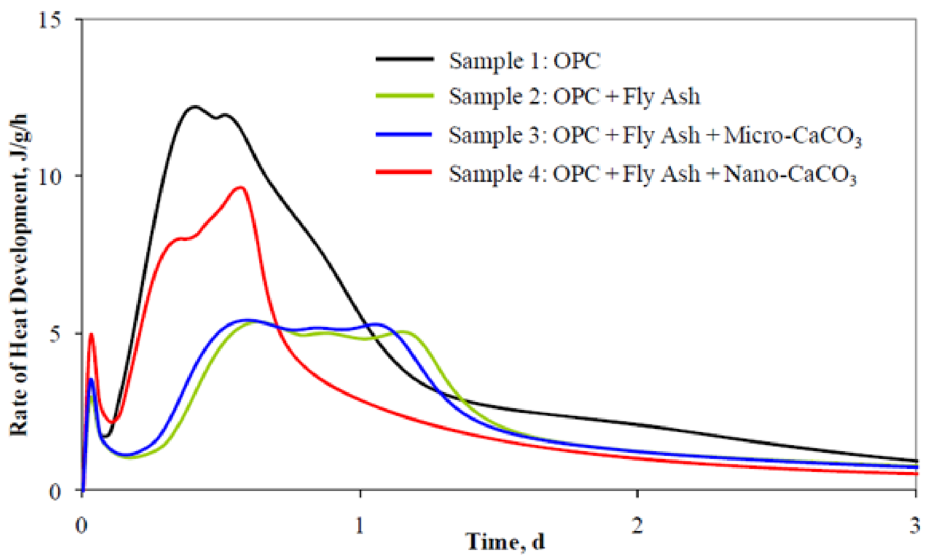

Figure 2.44. Rate of heat development measured by the conduction calorimeter (Raky *et al.* 2010)

Additionally, concrete used in building facades or paving can possess the ability of self-cleaning. Nano-TiO_2 decays pollutants via photocatalytic degradation. Furthermore, NS can help incinerator bottom ash to be used as aggregates with an improved mechanical properties (Birgisson *et al.* 2013).

2.3.5. Nanotubes

Traditionally tensile and flexural weakness of concrete has caused limits in designing. The first solution for this weak point through history was application of straw in sun backed bricks of 57 m height Agar Quf 3500 years ago (Newman 2003). Although, steel rods and pre-stressing are used to accommodate such stresses, nanofibers inhibits growth and interrupting propagation of cracks (Ferro *et al.* 2011)

Carbon nanotubes are hallow tubular channels by diameter range between 0.4-10 nm for single-walled and 4-100 for multi walled and length reaching to even millimeter range which. These walls are rolled graphene shits.

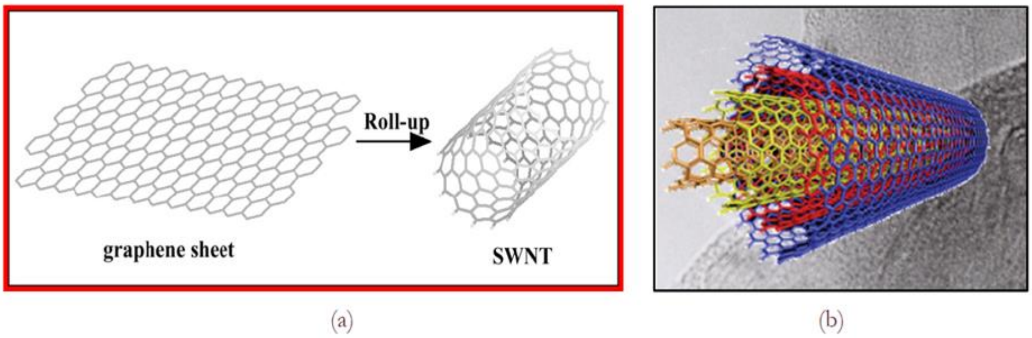

Figure 2.45. Illustration of SWCNTs (a) and MWCNTs (b) (Ferro et al. 2011)

Presence of carbon nanotubes (CNT) and carbon nanofibers (CNF) in concrete can be considered as a nanoreinforcement which not only considerably increases the strength, but also shows exclusive chemical and electronic influences. Incorporation of CNTs and CNFs compensate the lower tensile strength flexural strength, and ductility of concrete. Bridging cracks and voids as well as helping to load transferring they produce more strong and much durable concrete. Due to nanoscale characterization of ITZ, a reduction in tensile-creep is reported in fiber reinforced UHPCs (Raki *et al.* 2010).

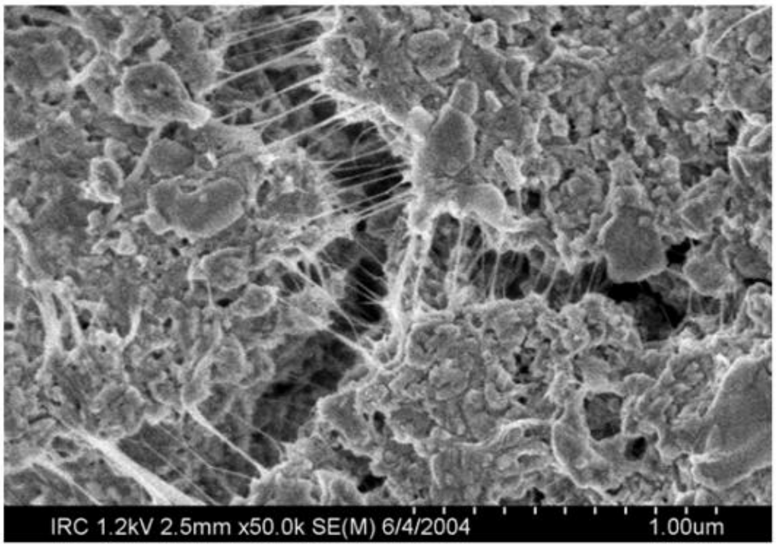

Figure 2.46. Example of crack bridging SWCNT (Raky *et al.* 2010)

Single walled CNTs (SWCNTs) also acts as a nucleation site to lead for a denser C-S-H formation.

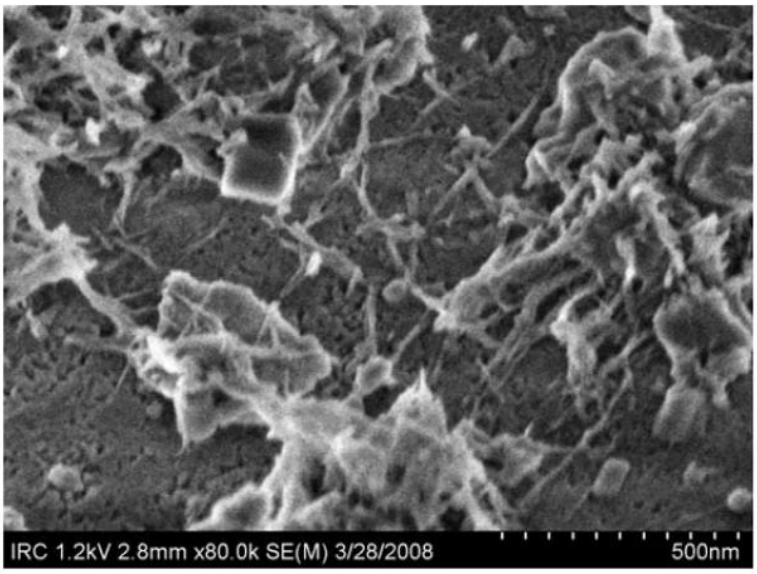

Figure 2.47. Growth of C-S-H around SWCNT bundles (Raky *et al.* 2010)

Additionally, the usage of nanofibers alongside with microcapsules and silica fume has resulted in self-feeling concretes with the capacity to heal microcracks. Intelligent and self-sensing concretes are another products using such fibers electrical conductivity which possess diagnostic properties.

2.3.6. Applications of nanoparticles and nanotubes

In addition to precisely before mentioned influences of nanomaterials on concrete, some main applications can be summarized in this way:

Concretes with photocatalytic properties are used for aesthetic and architectural purposes. White cement containing nano-TiO_2 removes pollutants and dirt to protect decorative properties of concrete via self-cleaning.

Self-compacting concretes, the main field of interest in this work, benefits appreciably from nanoparticles either for workability and strength or durability. Improved segregation resistance, refined pore system and stiffer paste are some reasons for this. Furthermore, inclusion of nanoclay is vital for self-consolidating concrete of slip form paving or SF-SCC. Moreover, the high reactivity of such particles plays a great role in characteristics of ultra-high performance concretes (UHPC) (Raky *et al.* 2010; Birgisson *et al.* 2013).

2.4. Conducted Relative Researches

Domone (2005) conducted an analysis of 68 case studies of the application of SCC on the basis of formulation details and properties. It was revealed that the main reason for use of SCC in most of the cases, is technical advantages compared to NVC, for instance, the difficulty of vibration in congested reinforcement. Economic benefits and novel construction were found to be the basic cause of use in the other cases. Reduced construction time and labor cost as well as thin-section precast or composite construction are examples of the latter reasons.

In almost all of slump flows were between 600-750 mm and about 80% of samples showed a compressive strength greater than 40 MPa which was mainly controlled by the binder composition rather than w/b ratio. Considerably varied values of other fresh properties, namely T500, V-funnel or L-box indicated the independence of this parameters.

Crushed rock was used as aggregate according to its local availability with 16-20 mm maximum size in 70% of cases. All but two of mixes possessed a binary or ternary powder compound of cement with LSP, GGBS, CSF or PFA among which LSP was the most common addition. Reducing hydration temperature or avoiding excessive cement content were the most general explanation of choice of SCMs.

The applied superplasticizers (SP) were polycarboxylic acid-based. Air entraining agents were used in some cases to improve the freeze and thaw resistance whereas VMAs were included to protect stability of the mix against sensitivity materials variation.

Aggregate grading seemed more important than type or size. Average fine aggregate content was approximately 50% but lower coarse aggregate content, average about 30%, was used to be lubricated by fine ones or mortar, also to prevent blocking. Paste content was averagely about 35% and powder content near to 500 kg reducing something about 30 kg if VMA is used. The median value of w/c ratio was 0.34% affected by hydration process, heat of hydration or strength gain.

According to all mentioned above, SCC should be considered as a family of variety of mixes for various requirements which owns lower w/p ratio and coarse aggregate content but higher sp dosages and powder contents, materials with a size smaller than 0.125 mm and sometimes containing a VMA.

In another review of 70 studies performed by P.L. Domone (2006) about the hardened mechanical properties of SCC in comparison with NVC, some interesting results obtained. The two main requirements to attain the special properties of SCC, fluidity, stability or passibility, are a lower yield stress and a reasonable plastic viscosity. Therefore, SCC needs both higher powder content and lower w/p ratio which highlight the necessity of SPs and VMAs. According to the various possibility of powder content in SCC such as PC, LP, PFA, GGBS or CSF, the type and proportion of powder appear to be governing the strength rather than w/p ratio. The cement efficiency factor, k-value, represent this effect on compressive strength. To estimate the compressive strength an equivalent w/c ratio in which the total c is the sum of SCM content multiplied by k-value and actual cement content, is used.

As with NVC, the cube strength of crushed aggregate mixes is higher than uncrushed ones but the average difference is 4 MPa instead of 8 MPa for NVC. However, the behavior of cylinders is contradictory.

The wide range between 0.8-1.0 achieved for cylinder/cube strength ratio which is completely different from the suggested range of 0.8-0.83 by BS EN 206. This perhaps be due to smoother crack surface of SCC which contains lesser coarse aggregates. Because the interlock of aggregates is believed to contribute in shear stress of cracked section and SCC of similar compressive strength shows 10% lesser shear stress than NVC.

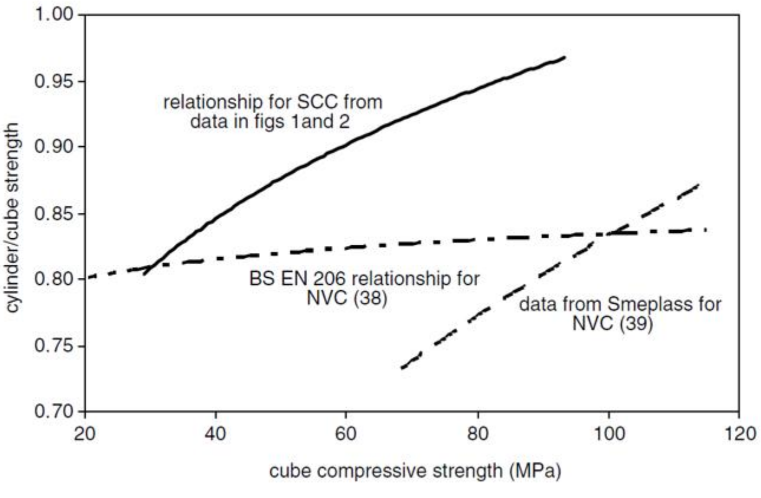

Figure 2.48. Cube and cylinder compressive strength relationship (Domone 2006)

Ignoring the scattering magnitudes of k-value for different powders except lp due to scattering in both achieved compressive strength and used materials, table below summarized the k-values.

Although limestone powder was accepted in many works to be in type I addition category acting just as filler, here, it is believed to affect the mix by means of two actions. First, acts as nucleation site for calcium silicate hydrates resulting in early age strength development. On the other hand, compounds with C3A as well as C2A and C3A to produce more cemetitious products.

Table 2.10. Cementing efficiency from strength data analysis (Domone 2006)

Addition	Range of addition rates	K factor		
		1 day	7 days	28 days
LSP	15-55	0.22 (14)*	0.36 (12)	0.29 (123)
PFA	20-60	-	-	0.56 (21)
GGBS	37-44	-	-	0.86 (5)
Chalk powder	25-55	-	-	0.23 (6)

*Number of results in brackets

No considerable difference observed for cylinder splitting versus modulus of rupture or compressive strength against static modulus of elasticity between SCC and NVC. Although, average stiffness of SCC was about 40% lower than that of NVC in higher strengths which was reduced to 5% for lower strengths.

Although SCC is expected to exhibit more brittle behavior, there are opposite results in fracture process of SCC which is used in ultimate load characteristics of concrete.

Regarding to its high fluidity and less bleeding, SCC should exhibit better bond to steel in both reinforcement anchorage length and wire transmission length in precast as well as corrosion protection due to its reduced top bar effect.

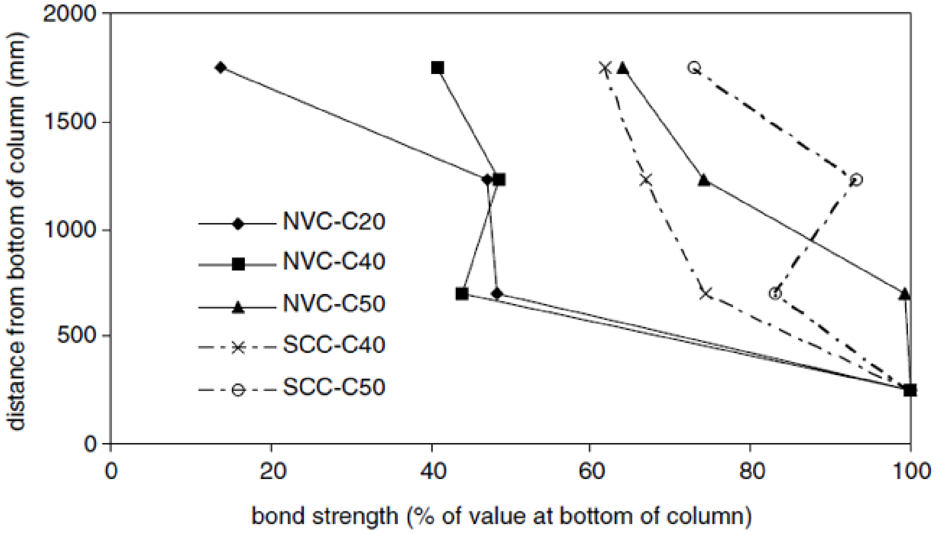

Figure 2.49. Variation of bond strength to 10 mm dia. Plain reinforcing bars with height in a columns element (Domone 2006)

Coefficient of variation from core strength, an in situ property for walls and columns, is slightly higher for SCC and totally it has no greater problem than NVC. Having the same load capacity with NVC, SCC tends to greater deflections and ultimate stains which is consistent with its lower E whereas its higher shear strength demonstration is inconsistent with before mentioned lower shear strength.

Türkel and Kandemir (2010) investigated the effects of two types of both powders and coarse aggregates on fresh and hardened properties of SCC. Type C fly ash and limestone powder each were used with either limestone or olivine basalt aggregates of particle size range between 5-15 mm alongside a polycarboxylate based SP.

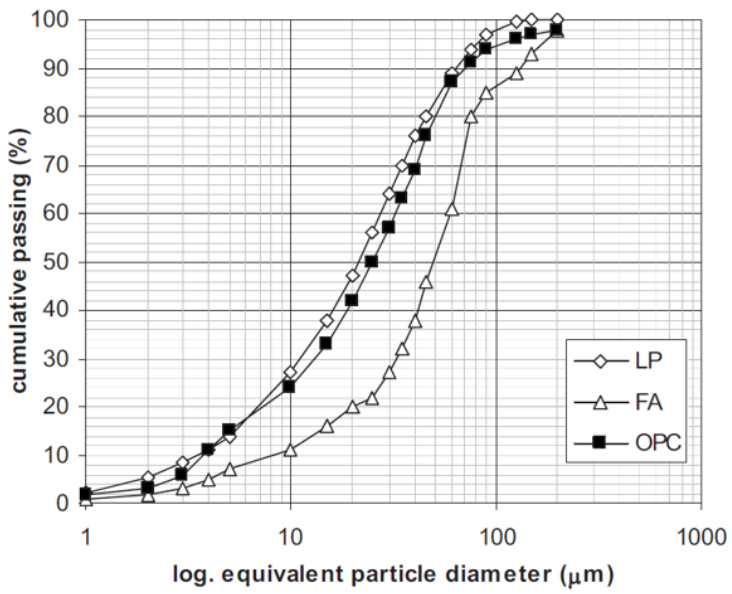

Figure 2.50. Particle size distribution of OPC, FA, and LP (Turkel and Kandemir 2010)

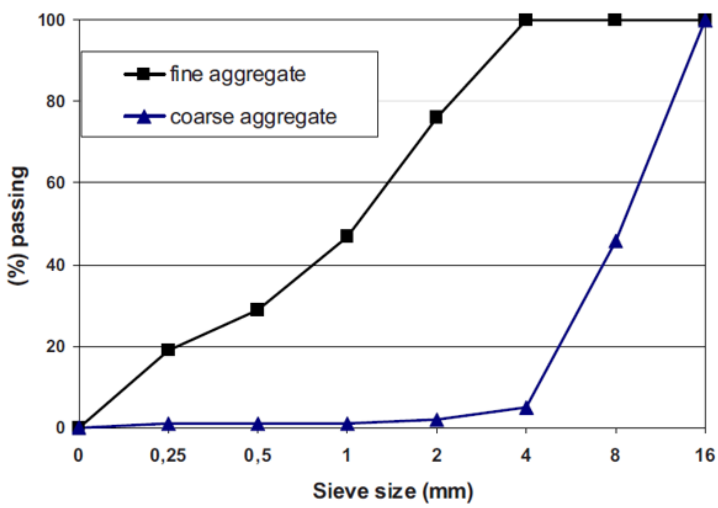

Figure 2.51. Gradation curves of fine and coarse aggregate for both limestone and olivine basalt (Turkel and Kandemir 2010)

Self-compactibity tests were performed in accordance with The European Guidelines for Self-compacting Concrete (2005). Slump flow of all mixes were in suggested range. However, it could be generally concluded that the type of powder and aggregate influenced SF, T_{500} time and V-funnel time. The highest self-compactibility achieved by limestone powder and limestone aggregate with V-funnel time of 11 seconds whereas fly ash and basalt aggregates negatively affected slum flow. Visual stability index of all mixes was between 0-1 and the mineral additives had a greater influence than aggregate type.

In terms of mechanical properties, the combination of fly ash powder and limestone results in the highest compressive and flexural strength. This can be attributed to the surface texture of aggregates and positive effect of fly ash on ITZ. The earliest strength development was related to limestone powder and limestone aggregate, however. It can be added that basalt aggregates and fly ash powder were beneficial in segregation and frost resistance, respectively.

In another work, Dinakar and Manu (2014) used metakaolin as a mineral admixture to obtain a new mix methodology resulting in high strength SCC. Despite FA, GGBS or SF which are by-products, metakaolin is a manufactured product with 12 000 m^2 specific surface area and average particle size of 1.5-2.5 μm lying between fly ash and silica fume.

There are several earlier suggested mix design methods such as Okurama, Ochie *et al.* CBI, Sedran *et al.* or UPC methods but Dinakar was the first to introduce a methodology including different replacements of FA with respect to efficiency factor, the portion of pozzolanic material equivalent to PC. K-value is used in w/(c+k×m). Silica fume and metakaolin with a greater than unit value for k which indicates a pozzolanic performance higher than PC can be used in concrete with compressive strength above 100 MPa. The suggested method which includes seven steps has been summarized in figure below.

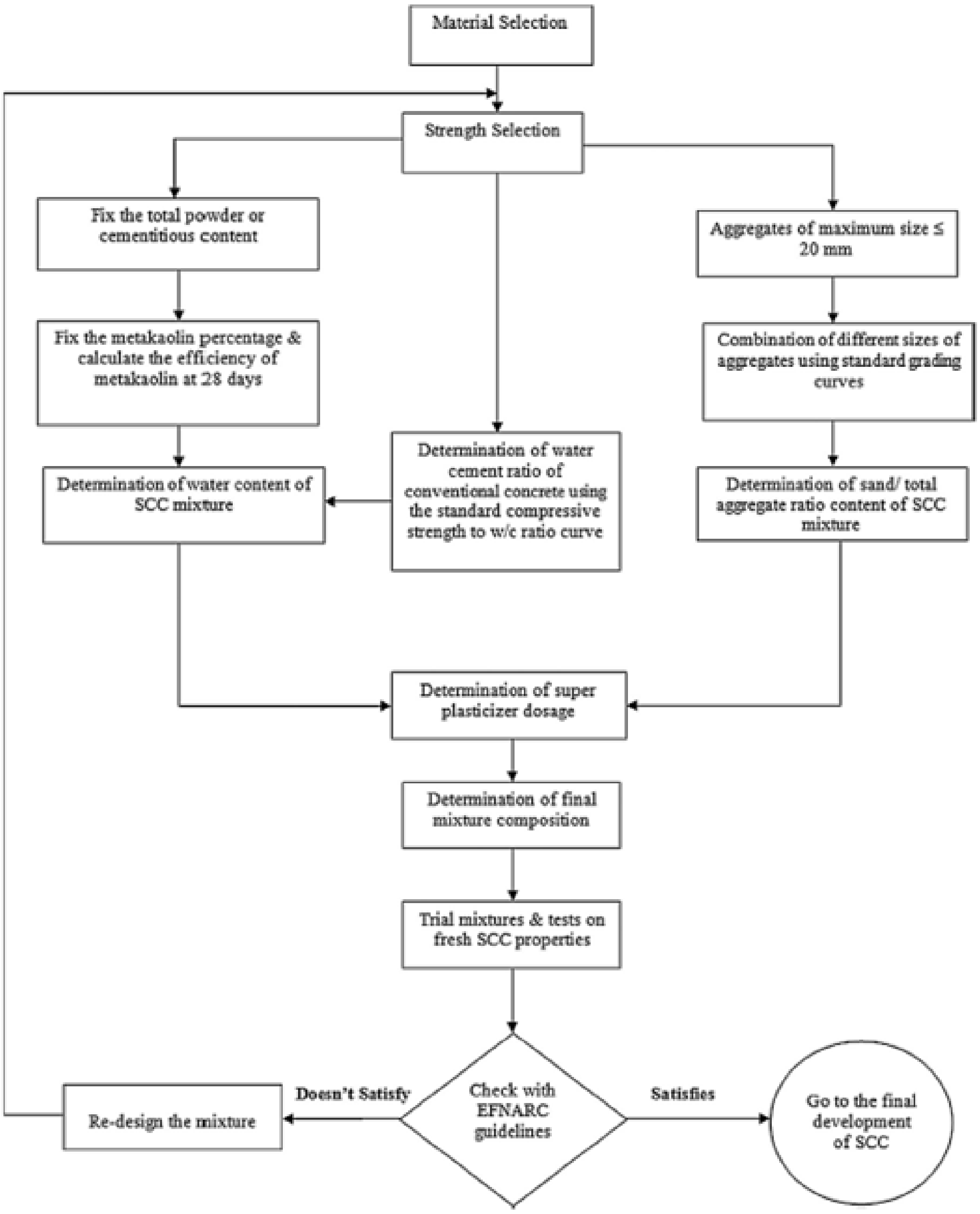

Figure 2.52. Outline of the proposed mix design methodology (Dinakar and Manu 2014)

Samples designed and calculated for 80, 100 and 120 MPa to validate the methodology. Cement and metakaolin selected in accordance with ASTM with 550kg/m^3 total cementitious materials. Different fractions of coarse and fine aggregates together with HRWR SP and PCE VMA introduced according to given figures and tables. Although, 20% metakaolin seems to be the best content according to Figure 2.54, 7.5, 15 and 22.5% were selected for 80, 100 and 120 MPa respectively.

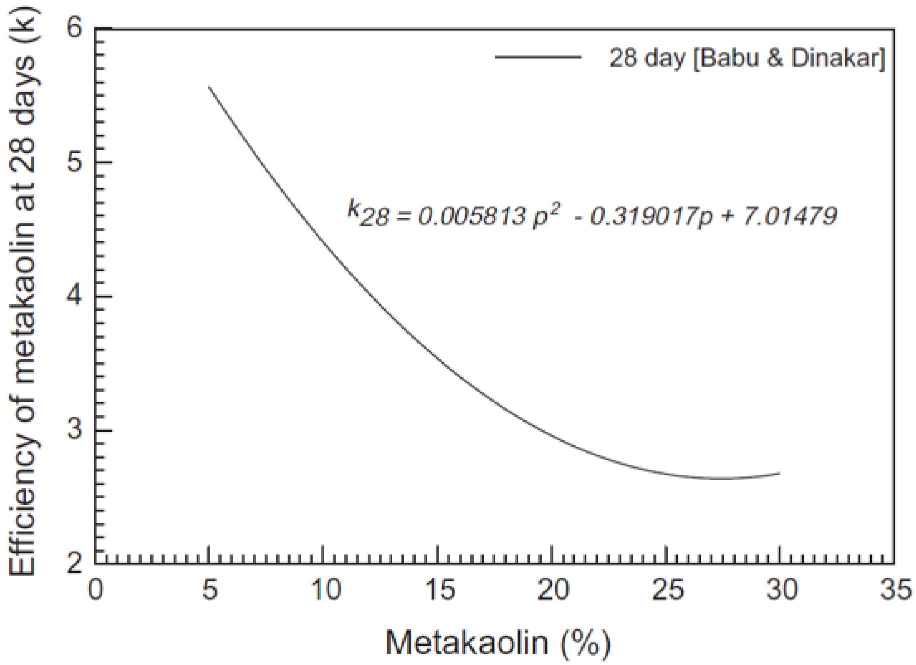

Figure 2.53. Variation of efficiency factor (k) with percentage replacement of metakaolin (Dinakar and Manu 2014)

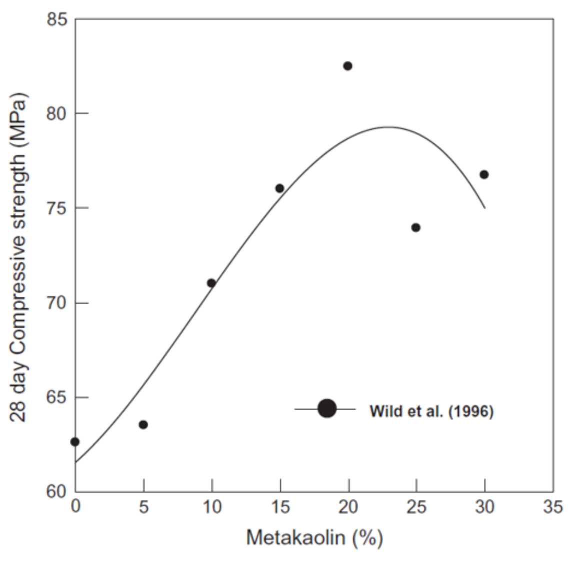

Figure 2.54. Maximum possible percentage replacement vs. compressive strength (Dinakar and Manu 2014)

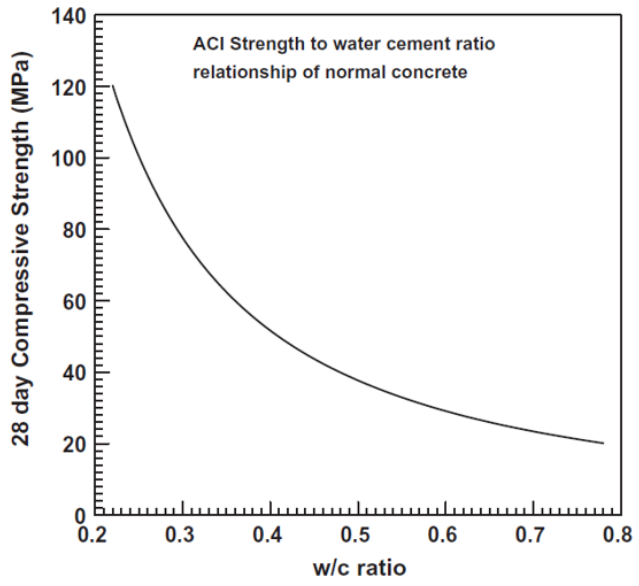

Figure 2.55. Strength to w/c relationship of conventional concrete (Dinakar and Manu 2014)

The mix with 22.5% metakaolin content showed the highest T_{500} result and revealed that metakaolin replacement significantly affect the values of T_{500} and V-funnel tests.

Table 2.11. Regulations for SCC (The European Guidelines for Self-Compacting concrete 2005)

Parameters	EFNARC guidelines
Volume of paste (liters/m^3)	300-380
Powder content (kg/m^3)	380-600
Water content (kg/m^3)	150-210
Fine aggregates in total aggregates (%)	48-55
Slump flow (SF) class (mm)	
SF1	550-650
SF2	660-750
SF3	760-850
Viscosity class (V-Funnel time in s)	
VF1	≤ 8
VF2	9-25
VS1 (T_{500})	≤ 2
VS2 (T_{500})	> 2
Passing ability class (L-Box)	
PA1	≥ 0.8 with 2 rebars
PA2	≥ 0.8 with 3 rebars

Table 2.12. Characteristics of cement and metakaolin (Dinakar and Manu 2014)

Chemical composition	Cement (%)	Metakaolin (%)
Silica (SiO_2)	34	54.3
Alumina (Al_2O_3)	5.5	38.3
Ferric oxide (Fe_2O_3)	4.4	4.28
Calcium oxide (CaO)	63	0.39
Magnesium oxide (MgO)	1.26	0.08
Sodium oxide (Na_2O)	0.1	0.12
Potassium oxide (K_2O)	0.48	0.50
Sulphuric anhyrided (SO_3)	1.92	0.22
Loss on ignition (LOI)	1.3	0.68
Blaine (m^2/kg)	360	15 000
Specific gravity	3.15	2.5

For normal concretes the strengths of 80 and 100 MPa achieved at 28 days but for 120 MPa the result was 111 after 90 days. On the other hand, values even greater than 80 and 100 recorded at 28 days and 120 MPa after 90 days.

Sfikas *et al.* (2014) carried out a work in relationship with SCC and metakaolin but they considered the influence of the replacement by both cement and limestone powder on rheological and mechanical properties of SCC. The physical and chemical actions of SCMs provides a better cohesiveness for SCC as a result of improved grain size distribution and particle packing. Utilization of metakaolin, product of calcination of purified kaolinite clay, can firstly refine the pore structure of the mix due to its higher degree of purity, pozzolanic reactivity or finer grading. On the other hand, it reduces the amount of calcium hydroxide to produce secondary calcium silicate hydrates. All these are beneficial to reach a more durable SCC reminding this important fact that the less the utilization of OPC, the lower the emission of carbon dioxide. The replacement of limestone powder was 6.9-20% and for cement it was 13.7-40%. The rheological classification was in accordance with European Guidelines for SCC (2005) using slump flow, fresh visual stability (FVS), V-funnel, and L-box test to evaluate the workability, segregation tendency, viscosity and passing ability of the mix, respectively. Moreover, compressive and tensile strength were evaluated using EN 12390-4 and 6 (2009).

An evident effect of the replacement of both cement and limestone on rheology observed. The lower slump flow could be as a result of irregular and plate like shape particles. The higher V-funnel time could be for the same reason as well. A lower L-box ratio and FSV value obtained. The latter ensures the absence of bleeding or segregation. Lubrication effect of finer sizes resulted in an accelerated T_{500} time. Although there was not any difference in the rheological class with reference samples.

For compressive strength, the higher the content of metakaolin, the higher the compressive strength even for 360 days but the rate of development for 28 days was greater.

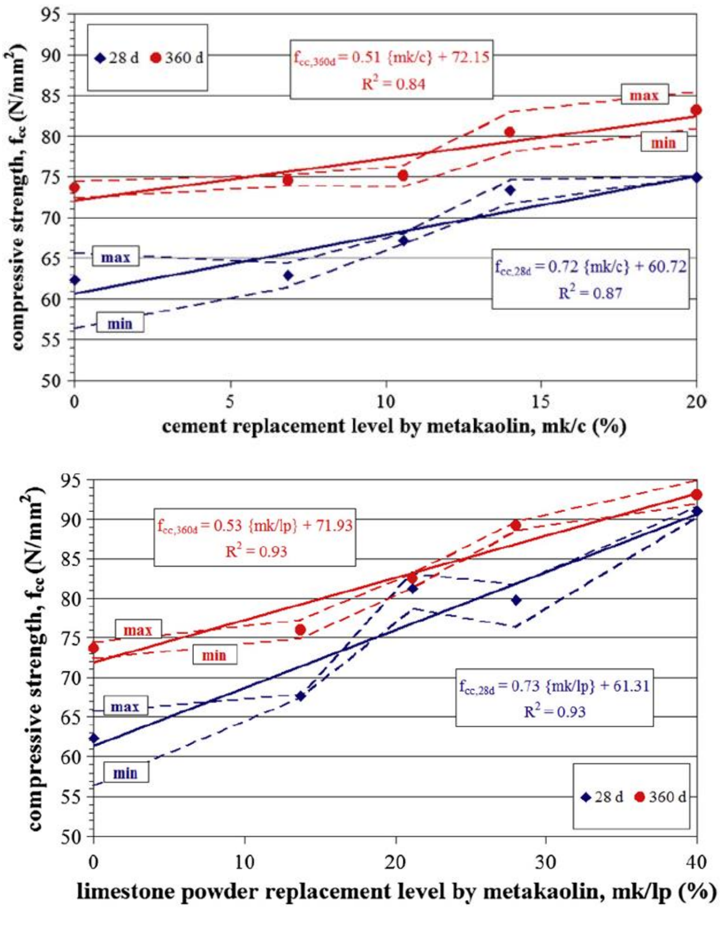

Figure 2.56. Effect of metakaolin and limestone powder level of cement replacement on the compressive strength (Sfikas *et al.* 2014)

The results for limestone and cement replacement were similar. However there was a convergence tendency for both 28 and 360 days strength gain at 40% replacement case. In terms of tensile strength, although it was rising by increasing the metakaolin content, in limestone replacements there a good correlation between compressive and tensile strength was evident despite of the cement replacements which demonstrated a weak correlation.

As an introduction to the influence of nano particles, the work of Quercia and Brouwers (2010) in application of nano-silica (NS) in concrete mixes is used. As the ingredient of the most common used construction material, there is a great environmental merit to reduce the amount of cement through utilization of nanoparticles.

On the other hand, concrete contains particles from 300 nm to 32 mm. Particle size distribution (PSD) determines the fresh state properties of the mix but hardened properties, strength and durability, is governed by particle packing resulted from mix grading. Thus, the employment of nanoparticles with sizes below 300nm is an effective way of packing improvement to increase solid size range.

There are different procedures to produce NS. In sol-gel method, starting materials are solved in a solvent and reduced pH of solvent results in precipitation of silica gel to be a xerogel after filtering, aging and stabilizing. Otherwise it can be produced via vaporization of silica fume. Other method are by-product of silicon metals, biological method, precipitation method or the alternative production route.

Due to its high surface area, NS accelerates the hydration process through creating nucleation sites for precipitation of C-S-H which is established via viscosity tests. The results revealed the increased need for water and stronger tendency towards adsorption of ionic species considering necessary dispersing to avoid agglomeration.

Different researches confirmed the significant effects of NS on microstructure improvement, permeability reduction, pore size diminution and ITZ densification.

Because NS can react $Ca(OH)_2$ and reduce their size and amount. It also fills the C-S-H voids, tightly bonding with them, and avoid calcium leaching. Increased density, reduced porosity and improved bond with aggregates make NS concrete to demonstrate a higher compressive and flexural strength alongside the excellent durability properties.

Owing to all mentioned above, NS has been made a necessity for HPC and SCC. It is added to increase cohesiveness as long as avoiding segregation and bleeding. In eco-concretes where cement replaced by waste materials of fly ash, it is used to compensate the drawbacks such as low compressive strength and long setting period.

Durability performances of concrete NS investigated by Hongjian *et al.* (2014). Thanks to its ultra-fine particles, application of NS seems to be promising for blended cements because of its early age pozzolanic reactions provided a correct dispersion. Some conducted researches with different percentages of NS had demonstrated beneficial results in uniform microstructure, calcium leaching or chloride penetration. Transport related durability performance of concrete considered here using 0.3-0.9% NS with average particle size of 13 nm and surface area of 200 m^2/g which highlights the risk of agglomeration. Therefore, both surfactant SP and ultra-sonication were used.

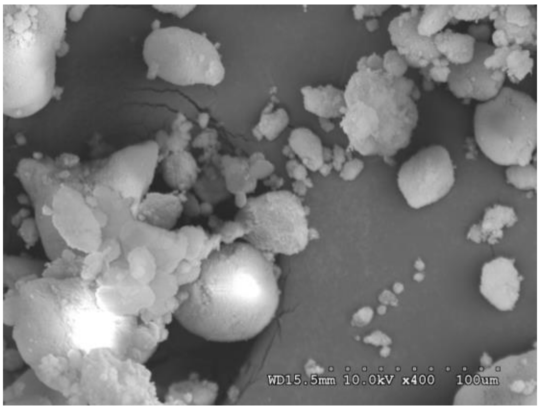

Figure 2.57. Agglomeration of nanoparticles (Hongjian *et al.* 2014)

Portlandite content measured using TGA by recording the weight loss relevant to the calcium hydroxide. As it is evident in the figure below, 0.9% NS makes the level of

Portlandite to be remained at 15% after 24 hour in contrast with OPC which reaches to the level of 22% after 7 days. Therefore, before mentioned acceleration effect of NS proved again predicting a denser microstructure as a result of this pozzolanic reaction.

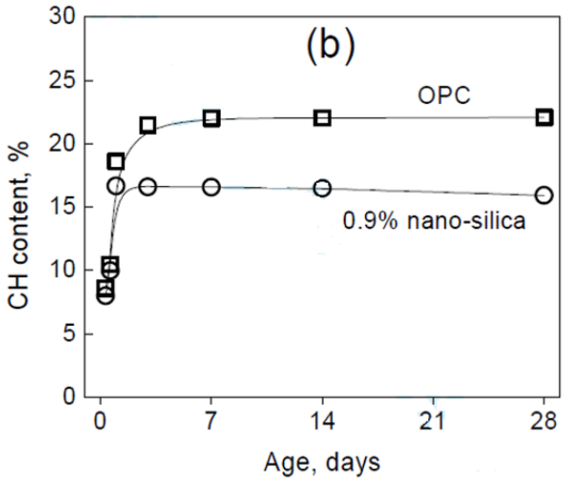

Figure 2.58. TGA results and portlandite content at different ages of cement paste with NS (Hongjian *et al.* 2014)

The result of MIP test demonstrate the identical total porosity, 13.5%, for both mixes but large capillaries which govern the permeability and diffusivity reduced with 0.9% NS while the medium one increased. The pozzolanic reaction refines and blocks the capillary pores to reduce permeability.

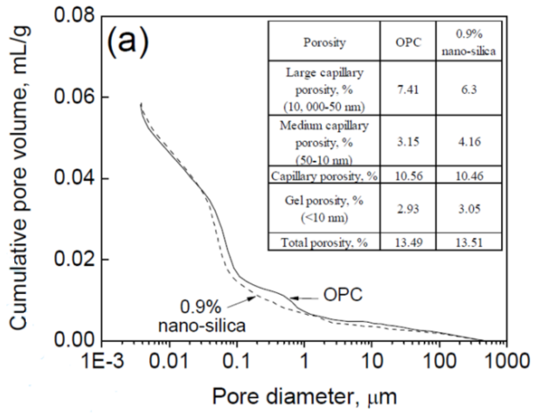

Figure 2.59. Pore size distribution of concrete with NS and cumulative pore volume curves (Hongjian *et al.* 2014)

There are crystalline CH, needle-shape AFt and various size of voids in SEM images of OPC. In contrast, NS concrete possess a homogeneous matrix with adenser ITZ.

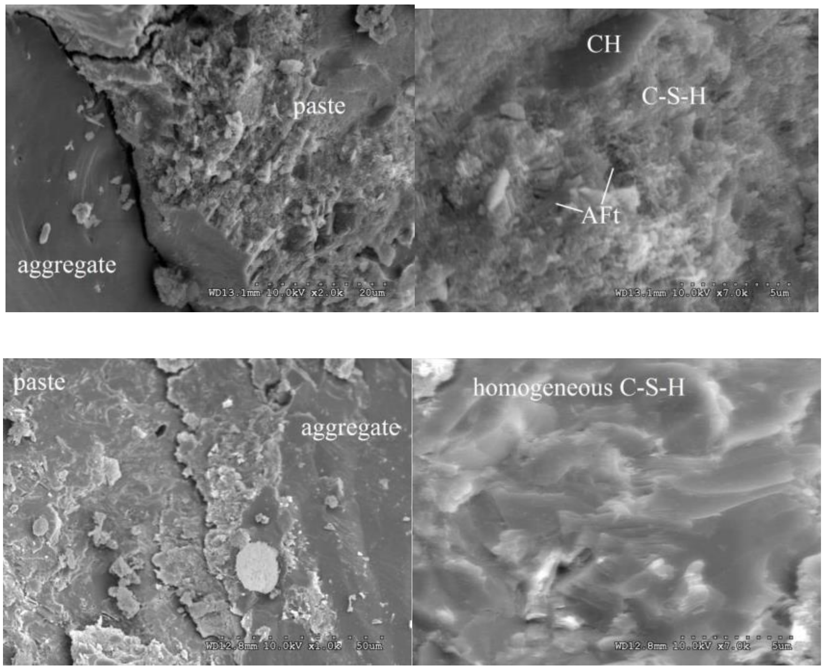

Figure 2.60. Micro structure morphology at the ITZ (Hongjian *et al.* 2014)

Compressive strength increased regardless of testing age with the increase of NS content as a result of both filling effect and pozzolanic reaction. These effects by which the porosity is refined and crystal size reduced are more pronounced in ITZ.

Water penetration depth reduced specially for 0.3% NS concrete at 28 days and continued noticeably at 91 days for 0.9% NS concrete. These can be interpreted as the agglomeration of high content of NS for first case and continuously modification of microstructure with NS for the second result.

Increase in NS percentage affected mainly the secondary sorptivity and both initial and secondary sorptivity were influenced at 91 days age. It was again due to blockage of connectivity and size reduction of voids via filling or pozzolanic reaction.

RCM results were very similar to those of water penetration depth. Meanwhile, the chloride content of each depth in chloride diffusivity was higher than OPC. The results were in consistence with RCM in the matter of agglomeration and NS content.

Yu *et al.* (2014) used NS to study its effects on UHPC with a low binder amount. Due to this fact that cement production is responsible for 7% of the total anthropogenic emission of carbon dioxide, it seems reasonable to focus on such particles to produce concretes with less clinker consumption together with better durability and smaller cross section.

To further improvement in mechanical properties short straight steel fibers applied alongside the slurry NS in the mixes.

According to the importance of an optimal packing in mechanical and durability, different models such as LPDM, SSM or CPM reviewed and Modified Andreasen & Anderson Model finally used in this research.

$$P(D)=(D^q-D^q_m)/(D^q_{max}-D^q_{min})$$

Ds are the particle size in µm and P(D) is a fraction of total solids smaller than D. Distribution modulus, q, is taken greater than 0.5 for coarse mixtures and smaller than 0.25 for fine ones. Meanwhile, it is 0.22-0.25 for SCC and it is equal to 0.23 in this study. The NS content increased from 1% to 5%. The increased NS resulted in linear decrease of slump flow because of the raised demand for water which reduced the amount of lubricating water.

The increased viscosity limited the easily scape of air from mix and raised the air content. However, the increase of NS, of course up to 4%, reduced the porosity through nucleation effect.

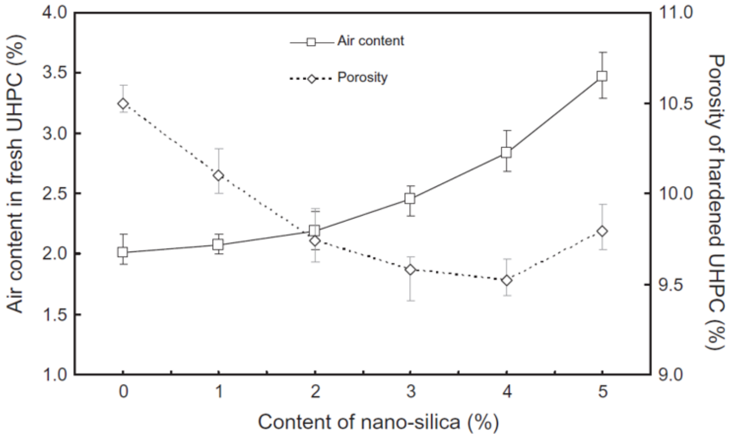

Figure 2.61. Air content and porosity of UHPC with different amount of NS (Yu *et al.* 2014)

There was a parabolic growth tendency in either flexural or compressive strength by increasing content of NS.

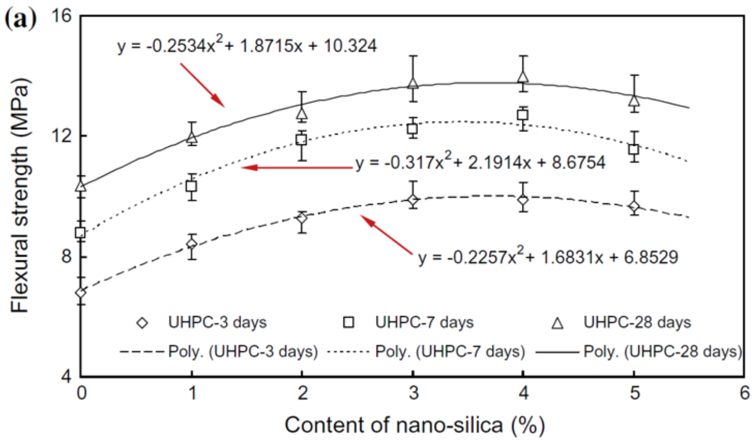

Figure 2.62. Variation of flexural strength of UHPC as a function of NS (Yu *et al.* 2014)

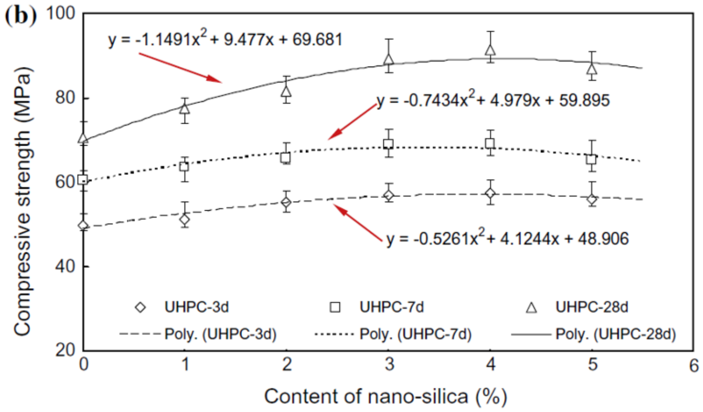

Figure 2.63. Variation of compressive strength of UHPC as a function of NS (Yu *et al.* 2014)

Since the hydrate products diffuse and envelop nanoparticles like kernels a reduction in time to reach the maximum rate observed in calorimetry test results with increase of NS. It was a compensation for dormant period for reference samples.

There were three main peaks in the vicinity of 105, 450 and 800°C attributed to the evaporation of free water, decomposition of calcium hydroxide and decomposition of $CaCO_3$, respectively. The lowest free water and ettringnite loss of reference mix rose as NS increased whereas the largest $Ca(OH)_2$ loss of this mix decreased by reduction of NS. All these can be interpret by two way: First, promotion of hydration to produce more products by NS. Second, NS reaction with $Ca(OH)_2$ to produce more C-S-H.

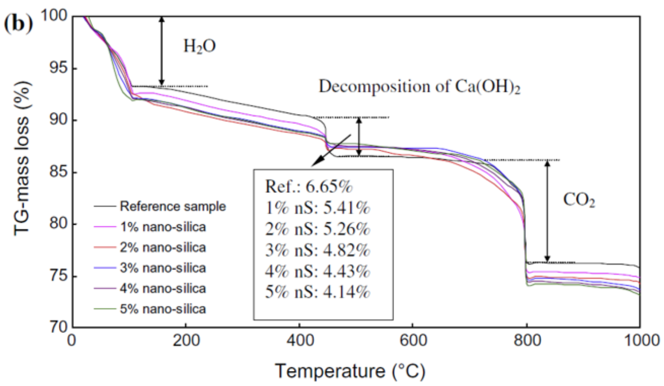

Figure 2.64. TG (mass loss) curves for UHPC with different NS amount (Yu *et al.* 2014)

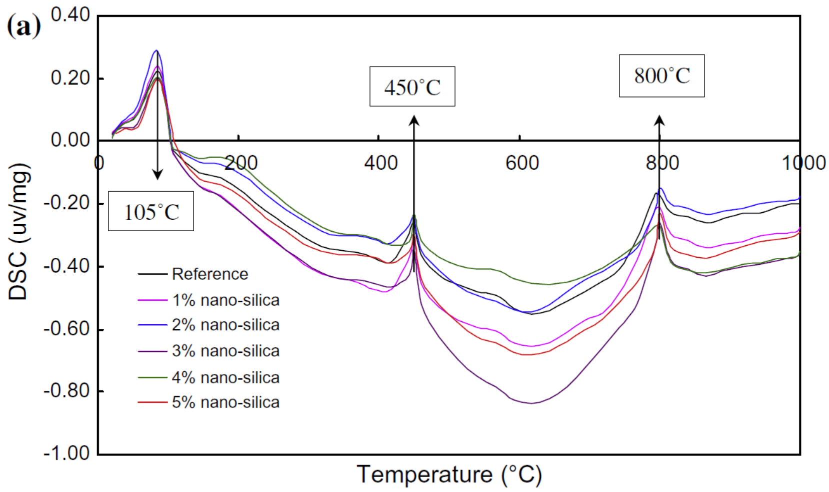

Figure 2.65. DSC (deferential scanning calorimetry curves for UHPC with different NS amount (Yu *et al.* 2014)

Combining results from calorimetry and thermal tests, it concluded that the dormant period caused by utilization of SP can largely be compensated by promotion impact of NS.

This figure presents the nucleation mechanism of NS. Normal cement grains grow thicker and initial hydration is limited to the surface due to difficulty of ionic transfer between the unhydrated cement grains and surrounding solution which results in higher porosity and lower strength.

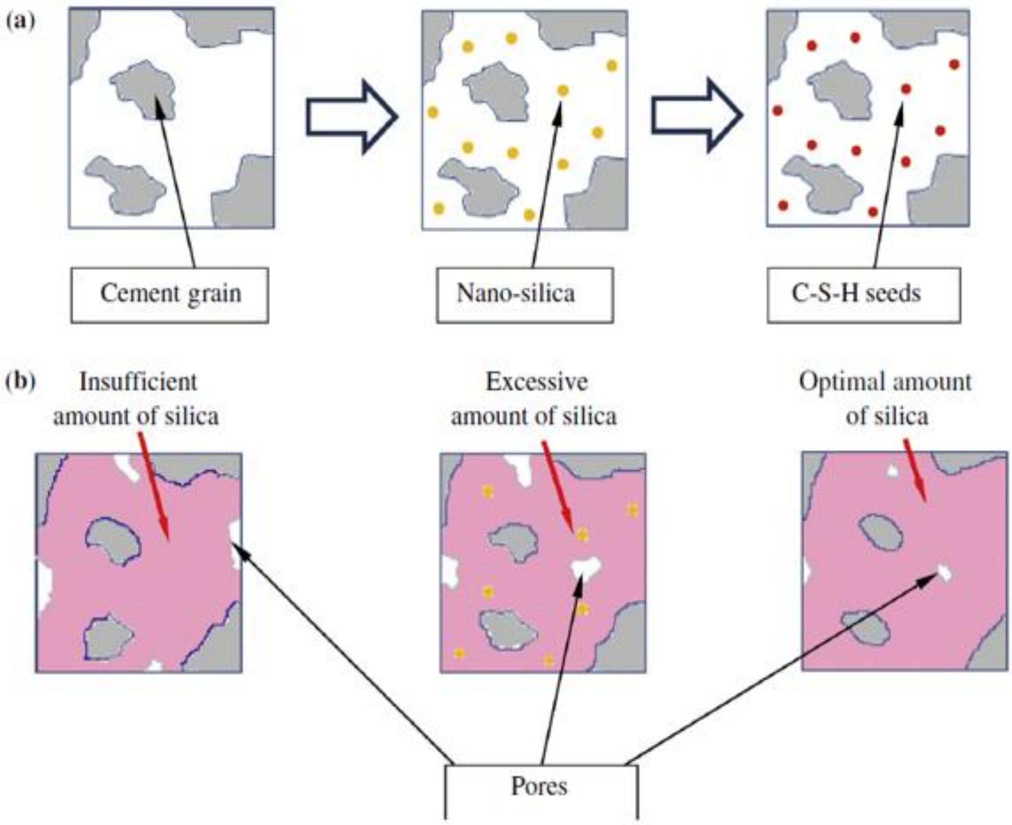

Figure 2.66. Schematic diagram of nucleation effect of NS on UHPC (Yu *et al.* 2014)

But formation of C-S-H is no longer limited to the grain surface in presence of NS which cause early pozzolanic reaction on the silica surface to produce C-S-H. It is evident from the SEM images that well developed calcium hydroxide plates are implying more porosity. Meanwhile, NS reaction with Ca(OH)2 has produced fine and foil like C-S-H. However, increasing NS from 4% to 5% has resulted in more air voids.

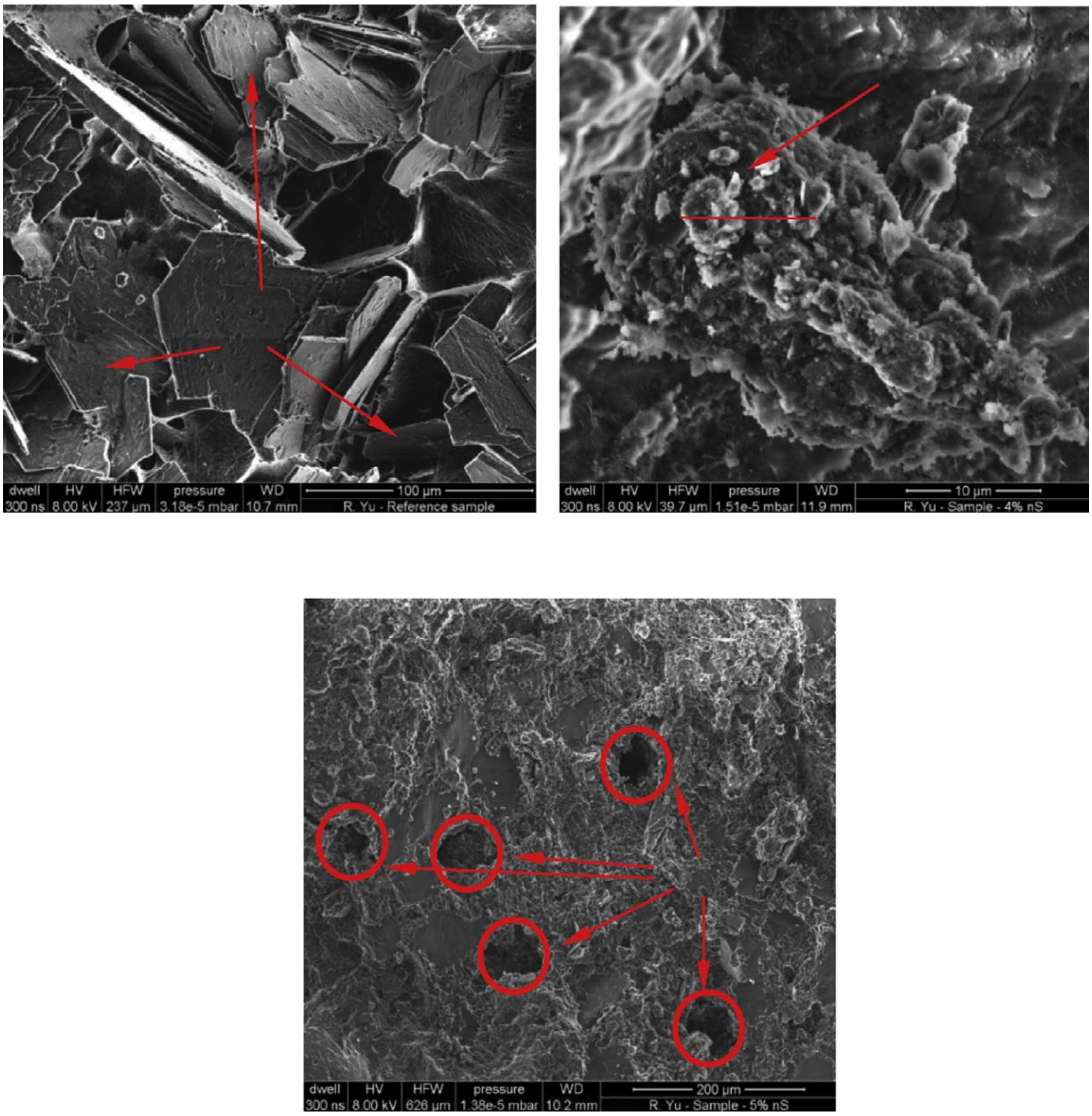

Figure 2.67. SEM images: (a) reference sample (b) UHPC with 4% NS (c) UHPC with 5% NS (Yu *et al.* 2014)

Behfarnia and Salemi (2013) compared the effects of nano-silica (NS) and nano-alumina (NA) on frost resistance of concrete. There were mixes containing 3,5 and 7% NS as well as 1, 2 and 3% NA. The compressive strength of the samples increased by inclusion of NS up to 5% but there was a reduction in 7% NS. As mentioned before, by commence of hydration products diffuse to envelop NS like a kernel and restrict the crystallization of calcium hydroxide to increase strength. The more increase in NS decrease the distance between them to reduce the ratio of crystal to gel to produce a loose matrix and reduce the strength. The strength reduction may also be attributed to the agglomeration phenomenon which produce a large weak zone in matrix. Due to high reactivity of NA and its particle packing recovery effect, mixes gained higher strength by increasing NA.

Water absorption test results complying with ASTM C642 revealed a remarkably lower permeability with these nanoparticles.

Frost resistance test by different cycles conducted in accordance with ASTM C666A through measuring the decrease in compressive strength, length change, mass loss and increase in water absorption. A much lower strength loss observed for concretes containing nanoparticles. It was true again with respect to the length change and mass loss and water absorption regarding the better performance of NA in frost resistance. However, ignoring the surpass NS effects, NS was better in strength gaining.

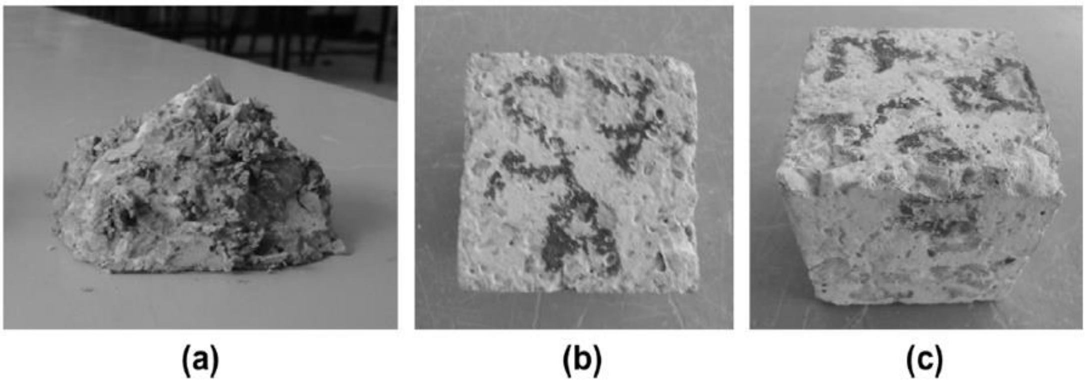

Figure 2.68. After 300 cycles of freeze and thaw (a) control sample (b) sample with 5% NS (c) sample with 3% NA (Behfarnia and Salami 2013)

As an alternative nanoparticle, nano-CuO (NC) addition in SCC investigated by Nazari and Riahi (2011). Two series of samples prepared. The first included dosage of polycarboxylate SP between 0 and 1%. The second contained NC of 1-5% in addition to 1% SP. In first series compressive strength dropped by SP rising which could be attributed to the creation of greater CH crystals in presence of SP. Compressive strength increased as expected by increasing the NC. However, NC content above 4%

demonstrated an inferior effect on strength. Moreover, the total specific pore volume and pore dimension fell in the range of low harm-pore. The reasons for superior and inferior effects discussed similar to previous works such as filler effect and nucleation and pozzolanic reaction or inappropriate distance between particles. Acceleration of peak time and drop in heat release rate fallowed the same order in thermal tests.

The same researchers, Nazari and Riahi (2010), investigated the effects of NS on SCC from different points of view. The mixes were in an identical condition with previously mentioned work. Just, the NC was substituted with NS in SCC.

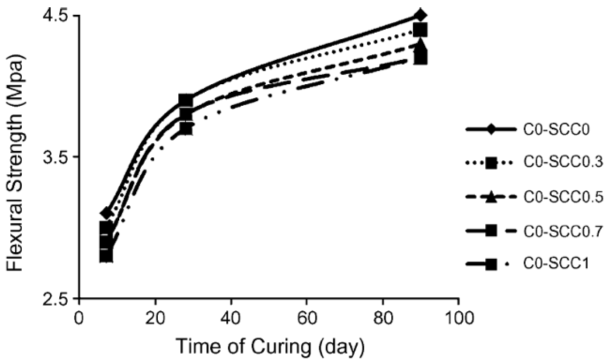

Figure 2.69. Flexural strength of specimens with SP (Nazari and Riahi 2010)

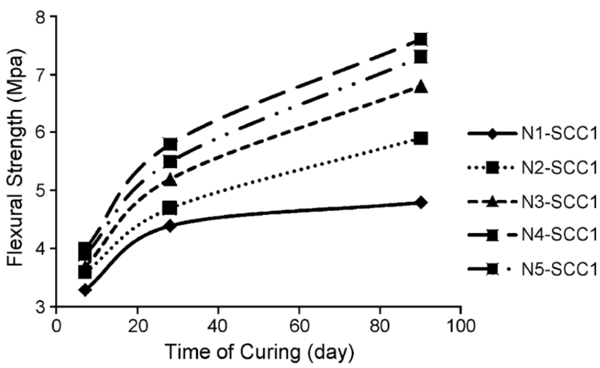

Figure 2.70. Flexural strength of specimens with NS (Nazari and Riahi 2010)

As it is obvious from the figures above, the all results about the flexural strength amazingly is similar to those of compressive strength in previous work of them. Even the optimal percentage of NS in SCC is 4% similar to NC in prior work. The influence of NS here is the same as with NC. Thermal tests gave similar results as well. This similar influences in two different work with different nanoparticles seems a little odd and more investigations may be necessary.

Qurica *et al.* (2014) carried out a research about the influence of addition of 3.8% nano-silica particles with same PSD but different production methods, colloidal NS suspension and powder NS, on mechanical properties and durability of SCC. Characteristics of utilized materials are given in figure and table below.

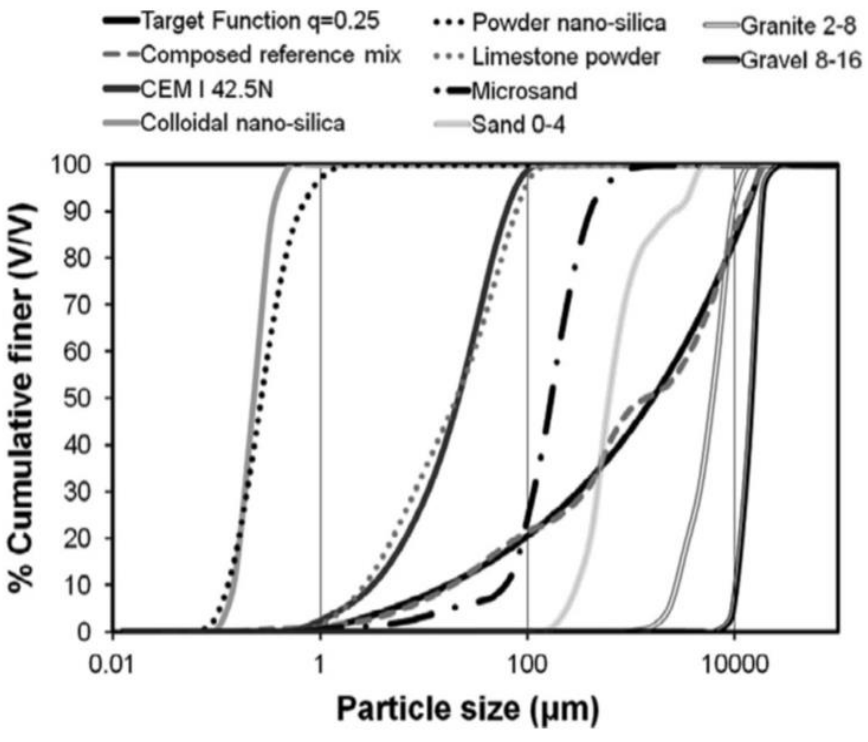

Figure 2.71. PSD of used materials (Querica *et al.* 2014)

Table 2.13. Properties of the used materials (Qurica *et al.* 2014)

Materials	Specific density (g/cm^3)	BET (m^2/g)	pH	Solid content (%w/w)	Loss in ignition (LOI)	Computed SSA (m^2/m^3)
CEM I 42.5n	3.14	1	-	-	2.8	1 699 093
Colloidal NS	1.40	50	9.5	50	-	46 110 081
Powder NS	2.15	56	5.0	-	0.5	48 175 461
LSP	2.71	-	-	-	-	1 234 362
Microsand (sandstone)	2.64	-	-	-	-	193 514
Sand 0-4	2.64	-	-	-	-	14 251
Granite 2-8	2.65	-	-	-	-	1740
Granite 8-16	2.65	-	-	-	-	515
SP	1.10	-	7.0	53	-	-

Initially, the fresh properties assessed in accordance with EFNARC. Apparent from the results presented in table below, flow class of all mixes was in the required range, emphasizing the vicinity of the mix containing colloidal NS to the lower limit. All but the reference mix fulfilled viscosity class. Higher air content due to inclusion of nanoparticles with high SSC was obvious again as a result of increased viscosity.

Table 2.14. Properties of the prapered SCC mixes in fresh state (Qurica *et al.* 2014)

Value	Reference	Cooloidal NS	Powder NS
SF (mm)	690-720	664-701	685-720
VF	35	20.5	24.5
Fresh density (g/cm^3)	2.399	2.384	2.392
Air content (V%)	1.15	1.79	1.58
Paching density (%)	83.55	82.91	83.12

As the second point, hardened properties was under investigation. The mix with colloidal NS demonstrated the highest compressive strength except first day but the gain rate was pretty low after 28 days due to early consumption as a result of higher reactivity. Some other interesting results obtained. The mix with powder NS showed interestingly a similar compressive strength to the reference mix at 7 days and colloidal NS presented a higher standard deviation.

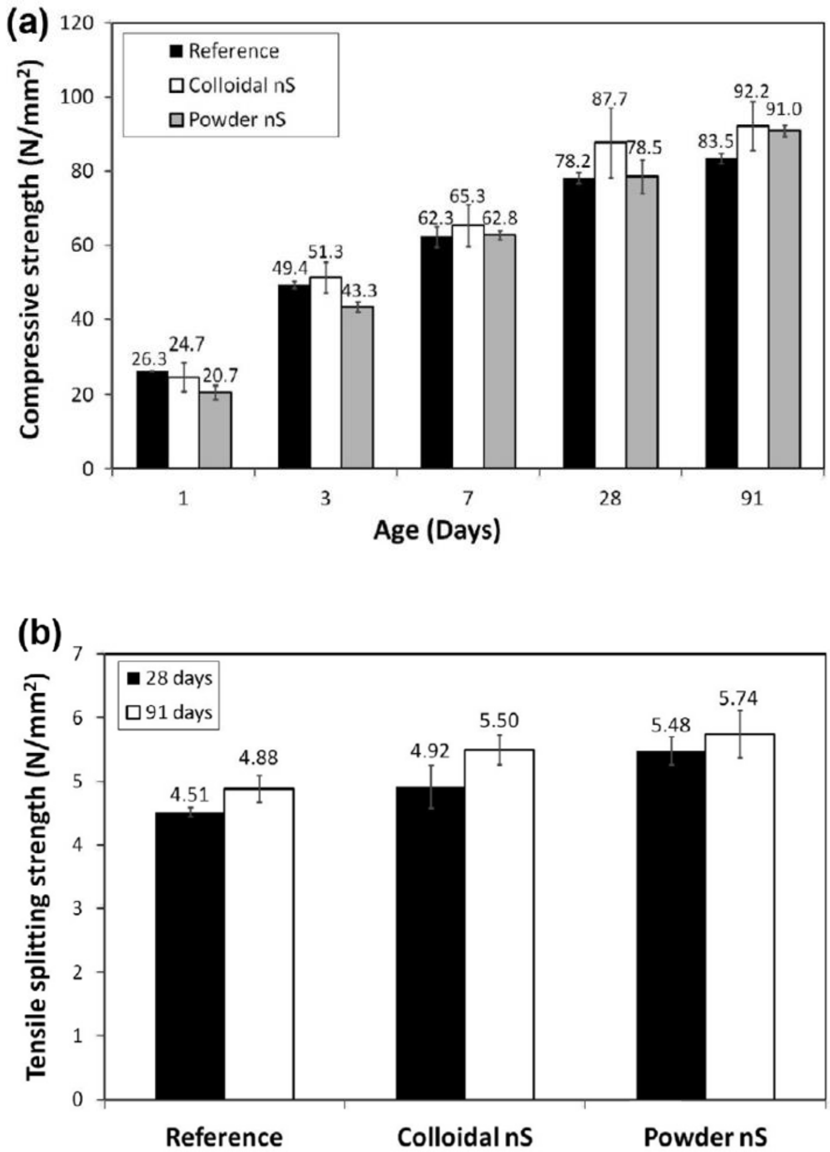

Figure 2.72. Mechanical properties of tested SCC mixes (Querica *et al.* 2014)

Precipitation of smaller and stiffer C-S-H together with acceleration of hydration results in a remarkable improvement in ITZ which is the main cause of higher tensile strength with NS. It is noticeable that less reactivity of powder NS leads to a better wet packing due to lower viscosity to provide an improved bond between matrix and aggregates.

Regardless of slightly higher total porosity of SCC mixes containing NS, the results suggested a considerable decrease in water penetration. In other words, NS modifies the pore structure to a finer and lesser interconnected system as found out in some researches.

MIP test was carried out to support the findings. The results revealed reduction in median pore diameter by both volume and area as well as average pore diameter. The bulk density and apparent density increased. Additionally, an increment in dead-end and ink-bottle shape pores versus cylindrical ones demonstrated improvement in effective porosity.

The results of the RCM and conductivity tests declared a significant reduction in both. The degree of conductivity or its inverse value, resistivity, not only is in a close relation with other pore structure factors such as tortuosity or connectivity, but also can be considered as an estimation facility for compressive strength in a high level of reliability. On the other hand, the RCM test results was promising a longer service life by a similar reduction which proved in chloride diffusion test. The better performance of colloidal NS was emphasized due to its higher reactivity.

In freeze-thaw resistance test, the reference SCC mix surpassed the recommended value of scaling criteria which is 1.5 kg/m^2 at 28 cycles at the 11_{th} cycle. While the mixes containing NS remained lower than this value until 48 cycles.

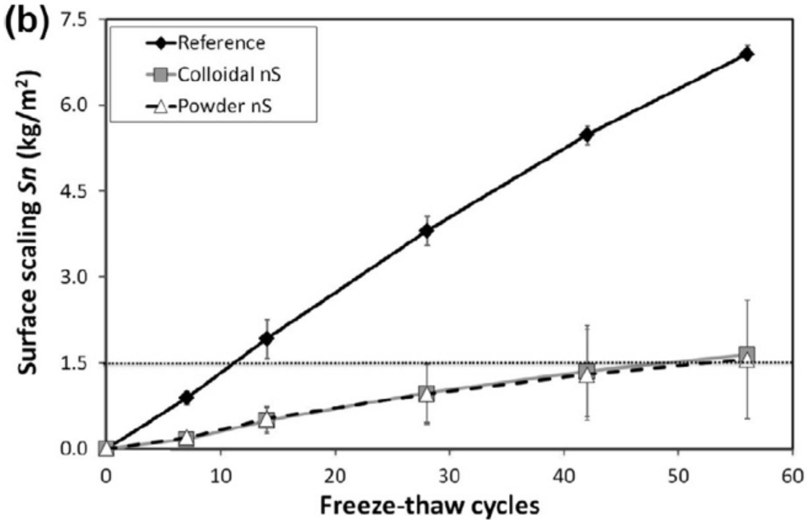

Figure 2.73. Cumulative scaling factor after 56 freeze-thaw cycles (3% NaCl solution) (Querica *et al.* 2014)

It can explained due to stiff C-S-H gel and refined pore structure with higher tortuosity and constrictivity. However, it is important to notice that the air entrainment is needed to achieve a good resistance to frost.

Shaikh *et al.* (2014) inspected the influence of different dosages of NS with various percentage of replacement of fly ash in both high volume fly ash (HVFA) concretes and mortars. The necessity of utilization of SCMs well discussed before and their inferior impacts in early age pointed out. The merit of this study was due to investigation of compensatory effects of NS as HVFA is applied.

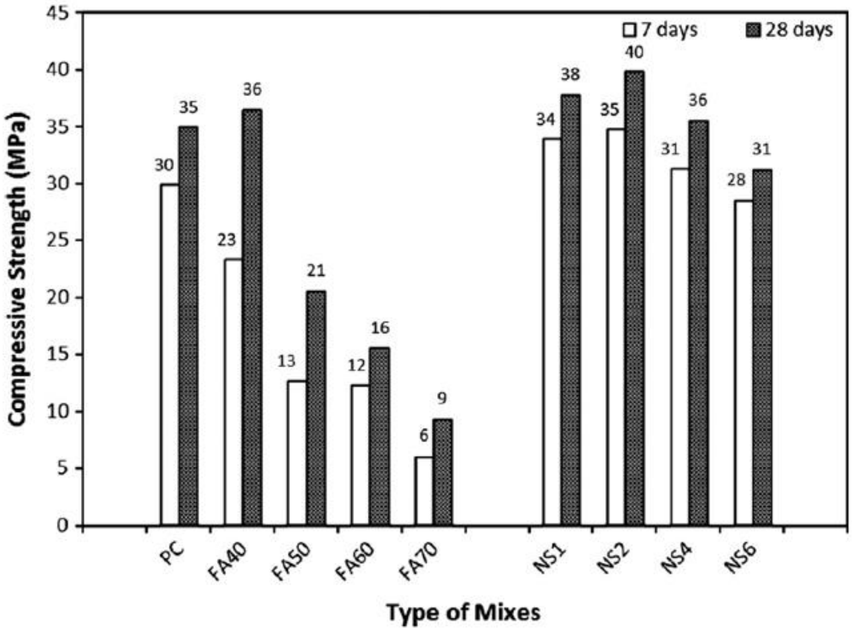

Figure 2.74. Compressive strength of mortars containing nS and fa (Shaikh 2014)

At first step, two series of mixes including 40-70% FA and 1-6% NS were prepared. 40% for FA and 2% for NS was found to be best with respect to compressive strength in first and second series, respectively. This 2% optimal NS content applied in HVFA mortars. It is evident from the figure that compressive strength of mortars with 60-70% FA are significantly influenced.

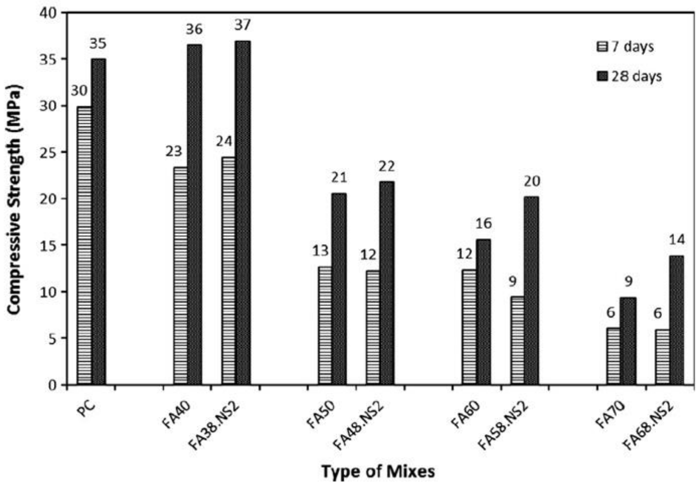

Figure 2.75. Effects of 2% NS on compressive strength of mortars containing HVFA (Shaikh 2014)

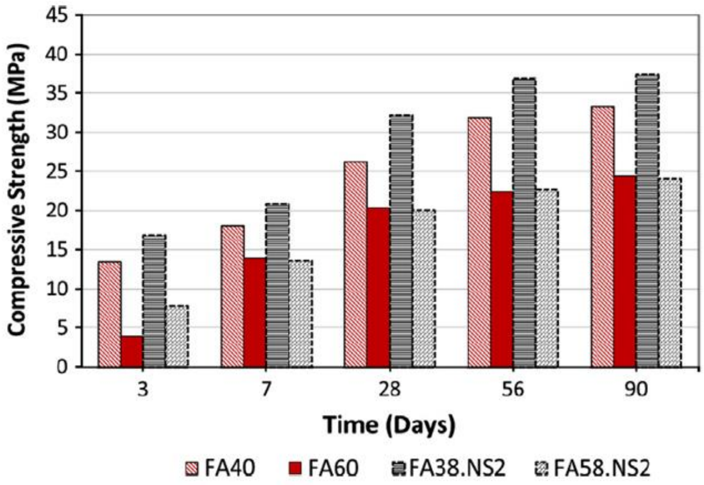

Figure 2.76. Effects of 2% NS on compressive strength of HVFA concretes containing 40% and 60% FA (Shaikh 2014)

In context of concrete, the influence of 2% NS was outstanding for 60% FA but it did not continued for later ages to the extent that in 7 days a slight reduction observed in consistence with mortar counterpart. Meanwhile, the results were promising for 40% FA.

SEM images demonstrated many spherical unreacted FA particles and voids in 40% whereas inclusion of 2% NS provided a denser microstructure with no voids due to formation of secondary C-S-H.

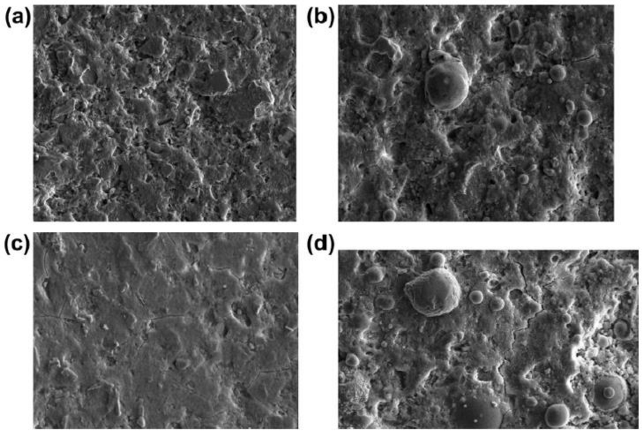

Figure 2.77. SEM images of (a) control paste (b) paste containing 40% FA (c) paste containing 2% NS (d) paste containing 38% FA and 2% NS (Shaikh 2014)

In backscattered electron (BSE) images, a useful method to identify the constituent phases, unhydraed cement particles, voids/cracks and CH/C-S-H/other hydration products are implied by brightest/white, dark/black and gray/dark gray colors, respectively. There are many white and black areas in mixes containing 40 and 60% FA indicating unhydrated cement particles, FA particles or voids and cracks despite of the counterpart mixes including 2% NS which consumed the calcium hydroxide.

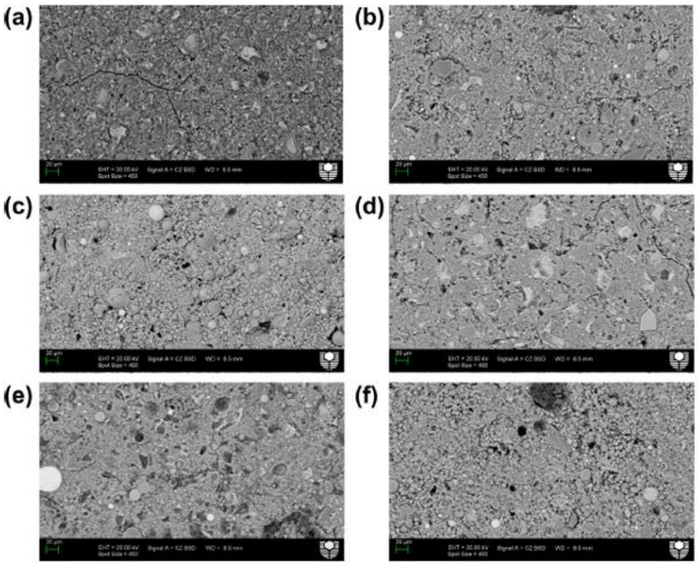

Figure 2.78. Backscattered electron (BSE) images of
(a) cement paste (b) paste containing 40% FA (c) paste containing 60% FA (d) paste containing 2% NS (e) paste containing 38% FA and 2% NS (f) paste containing 58% FA and 2% NS (Shaikh 2014)

According to X-ray diffraction (XRD) analysis, CH, C_2S/C_3S and SiO_2 are in majority. In both 3 and 28 days aged samples, the reduction in peak related to CH is obvious which indicates the early pozzolanic reaction of NS and consumption of CH. It is important to notice that due to its amorphous makeup, concentration of C-S-H is indirectly measured by CH since radiation will not diffract into measurable peaks for C-S-H.

Since agglomeration is the main problem with utilization of nanoparticles, both mechanical and ultrasonic methods with different NS percentages were used to focus on the effectiveness of these methods on dispersion process. The results not only did not revealed any improvement in compressive strength of the mix by different period of ultrasonicaction, but also there was a 10 % reduction in compressive strength.

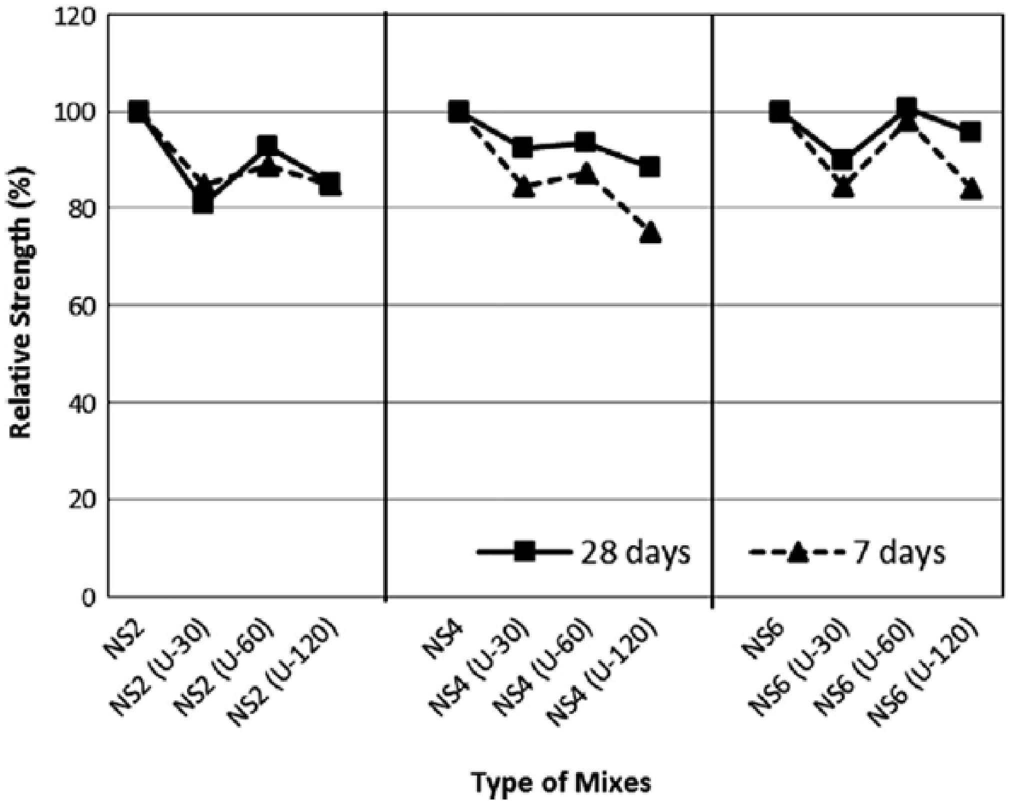

Figure 2.79. Effect of ultrasonic mixing of NS and its time on the strength development of mortars containing different NS contents (Shaikh 2014)

Zhang *et al.* (2014) tried to clarify the effects of steel fibers on the flexural toughness of HPC containing both FA and NS. The two methods of making HPC meet the special performance and uniformity requirements, addition of SP and SCMs, are used in this study. The proportions were 15% FA, 5% NS and 0.5-2.5% steel fiber. Three-point bending method was used in accordance with ASTM C1018 and DBV-1998.

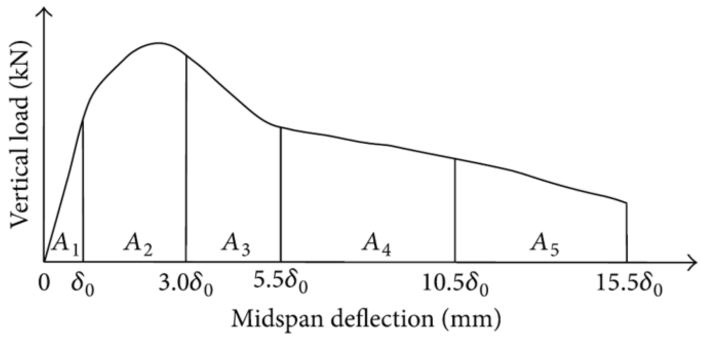

$$I_5, = \frac{A_1 + A_2}{A_1},$$

$$I_{10} = \frac{A_1 + A_2 + A_3}{A_1},$$

$$I_{20} = \frac{A_1 + A_2 + A_3 + A_4}{A_1},$$

$$I_{30} = \frac{A_1 + A_2 + A_3 + A_4 + A_5}{A_1},$$

Figure 2.80. Calculation diagram for flexural toughness of ASTM method (Zhang *et al.* 2014)

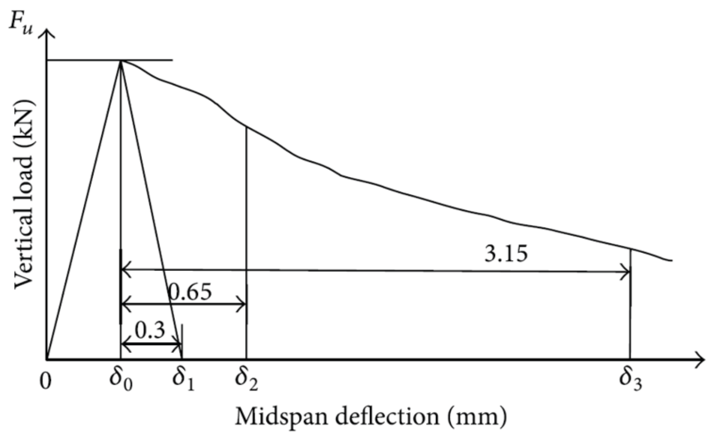

$$f = \frac{F_u l}{bh^2},$$

$$F_{eq,1} = \frac{D_1^f}{0.5},$$

$$f_{eq,1} = \frac{F_{eq,1} l}{bh^2},$$

$$F_{eq,2} = \frac{D_2^f}{3.0},$$

$$f_{eq,2} = \frac{F_{eq,2} l}{bh^2},$$

Figure 2.81. Calculation diagram for flexural toughness of DBV (Zhang *et al.* 2014)

It is clearly evident from the results that all parameters such as different flexural toughness indices, variation coefficient of bearing capacity, deformation energy and equivalent flexural strength increase by increment in steel fiber content up to 2%. Thus, the optimal percentage of steel fibers is determined to be 2% by which the all flexural indices not only increase but also meet the limits of ideal elastoplastic material.

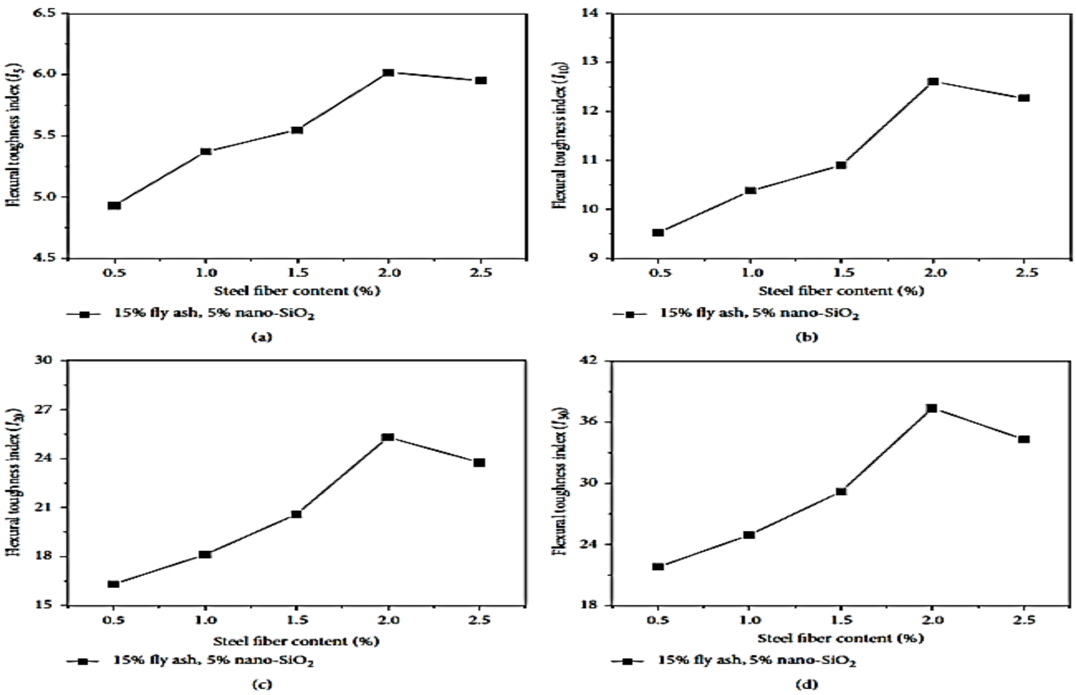

Figure 2.82. Effect of steel fiber content on flexural toughness indices (Zhang *et al.* 2014)

All these were in consistence with diagrams of vertical load versus mid-span deflection which were growing plumper by the increase of fiber content up to 2% and then got thinner by 2.5 % of steel fibers.

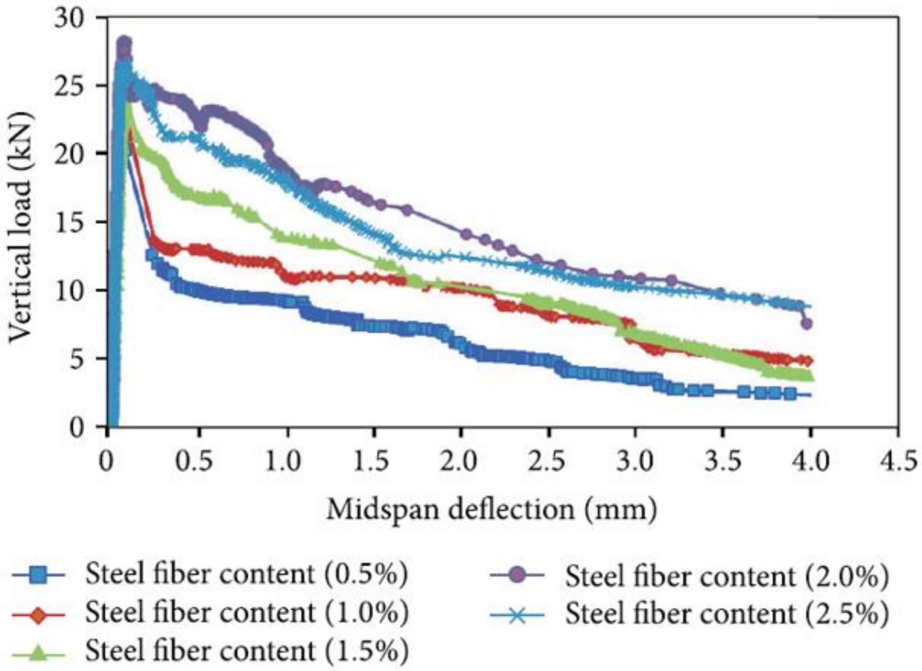

Figure 2.83. Contrast of "P_v-δ" curves of different steel fiber content (Zhang *et al.* 2014)

Wang *et al.* (2014) conducted a research to find out how MWCNT can influence the mechanical properties and durability of concrete. Despite of the superior properties achieved by mix through addition of CNTs, the two main related challenges remain considerable, hydrophobicity and agglomeration. On the basis of previous researches, this study investigated either physical or chemical methods of correcting these defects.

Three factors considered to observe the effects on compressive strength:

- MWCNT percentage from 0 to 2 in 0.25% wt% steps
- w/c of 0.4, 0.5 and 0.75
- chemical treatments by 0.1% dosage, namely, gum arabic, propanol, ethanol, sodium polyacrylate, methylcellulose, sodium dodecyl sulfate, and silane.

Optimum sonication time of 12 minutes achieved prior to mixing whereas 1.25% considered the best dosage of MWCNT as well as 1% content of SP result in ideal compressive strength.

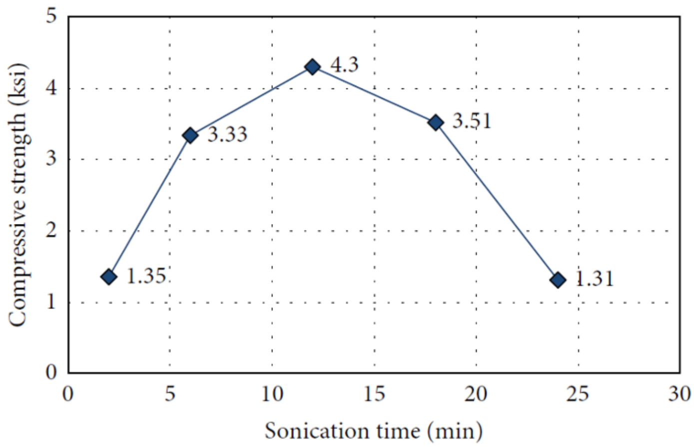

Figure 2.84. Effect of sonication time on MWCNT concrete compressive strength w/c = 0.5 & 0.75 (Wang *et al.* 2014)

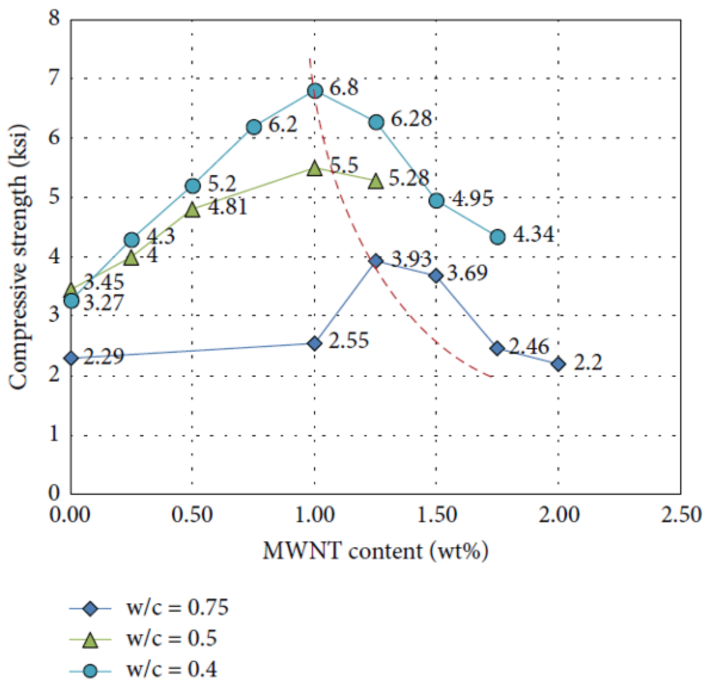

Figure 2.85. Compressive strength of MWCNT concretes with different w/c and MWCNT concentrations (Wang *et al.* 2014)

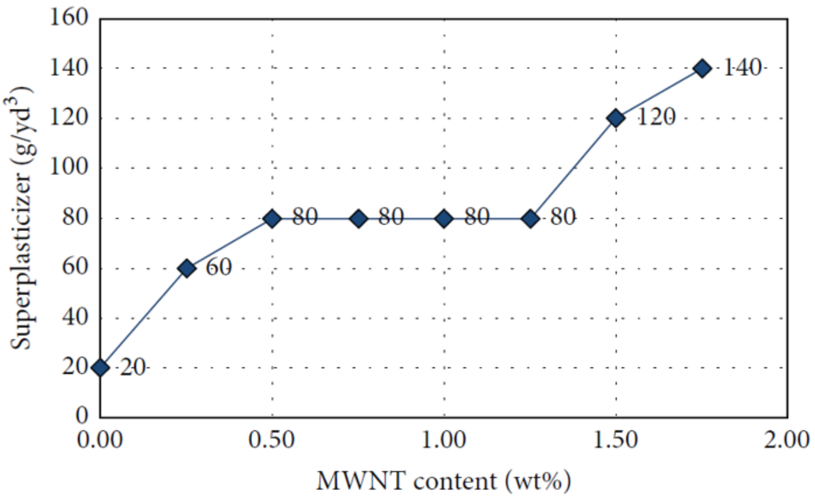

Figure 2.86. SP dosage (g/yd^3 at a w/c of 0.4 compared with the workability of fresh MWCNT concrete mixes (Wang *et al.* 2014)

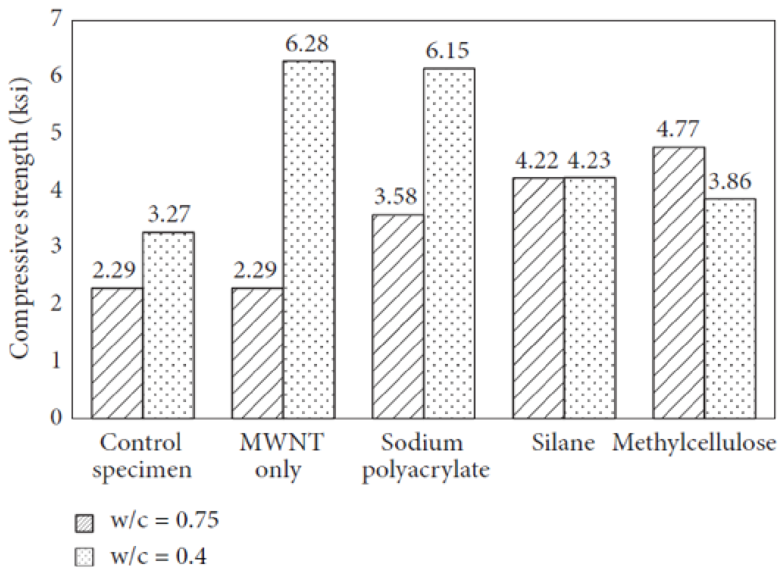

Figure 2.87. Effect of chemical treatments under two different w/c ratios (Wang *et al.* 2014)

Different chemical treatments investigated in various dispersion periods by w/c of 0.75. The best resulted ones compared with w/c of 0.4. It was evident that hydrophobicity of CNTs reduced the treatment effects of positively treating chemicals.

Three mixes with w/c of 0.4, MWCNT content of 1.25 wt% were treated by selected chemicals methylcellulose, sodium polyacrylate and silane to be subjected to durability tests. In ponding test based on ASTM C1543, sodium polyacrylate demonstrated the best results for chloride penetration. Moreover, in freeze-thaw test complying with ASTM C666, this chemical treatment found to be the most effective, again.

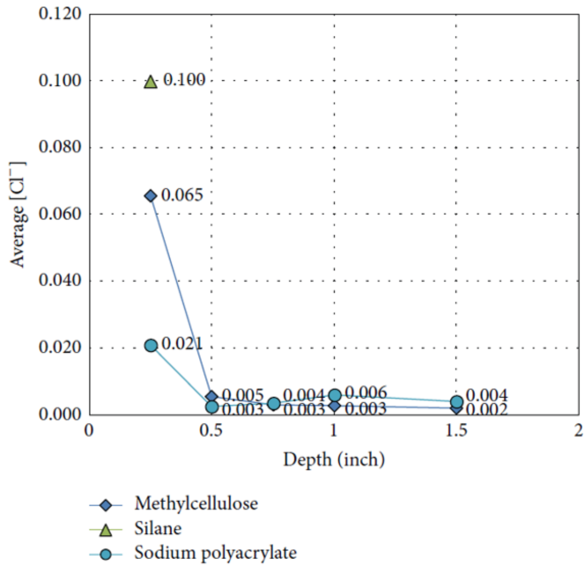

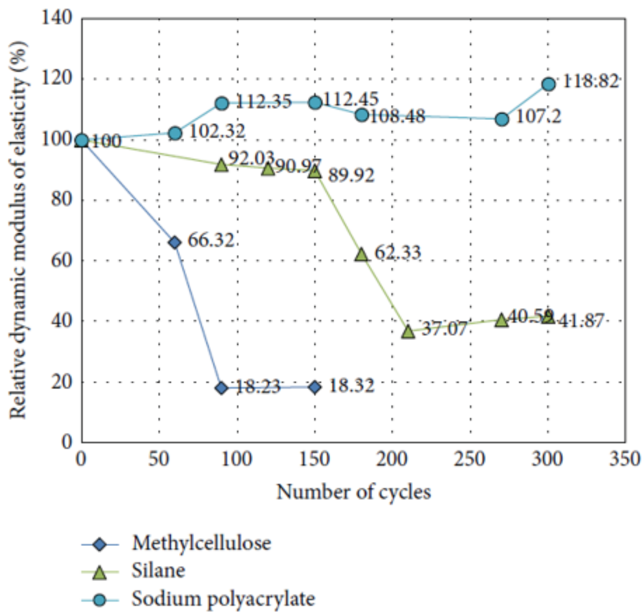

Figure 2.88. Chloride ions at different concrete depth and relative dynamic elastic modulus arising from different chemical treatments

The enhancing influence of different steel fiber ratios even on flexural strength of natural light weight aggregate concrete recorded by Duzgun *et al.* (2005)

Sahmaran *et al.* (2005), investigated various properties of HVFA self-compacting concrete containing hybrid fiber reinforcement. The decreasing effect of high proportion of fly ash on water demand of fresh state and compressive strength of hardened state verified in addition to other findings.

Banthia *et al.* (1995), investigated test methods for flexural toughness characterization of FRC which can be completely helpful in studies including such tests. ASTM C 1018 and JSCE S-F4 studied and compared and a new method was suggested. A number of very important concerns which emphasized in the article were:

- measuring true specimen deflection due to seating or twisting
- locating the first crack
- instability after peak load

Besides the suggested new method the usage of LVDT and Yoke was strongly recommended.

However, Nataraja *et al.* (2000) concluded that the JSCE approach is preferable due to its simplicity in characterization of flexural toughness.

3. EXPERIMENTAL STUDY

According to several studied articles from different researchers along with various available codes and guidelines, it can be concluded that SCC encompass a vast variety of materials, proportions and methodologies. In this thesis, the influence of nano silica and carbon nano tube on fresh properties, compressive strength and flexural toughness of self-compacting concrete containing fly ash has been investigated. According to previous studies, the best dosage for each particle was chosen to be used in solo and binary compositions in mixtures with and without fly ash. Conflicting results obtained to determine the optimal percentage of both SCMs and nanoparticles. Comparing fulfilled researches and referring to the study conducted by Shaikh *et al.* (2014) on influence of different dosages of NS and FA on HVFA NVC concretes and mortars, 2% NS and 40% FA proportions selected. Assessing various works again and using the graph provided in study conducted by Ferro G. re al. (2011) the proportion of CNT decided to be 0.08%.

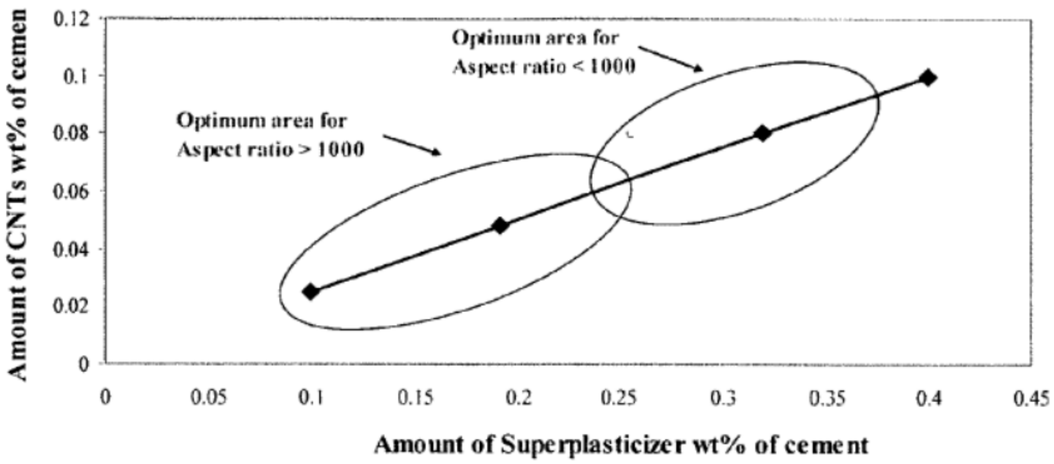

Figure 3.1. Optimum amounts MWCNT (Ferro 2011)

3.1. Materials of Study

3.1.1. Aggregates

Crushed 0-4 mm sand and 4-16 mm gravel was provided from Erzurum Ready Mix and Ilmi Ready Mix Concrete companies in Erzurum/Turkey as fine and coarse aggregates according to availability. Tables 3.1 and 3.2 present sieve analysis and physical properties of used aggregates and Figure 3.2 illustrates their grading curves. TS 706 and 802 used for this purpose. Minimum and maximum aggregate size of experiment were 4 and 16 mm whereas 4mm was the border size between fine and coarse aggregates. Proportion of fines was 62% and 38% for that of coarse ones.

Table 3.1. Sieve analysis of aggregates

Sieve Number (mm)	31,5	16	8	4	2	1	0,5	0,25	0,125	0,063	Remained
Passed (%)	100	100	80	62	47	37	18	8	4	2	0

Table 3.2. Properties of aggregates

Properties	Fine Aggregate	Coarse Aggregate
Fineness Modulus	1,64	5,65
Dry Weight	2,53	2,55
Cleaned Dry Weight	2,57	2,61
Specific Gravity	2,55	2,57
Absorption %	1,1	1,3

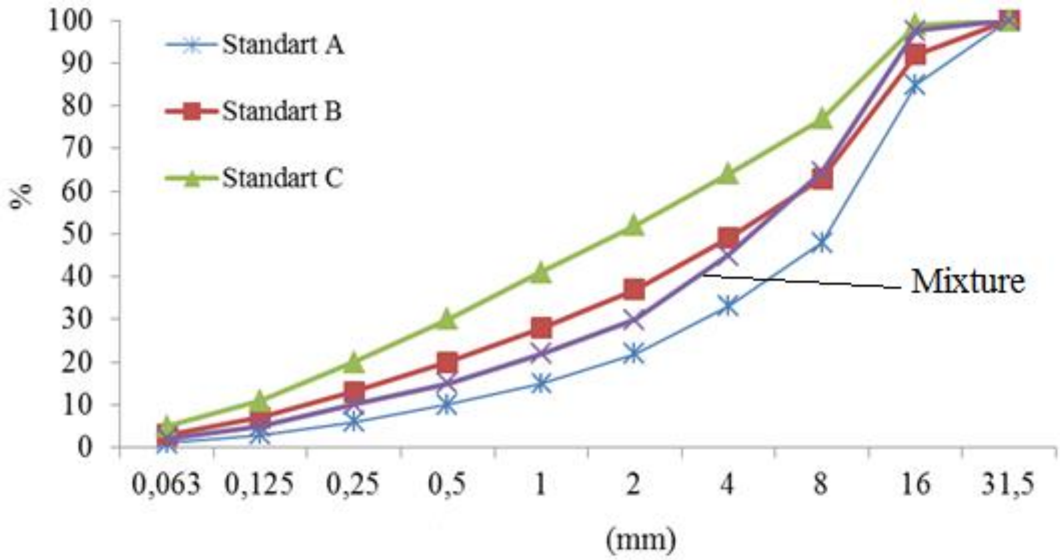

Figure 3.2. Grading curves of aggregates

3.1.2. Cement

In this study, an ordinary Portland cement (CEM I 42.5 R) produced by Askale cement factory in Turkey, used in all mixes. The all physical and chemical properties which are shown in tables below controlled according to TS EN 197/1.

Table 3.3. Chemical compositions of cement

CaO (%)	61,80
SiO_2 (%)	18,89
Al_2O_3 (%)	4,40
Fe_2O_3 (%)	3,46
MgO (%)	3,89
SO_3 (%)	2,97
K_2O (%)	0,59
Na_2O (%)	0,22
Cl^- (%)	0,0111
LOI (%)	3,14
Remain (%)	1,02
%45 µ	4,59

Table 3.4. Physical properties of cement

Day	Compressive Strength
2	26.7
7	-
28	55.9
Properties	Fine Aggregate
Specific Gravity (gr/cm^3)	3.13
Blaine Fineness (cm^2/gr)	3857

3.1.3. Water

Normal laboratory tap water complying with TS EN 206 and 1008 used for either producing or curing of all concrete mixtures.

3.1.4. Admixture

To achieve its particular plastic and hardened properties, presence of admixtures such as super plasticizers found necessary. A polycarboxylic ether base highperplacticizer of Draco Company was used to reduce water demand of mix and increase workability as is normal in SCCs. The proportion of hyperplasticizer was 2% in all mixes. Following table mentions all technical properties.

Table 3.5. Properties of hyperplasticizer

Properties of Hyperplasticizer	
Name	Draco-Levelcon FX10
Color	Light yellow
State	Liquid
Specific Gravity	1.023 – 1.063 kg/litre
Chloride content %(EN 480-10)	<0.1
Alkali content % (EN 480-12)	< 3

3.1.5. Fly ash

Owing to their fine particle size and high pozzolanic reactivity, SCMs demonstrated positive impacts on workability, mechanical properties and durability of SCC. Meanwhile, the results were conflicting about the percentage of replaced SCMs with respect to their type, accompanying other additives or the field they were under investigation. Therefore, an exact study is necessary for each of them in various textures.

A class F fly ash of Bekirly Termik/Turkey factory with properties shown in table 3.6 was used in second category of SCC mixes. The limits are in accordance with TS EN 450 and ASTM C 618(1998) since SiO_2+Al_2O_3+Fe_2O_3 >70% and CaO<10% and the class is F.

Table 3.6. Properties of fly ash

Analysis	Unit	Method of analysis	Limits	Results
LOI	%	TS-EN 196-2	< 5	4,38
Fineness(Wet Sieving)	%	TS EN 451-2	< 40 (45 µ upon)	24,12
Activity Index(28 day/90 day)	%	TS EN 196-1	> 70 / > 80	78,3 / 92,4[a]
Free CaO	%	TS EN 451-1	< 2,6	< 0,1
SiO_2 + Al_2O_3 + Fe_2O_3 Total Content	%	TS EN 196-2	> 65	90,05
Total Alkali content	%	TS EN 196-2	< 5,5	2,413
Reactive SiO_2	%	TS EN 197-1	> 22	62,2
SO_3	%	TS EN 196-2	< 3,5	0,3
Chloride	%	TS EN 196-2	< 0,1	0,01
MgO	%	TS EN 196-2	< 4,5	1,42
Particle Density	kg/m^3	TS EN 196-6	2,015 < Value < 2,465	2,33
Setting Time(start/end)	min.	TS EN 196-3	Twofold of setting time of the test cement + 20 min.	245 / 310 (Ash) 155 / 200 (Cement)
Reactive CaO	%	TS EN 197-1	< 11	2,14

3.1.6. Nano silica

Nanoparticles and nanotubes influenced SCC significantly in different aspects. There were a vast range of nanoparticles used in SCC mixes. The fresh properties of mixes were evaluated by the methods describes mainly in EFNARC and similar guidelines. Packing effect and filling property of these ultra-fine particles which act as ball bearing made SCC to show better fresh properties. The reduced w/c ratio leaded to lesser bleeding and improved hardened properties. On the other hand, due to their fine particle size which increases the specific surface area to be more reactive, they intense and accelerate hydration process, consume portlandite, refine the pore structure and strengthen the matrix. The results of tests such as TGA, MIP, SEM, XRD, Conductivity, Diffusion or Penetration confirms these results. In this study, the provision of NS was from Nanosany Corporation with properties given in Table 3.7.

Table 3.7. Properties of silicon oxide nano-particle

Properties of SiO2	
Purity	99+%
APS	11-13 nm
SSA	200 m^2/g
Color	white
Bulk density	<0.10 g/cm^3
True density	2.4 g/cm^3

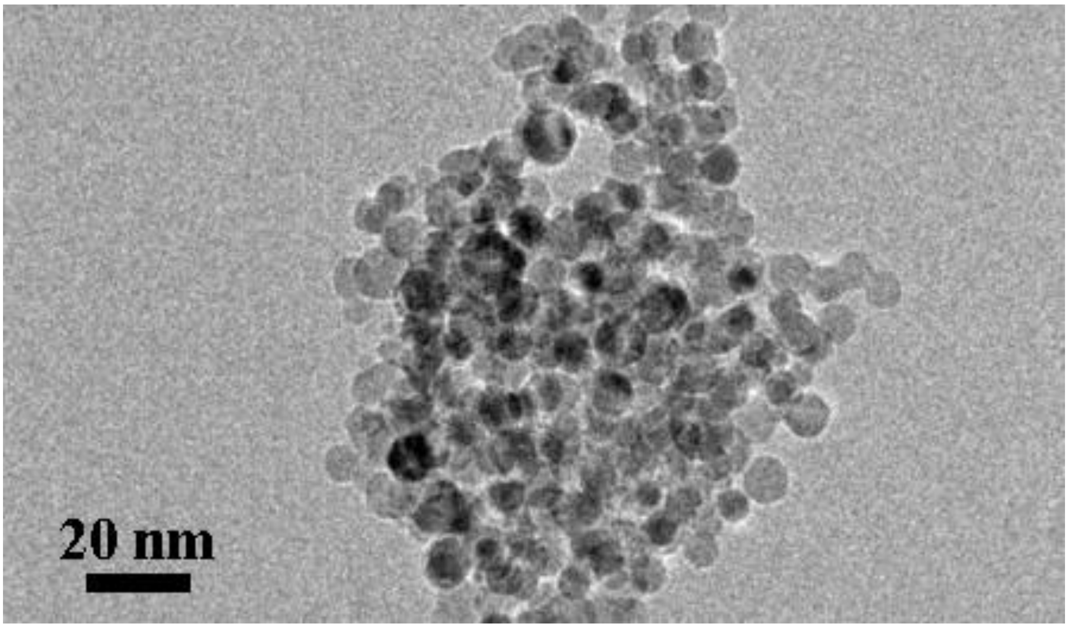

Figure 3.3. SEM image of silicon oxide nano-particle

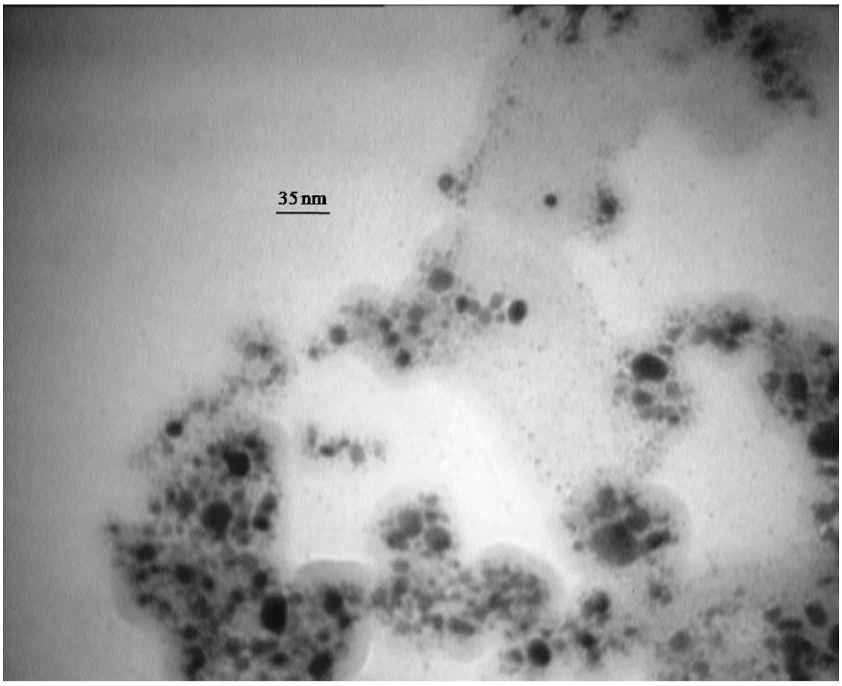

Figure 3.4. TEM image of silicon oxide nano-particle

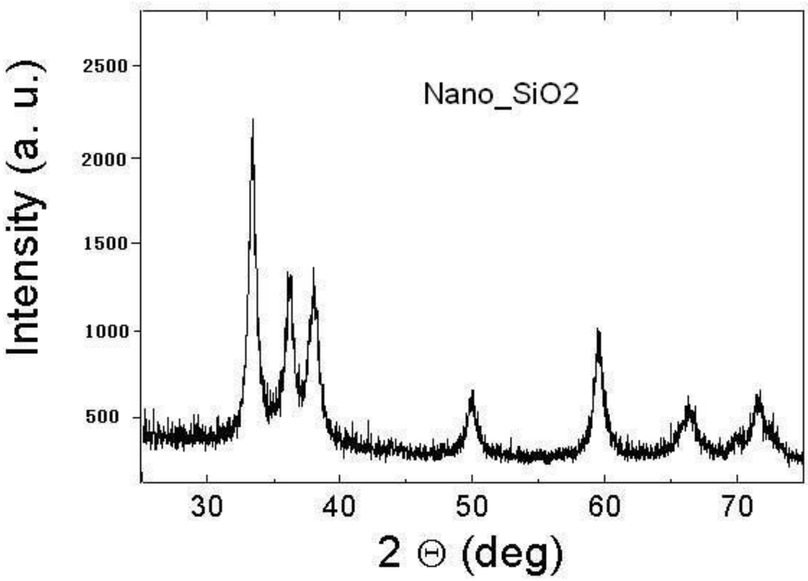

Figure 3.5. X-ray analysis of silicon oxide nano-particle

3.1.7. Nano carbon tube

Significant improvements observed by introducing steel fibers to mixes which include both nanoparticles and SCMs. Fibers improved flexural toughness indices or deformation energy of SCC mix which contains nano-silica and fly ash. In this study, fibers are replaced with CNTs to investigate their influence on this field. CNTs with a suitable dispersion (it is true about nanoparticles as well) can even improve the compressive strength more than 100%. However, the hydrophobic property should be considered. There were conflicting reports about the method of dispersion of nanoparticles. Either in mechanical, chemical treatment or sonication, it is important to avoid the agglomeration of such particles due to their high surface forces. In this research, CNTs were provided from Research Institute of Petroleum Industry by characteristics presented below:

Table 3.8. Properties of MWCNT

Properties of MWCNT	
BET	270 m^2/gr
Length	10 UM
Diameter	10-30 nm
Thermal conductivity	1500 w/mv

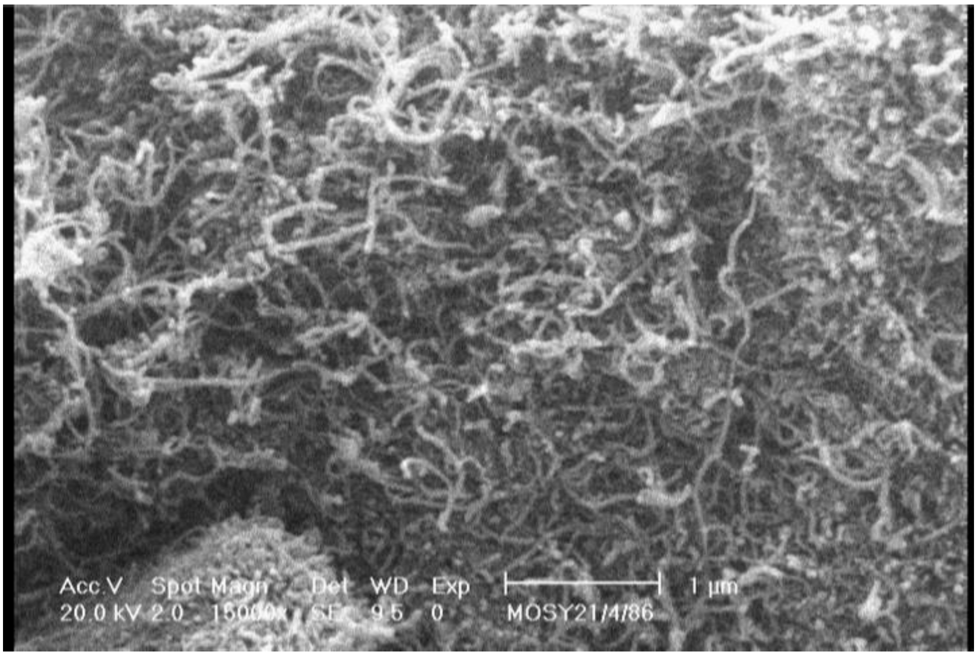

Figure 3.6. SEM image of MWCNT

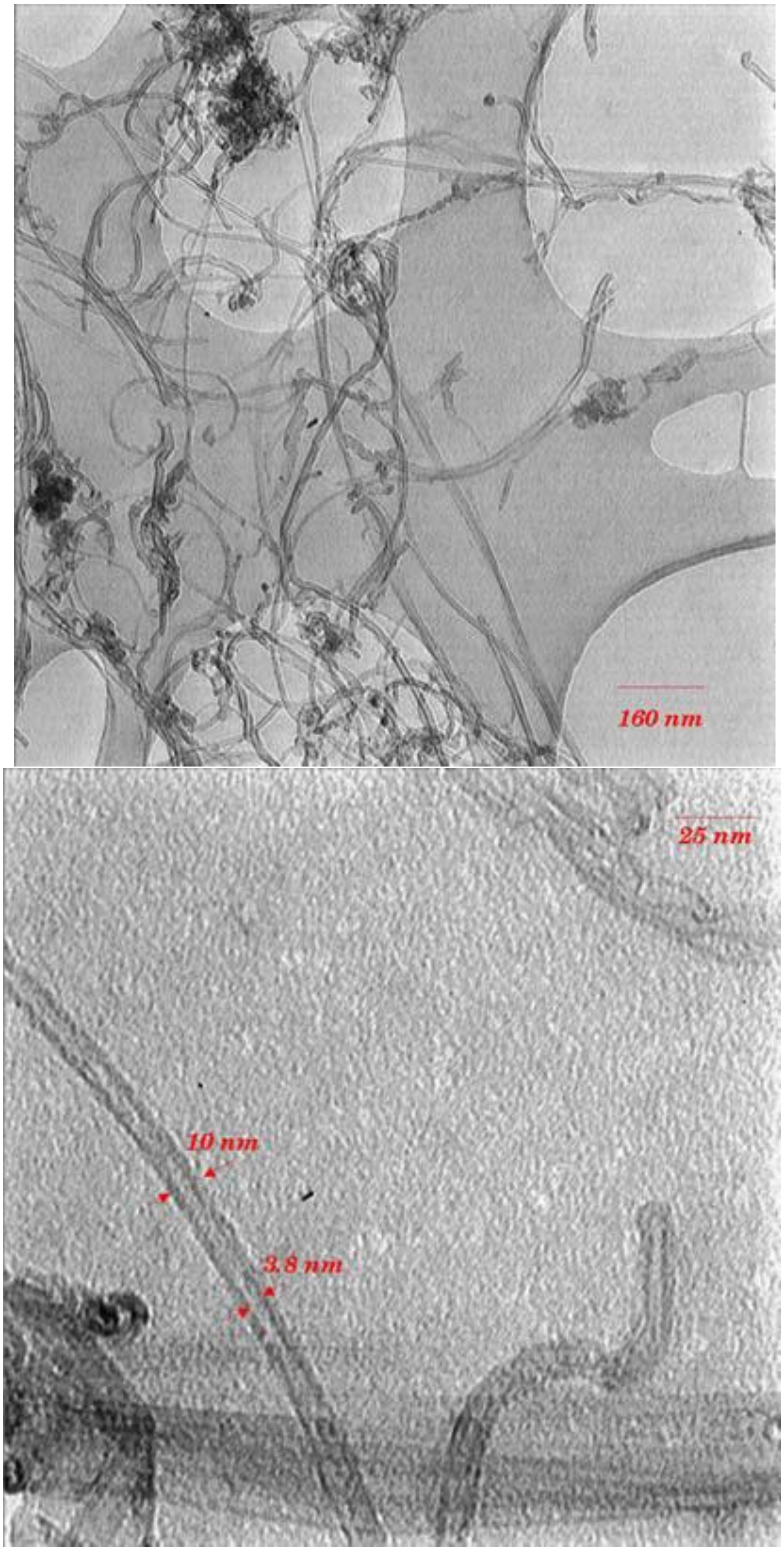

Figure 3.7. TEM image of MWCNT

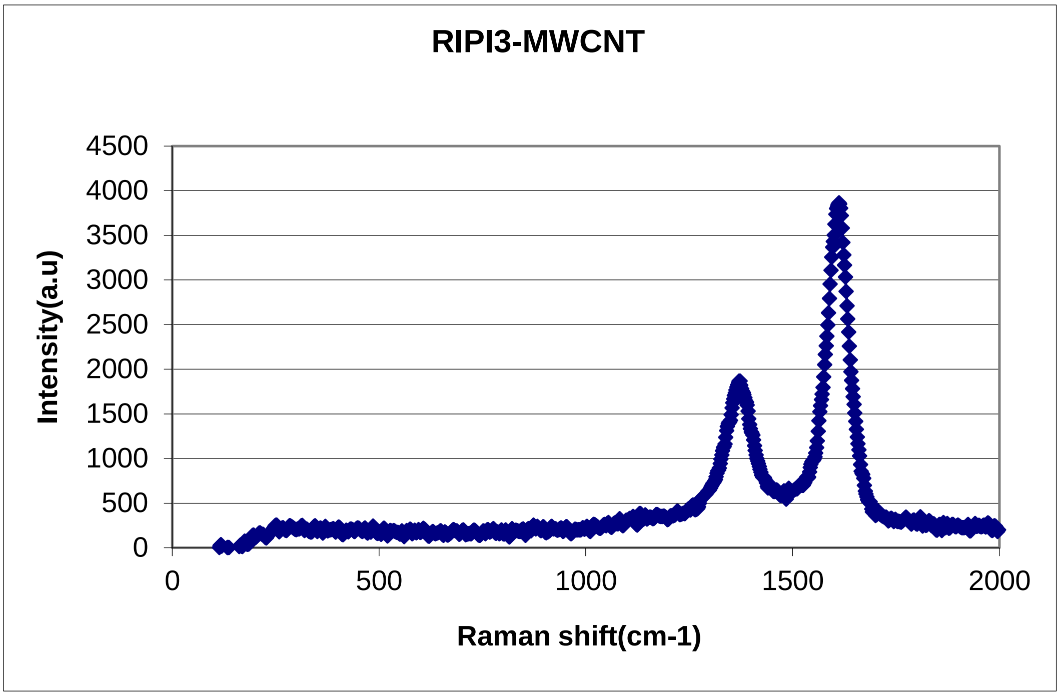

Figure 3.8. Raman analysis of MWCNT

3.2. Mix Design

There were different methods for mixing but the modified method of Andreasen and Anderson was most accepted. However, it needs exact investigation to determine a method for a mix with specific constituents such as nanoparticles or SCMs. First of all, in accordance with the sieve analysis and other properties, the mix design method used by Aydin A. C. (2007) selected as a base to satisfy all SCC criteria. This plain SCC group determined as G1 after several trials made some changes to achieve the best reference mix. There were two categories of mix groups and totally eight groups. The first category included G1, G2, G3 and G4 without fly ash besides the second category including G5, G6, G7 and G8 all with fly ash. Nano silica added to G2 and G6 and CNT involved in G3 and G7. G4 and G8 contained both NS and CNT. The w/c ratio fixed to 0.4 and cement content 500 kg/m^3 for all of groups together with 2% of binder weight for superplacticizer (SP) as it was recommended by manufacturer. The most effective dosages for FA, NS and CNT assigned as 40%, 2% and 0.08%, respectively, concluding from all researches before mentioned in chapter 2. Logically, the replacement level subtracted from cement amount. Table below gives details of mix proportions.

Table 3.9. Mix proportion details for groups

Category	Group	Cement (kg)	w/c	Water (kg)	SP (%)	SP (kg)	FA (%)	FA (kg)	NS (%)	NS (kg)	CNT (%)	CNT (kg)	Fine Agg. (kg)	Coarse Agg. (kg)
I	G1	500	0.4	200	2	10	–	–	–	–	–	–	1055	566
	G2	490	0.4	200	2	10	–	–	2	10	–	–	1055	566
	G3	499.6	0.4	200	2	10	–	–	–	–	0.08	0.4	1055	566
	G4	489.6	0.4	200	2	10	–	–	2	10	0.08	0.4	1055	566
II	G5	300	0.4	200	2	10	40	200	–	–	–	–	1055	566
	G6	290	0.4	200	2	10	40	200	2	10	–	–	1055	566
	G7	299.6	0.4	200	2	10	40	200	–	–	0.08	0.4	1055	566
	G8	289.6	0.4	200	2	10	40	200	2	10	0.08	0.4	1055	566

3.2.1. Mix production

A systematic sequences of operations employed in production of all SCC mixes to achieve a comparable results for all groups. Fine and coarse aggregates mixed in a rotary vertical axis mixer for 30 seconds to reach to a homogeneity of aggregates. In groups containing FA or NS, they were blended with cement and added to the mixer.

Then mixing continued for one minute. The half of water poured to the mixer and it rotated for another one minute. Thereafter the remained water was introduced to the mix and the concrete was mixed for minute again. In the matter of NS, the last mixing duration was 1.5 minutes. SP added with the second half of mix water. In groups including CNT, to avoid agglomeration, CNT was mixed first with water and blended sufficiently.

3.3. Test Methods

The three most important and wide spread tests for fresh state SCC conducted according to The European Guidelines for Self-Compacting Concretes 2005.

3.3.1. Fresh state tests

3.3.1.a. Slump-flow

As mentioned in section 2.1.4.4, this test measures the mobility and deformity of the SCC under a low rate of shear of self-weight by measuring free flow of concrete. Moreover, T_{500} helps to better evaluation of flowability.

A 900 × 900 mm metal tray placed horizontally and moisturized as in figure 2.3. The cone positioned at the center and filled by mix. All surplus concrete removed from top of the cone and from the base-plate. The cone lifted to allow the mix to spread and stop while another colleague was measuring $T_{500.}$ The longest diameter, d_m, and its perpendicular diameter, d_r, recorded to calculate their average. Potential bleeding or segregation visually checked by controlling paste zone in the age or coarse aggregate pile at the center.

3.3.1.b. V-Funnel

Once more, as stated in section 2.1.4.4, this inverted equipment, figure 2.5, is used to measure not only the filling ability of SCC but also considers high amount of coarse aggregate and high paste viscosity.

After wetting the V-Funnel apparatus and setting up, a container placed under it. The orifice closed and funnel filled. After removing and cleaning poured concrete the orifice opened to allow concrete flow to container until noticing the light through gate. The time between opening the gate and the seen light was measured as $t_{v\text{-}f}$.

3.3.1.c. L-Box

Referring to section 2.1.4.4 again, L-Box test method uses an L shaped container consist of a vertical and horizontal parts, figure 2.6, to evaluate properties such as mobility, passing ability, segregation and leveling.

First the device dampened and placed firmly in horizontal position. The gate closed and the vertical section filled with concrete. After removing all surplus concrete, the mix allowed to flow to horizontal part. The vertical distance of H_1, H_2 and their ratio obtained.

3.3.2. Hardened State Tests

For each group, nine cylinder samples of 100 × 200 mm and six prism samples of 70×70×280 mm produced.

3.3.2.a. Compressive strength

After curing period, compressive strength of 3, 7 and 28 days measured by three cylindrical samples for every age. For this purpose, a compressing device with 3000 kg loading capacity utilized. The samples capped with sulfur after demolding and located vertically to press. The pace of loading was set to be 5kgf/s and the maximum bearing load recorded. The compressive strength of each sample calculated by dividing the resulted load by the surface of sample and the average of three strains determined as the final compressive strength for every age of each group.

Figure 3.9. Compressive strength testing set up

3.3.2b. Flexural Toughness

In this part of the Study, Flexural toughness of various SCC mixes investigated. Among the several methods and standards for this issue, ASTM C1018 appeared to be more practical. JSCE SF-4 is similar to ASTM C1018 in test procedure and the only difference is in the way of curve analyzing. It is obvious that the P_v-δ diagram of plain concrete without steel bars or any kind of fibers would continue to a short distance after the pick point. Thus, the post-crack region does not seem suitable in PCS method.

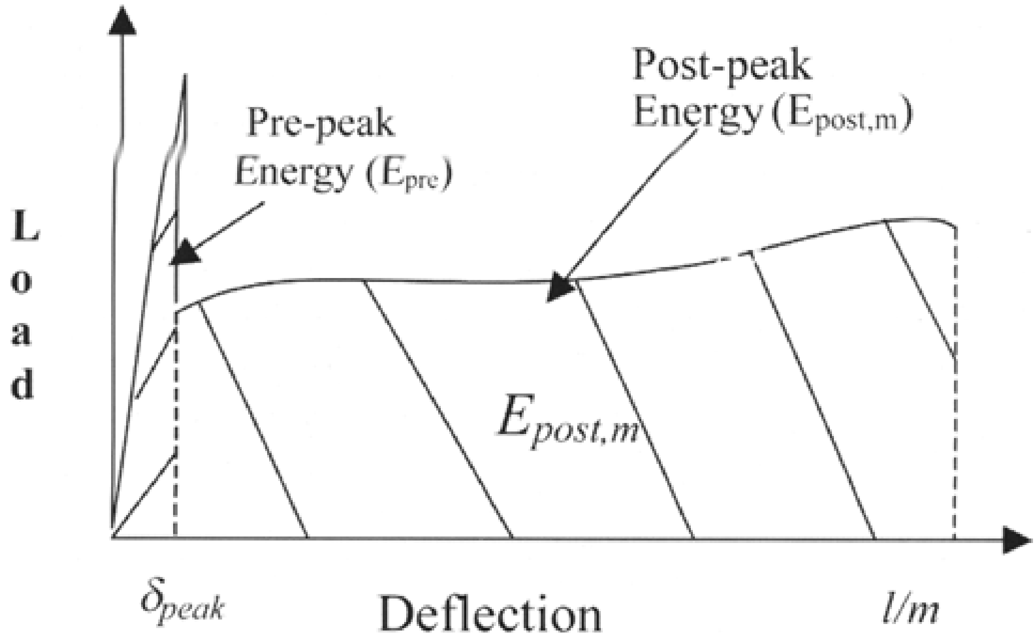

Figure 3.10. PCS analysis with pre-peak and post-peak region (Banthia 2004)

According to all above, ASTM C1018 with some tiny differences which were ignorable due to concept of comparison between different mixes, selected to be followed. A compressing machine with loading capacity of 3000 kg connected with a four-point bending set.

Figure 3.11. Flexural toughness testing set up

The specimens located on supports and a digital displacement meter positioned under the mid-span of them. A digital high resolution camera was recording all the procedure. The loading rate was selected as 5 kgf/s. After failure of the specimens, the recorded procedure reviewed slowly and precisely to obtain values of loading and displacement. Subsequently, the curves of load versus mid-span for all specimens acquired. By locating the first crack and measuring the areas, toughness indexes achieved to utilize in evaluation and comparison of flexural toughness of various SCC mixes.

4. RESULTS AND EVALUATIONS

4.1. Fresh State Results

4.1.1. Slump-Flow

In trial mixes the value of S-F for reference mixture had been decided to be close to average value of class SF2. Thus, the 73.5 cm of G1 was satisfying. At first category where mixes include no FA, the introduction of NS reduced the S-F value to the threshold limit of 52 cm in G2 and even G4 which was containing CNT. It can be contributes to the high surface area of NS and its higher water demand which causes problems of flowability in mixes with a constant amount of water. However, the addition of CNT in G3 improved the value to the 79 cm.

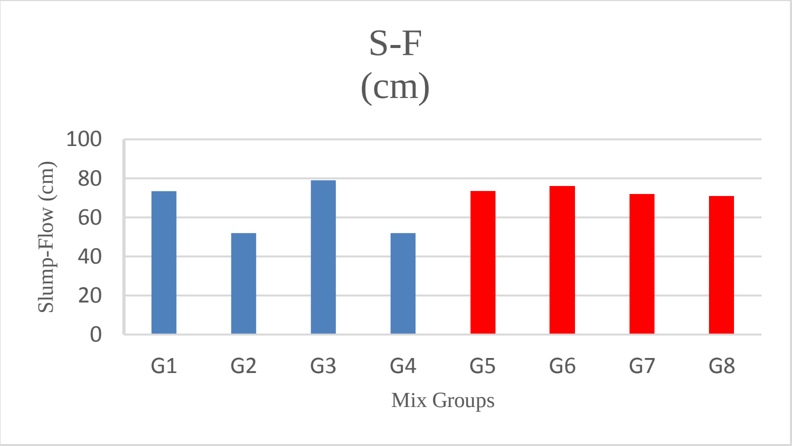

Figure 4.1. Slump-Flow test results

By contrast, in second category with mixes including FA, there was no evident altering in values by conclusion of NS, CNT or both of them. As it is obvious in Figure 4.1, there was not any noticeable fluctuation which means the inclusion of 40% FA has a dominating effect on the flow ability and deformability of the mix. FA conferred a better flow to mixes by reducing the sensitivity of all mix groups of the second category in which NS made the best result in G6 by a Slump-Flow of 76 cm.

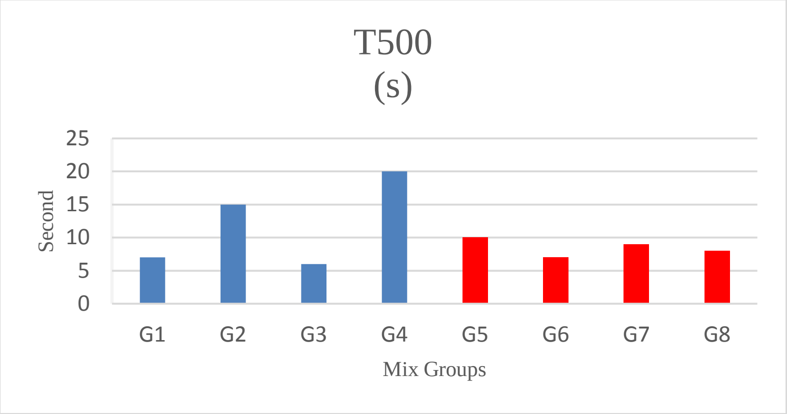

Figure 4.2. T_{500} test results

Figure 4.2 highlights the directly converse relationship between T_{500} test times and Slump-Flow test results. The longer the S-F value, the shorter the T_{500} period. The balancing effect of FA in controlling fluctuations was in the same manner. Here again, mix group G3 containing only CNT reduced T_{500} to the minimum of all by 6 s whereas G6 made the best time of 7 s possessing NS in mix groups with FA replacement.

4.1.2. V-Funnel

In the first category, the achieved 15 s for V-F time of G1 was reasonable. The inclusion of NS in group 2 and both NS and CNT in group 4 caused a remarkable increase of 67% and 87%, respectively. This can be due to increased paste viscosity as a result of higher reactivity of NS and its water consumption.

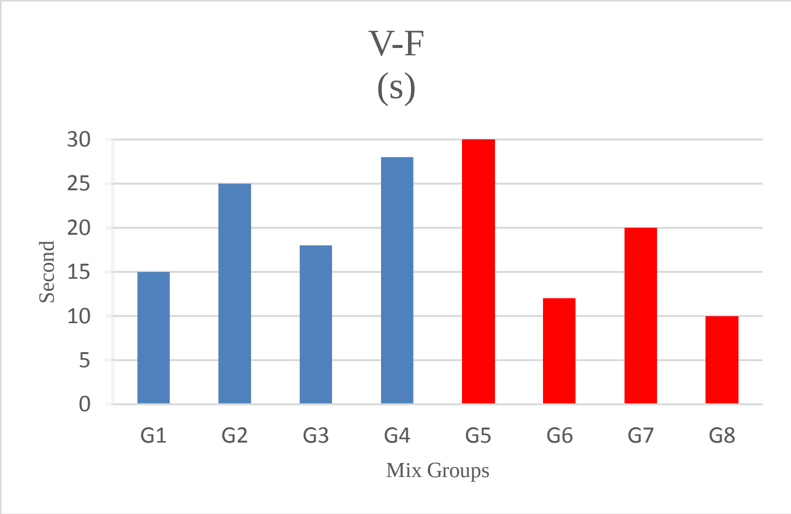

Figure 4.3. V-Funnel test results

In the second mix category, a completely contrast phenomenon observed by introducing 40% FA. FA permitted more free water in the mixture which trigger bleeding of mix. Thus, during V-Funnel test, normally the paste part of mix flowed out of the gate of apparatus in such vertical position and blockage happened. The more reactivity and higher water demanding properties of NS compensated this deteriorative effect of such huge proportion of FA replacement. Thus, the best results achieved by adding NS particles to mixes either with or without CNTs. This may can be interpreted by lesser K value of FA. As 40% FA replaced with cement the lower K factor of FA compensated the higher reactivity of NS and the best V-F time of 10 s was recorded for G8 with 40% FA, 2% NS and 0,08% CNT. All outcomes presented in Figure 4.3.

4.1.3. L-Box

The L-Box ratio of reference mix, G1, was 0.78. As a result of a small CNT proportion of G3, 0.08% the ratio remained constant. But, in groups 2 and 4, similar to previous tests, a great reduction happened so that the values fall to a smaller value than the lower limit according to The European Guidelines for Self-Compacting Concrete, 2005. Even though there was no bleeding or segregation in mixes of G2 and G4, less flow ability and high viscosity of the mixes were distinguished visually.

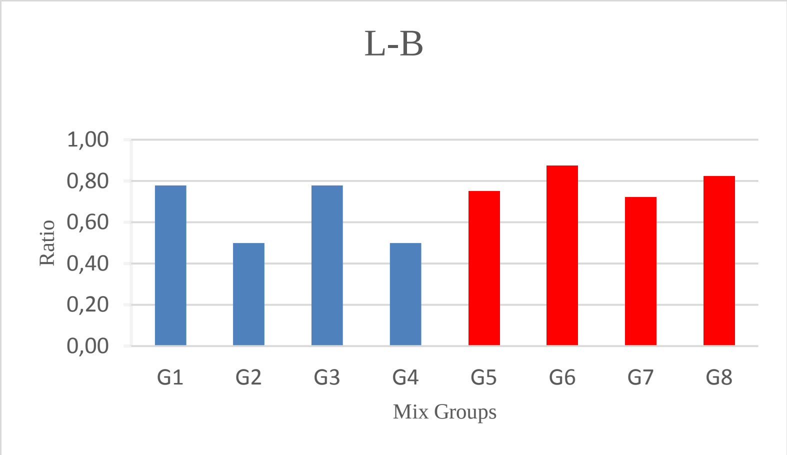

Figure 4.4. L-Box test results

In similar way to V-F experiences, the 40% replacement of FA in the mix resulted in much better consequences. NS increased this ratio from 0.75 for G5 to 0.88 for G6 and 0.82 for mixes with NS and both NS together with CNT, respectively, in spite of no sensible change for G7 containing only CNT in category II. G6 and G8 possessed very good condition of fresh state with no bleeding or segregation. Table 4.1 summarizes all results related to fresh SCC tests.

Table 4.1. Fresh state test results

Category	Group	S-F (cm)	T_{500} (s)	V-F (s)	L-B (-)
I	G1	73.5	7	15	0.78
	G2	52	15	25	0.50
	G3	79	6	18	0.78
	G4	52	20	28	0.50
II	G5	73.5	10	30	0.75
	G6	76	7	12	0.88
	G7	72	9	20	0.72
	G8	71	8	10	0.82

4.2. Hardened State Results

4.2.1. Compressive strength

All groups of both categories tested for their compressive strength of 3, 7 and 28 days. The summary of the results has been presented in Table 4.2.

Table 4.2. Compressive strength of 3, 7 and 28 days

Category	Group	f_c' 3 Days	f_c' 7 Days	f_c' 28 Days
I	G1	411	418	467
	G2	305	473	496
	G3	416	426	482
	G4	308	478	499
II	G5	173	208	361
	G6	258	290	512
	G7	149	234	349
	G8	205	377	495

In all groups, regardless of their various contents, compressive strength was increasing by aging, but the tendency was different. As illustrated in Figure 4.5, the mix with CNT of first category, G3, showed a similar normal model of getting strength with the reference mix G1. Nevertheless, mix G2 with NS and mix G4 with NS plus CNT experienced a sharper increase in first part of the graphs. This could be due to the high reactivity of NS. NS accelerates the hydration process by producing nucleation sites to precipitate C-S-H owing to its high surface area.

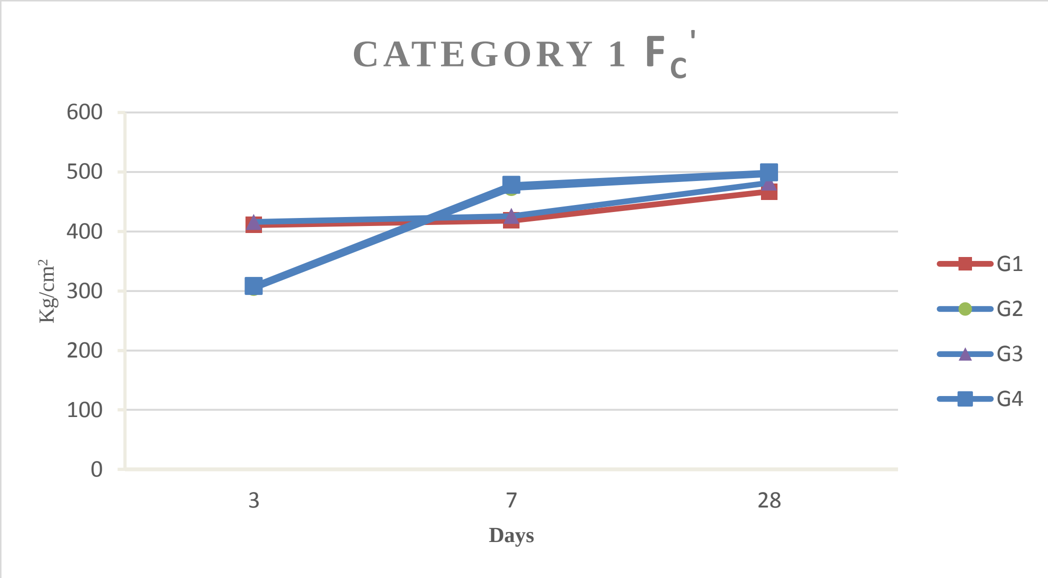

Figure 4.5. Tendency of gaining compressive strength for SCC mixes without fly ash

A different pattern was seen in Figure 4.6. A completely considerable retardation on early age strength of samples observed. The presence of FA in mixtures was the main cause of this event in G5 and G6. The creation of nucleation sites on the surface of FA retards the reaction of alite at early ages. On the other hand, in G7 and G8, the existence of CNT compensate at the day of 7 and produced a smoother graphs.

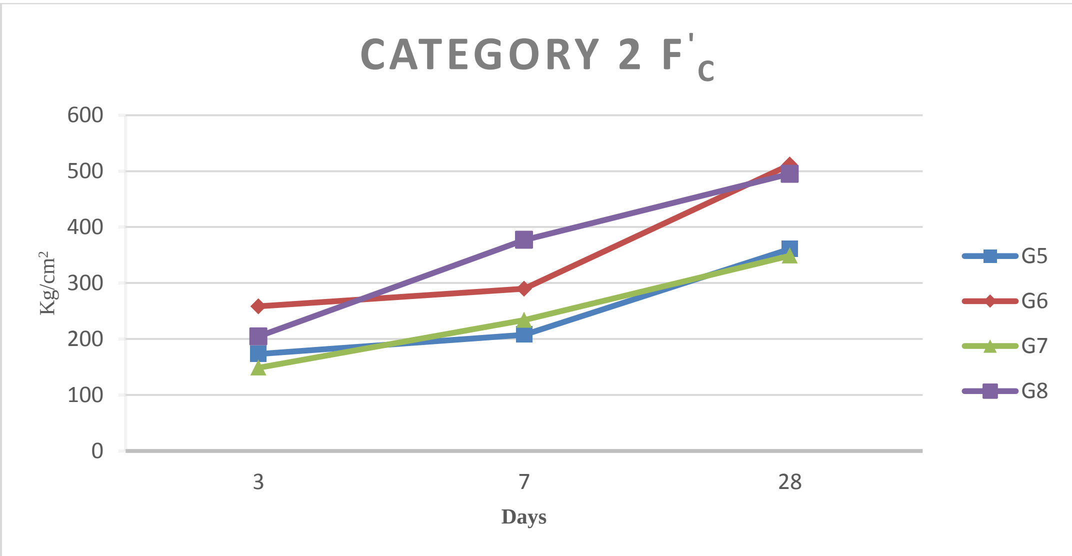

Figure 4.6. Tendency of gaining compressive strength for SCC mixes with fly ash

Figure 4.8 demonstrates the 3 day compressive strength of samples. In category I, despite addition of 2% NS, mix G2 and G4 lost 26% and 25% of their 3 day compressive strength. It seemed weird but this related to fresh state tests. Since the basis of study was on comparison of various SCC mixes of different particles and powder, the w/c ratio and SP content of all mixes were constant. Considering this fact that no vibration fulfilled during filling the molds to simulate self-compactibility, the weak rheological results of G2 and G4 had resulted in honeycombed and segregated weak hardened samples.

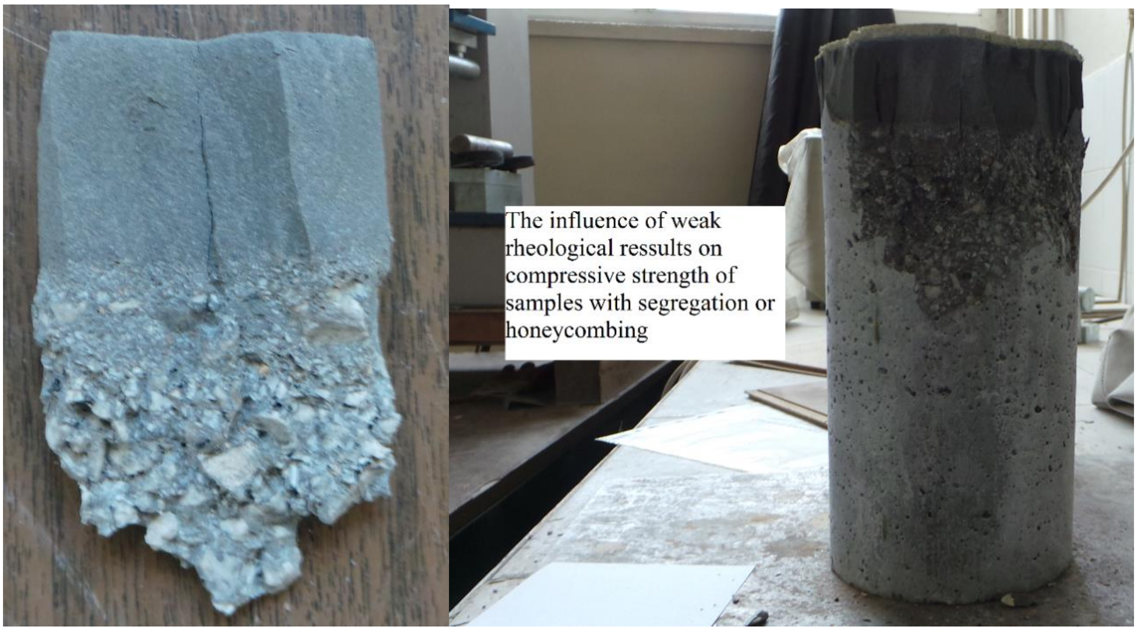

Figure 4.7. Negative effects of low fresh state results on hardened state results

Visual investigation of tested samples indicated that both of these mixes possessed distinguishable voids in the texture which caused great decrease of compressive strength in all samples of every ages. Although the compressive strength of mix G3 with CNT increased 1%.

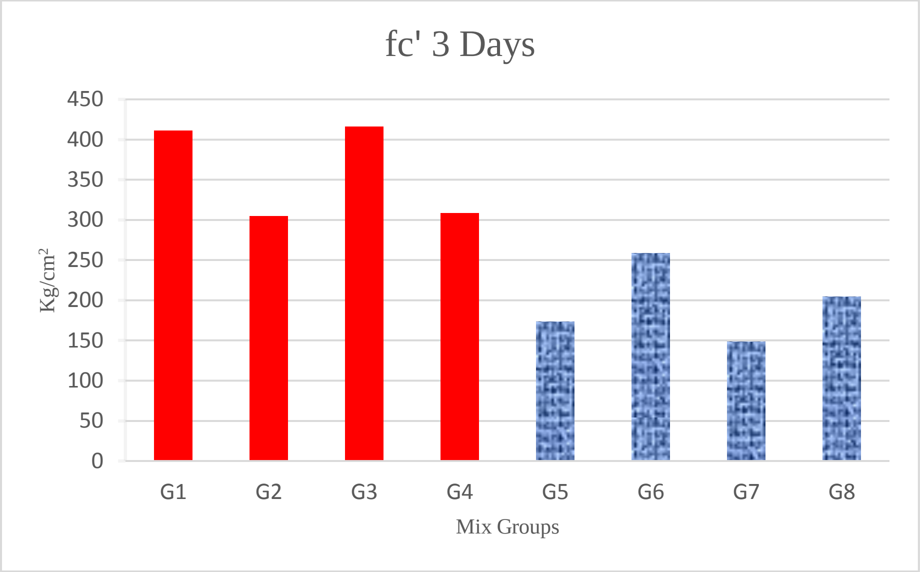

Figure 4.8. Compressive strength results after 3 days

The condition in category II was totally different. The 40% replacement of FA caused an approximately 58% reduction in G5, the reference group of this category, and similarly in other three groups. But, the inclusion of NS in G6 and G8, resulted in 49% and 18% increment of 3 day compressive strength, respectively, compared to reference mix group of this category, G5. The 14% reduction of G7 and lesser rise of G8 in comparison with G6 may be contributed to agglomeration of CNT in some points of the mixtures.

As seen in Figure 4.9, the higher reactivity NS compensated the void deficiencies of G2 and G4 and resulted in even 13% and 14% increase of strength. 2% higher 7 day compressive strength of G3 indicates the positive influence of CNT regarding its tiny proportion.

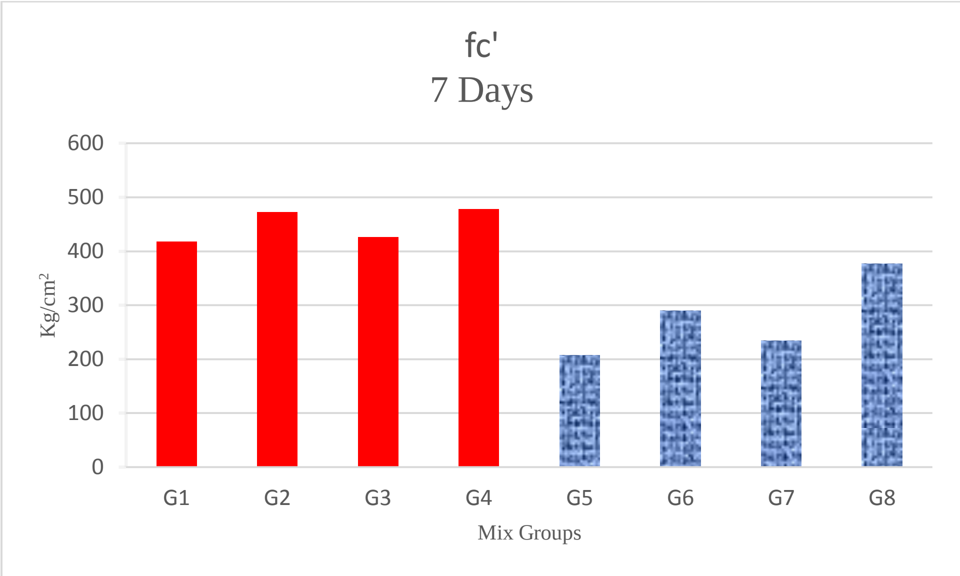

Figure 4.9. Compressive strength results after 7 days

In the second category, the 50% reduction was predictable due to 40% replacement of FA in G5. NS and CNT caused 40% and 13% higher 7 day compressive strength in G6 and G7 compared with G5. Simultaneous inclusion of CNT and NS resulted in the best 7 day compressive strength rise of 82% in mixes with FA for G8.

Figure 4.10 revealed a tendency similar to 7 days graphs of getting strength in 28 days for the first category. NS made 6% and 7% increase for G6 and G8, respectively. On the other hand, the little positive influence of CNT in G3 and G4 was indicated due to its small proportion in the mix. Conversely, the remarkable influence of these particles observed again with 42% and 37% in mixes G6 and G8, respectively, by presence of FA causing suitable self-compacting properties.

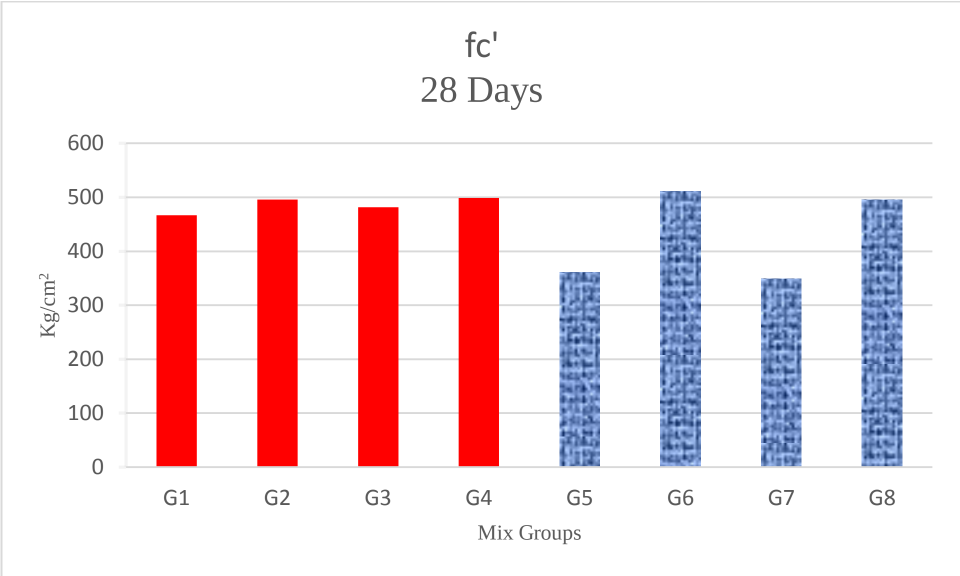

Figure 4.10. Compressive strength results after 28 days

4.2.2. Flexural toughness

Figure 4.11 and 4.12 show the load versus displacement diagrams of the mix groups of category I and II. The flexural toughness of concrete is evaluated by toughness indices. Since the calculation of these indices is on the bases of determination of first crack occurrence, all diagrams magnified to achieve this important and sensitive goal accurately. It was predictable that the plastic area after observing the first crack would not be so long. The maximum displacement never reached to triple δ_0 which results in equal areas for A_2, A_2+A_3, $A_2+A_3+A_4$ and $A_2+A_3+A_4+A_5$. Therefore, in all diagrams, toughness indices of I_5, I_{10}, I_{20}, and I_{30} measured with the same value in each mix group.

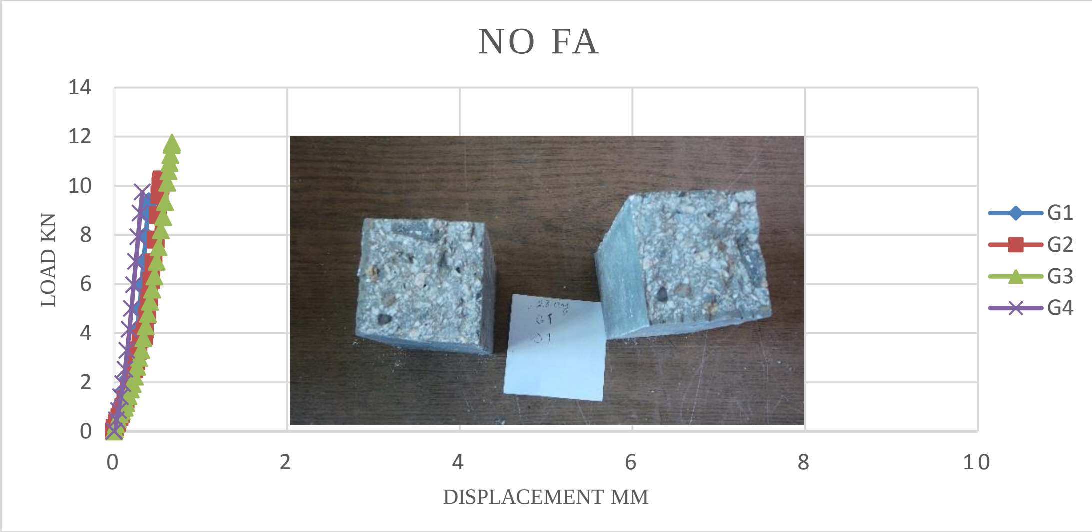

Figure 4.11. Load vs. Displacement graphs of mix groups without FA

In both categories with or without FA, the maximum loading recorded in groups containing CNT. It can clearly contributed to the crack bridging characteristics of CNTs which cause a higher moment bearing capacity for concrete profile in tensional area below the neutral axis.

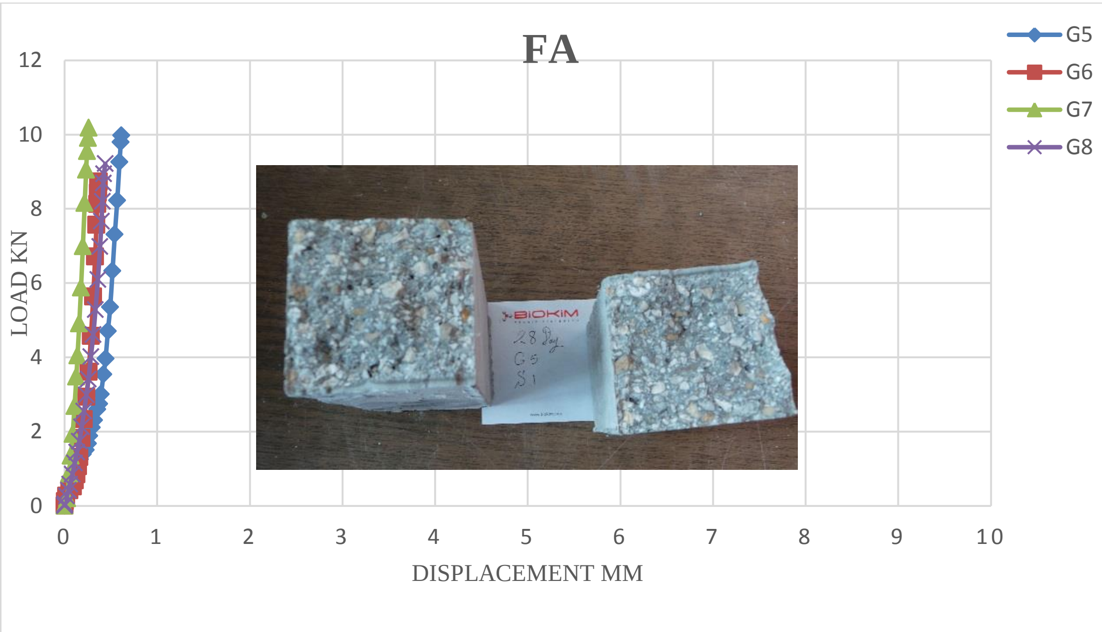

Figure 4.12. Load vs. Displacement graphs of mix groups with FA

Due to reasons mentioned above, the toughness indices for each category presented in a unit diagram. Figure 4.13 illustrates these indices for groups without FA. The toughness indices of reference group G1 were very close to unity as excepted. The inclusion of NS increased the values 3.68% in G2 whereas CNT raised them up to 20.83% for G3. This means that CNTs demonstrate a great influence on flexural toughness of self-compacting concretes. In G4, the mutual inclusion of NS and CNT made 17.45% increment, too.

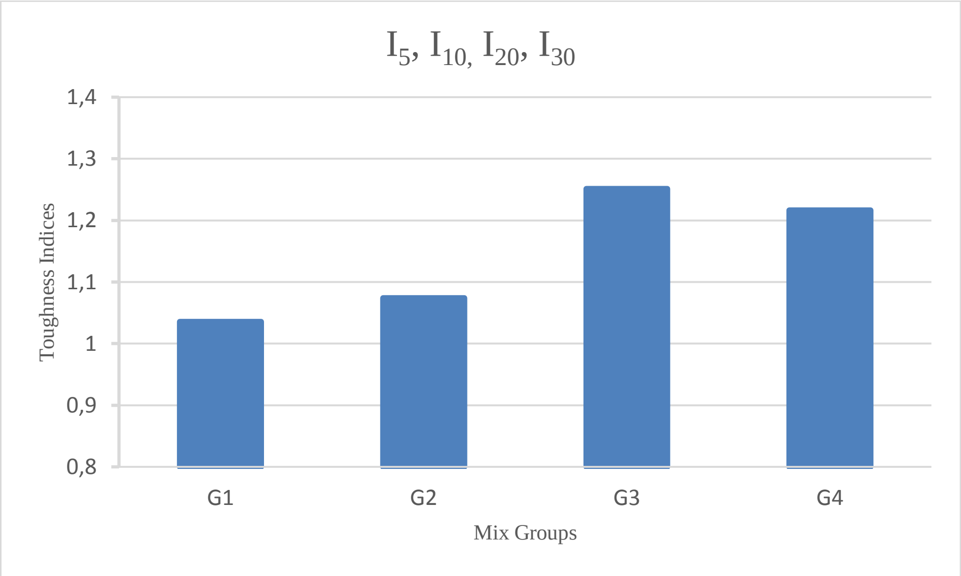

Figure 4.13. Toughness indices of mix groups without FA

As seen in Figure 4.14, the second category with mix groups containing FA followed a parallel pattern with category I. The mix G6 which contained NS possessed 6.98% further toughness indices than G5. CNTs again, increased the indices remarkably 17.96%. The joint impact of NS and CNT was 11.10% increment for G8.

All above mentioned demonstrates the outstanding effect CNT in improvement of CNTs on flexural toughness of SCCs. By restraining crack propagation and bridging them, CNTs interfere in tension bearing capacity of concrete sections owing to their tubular shape and extremely high strain bearing characteristics. It can also be contributed to the constructive role of CNTs in enhancing the quality of ITZ and microstructure of SCC.

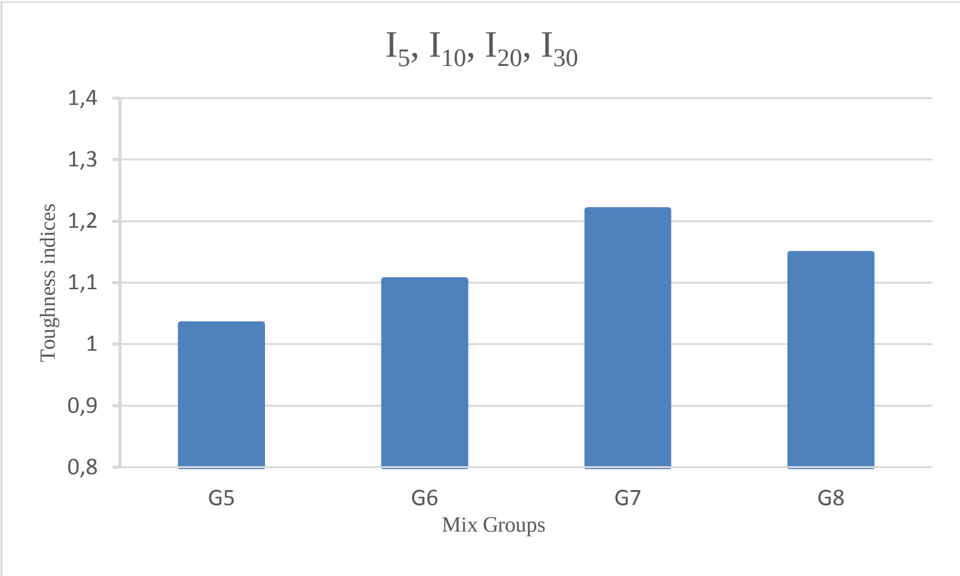

Figure 4.14. Toughness indices of mix groups with FA

5. CONCLUSIONS

Based on different tests carried out on various mixes of SCC, the following conclusions can be drawn:

- The maximum Slump-Flow time achieved by merely inclusion of CNT. Due to its higher water demand, NS significantly reduced this value in absence of FA. However, FA showed the strongest influence owing to its lesser water demand and reducing the sensitivity of SCC to changes of amount the free water in mix. NS demonstrated the maximum improving for mixes with FA.
- The mix containing solely CNT achieved the best result of all groups for T_{500}. On the other hand, FA controlled variations and NS resulted in minimum T_{500} time in mixes with 40% FA replacement.
- The higher reactivity of NS ruined V-Funnel test results causing high paste viscosity. In spite of NS, the enormous proportion of FA resulted in bleeding due its lesser water demand which worsened the time otherwise. The inclusion of NS and CNT in presence of FA prepared the best outcome.
- The destructive influence of NS in plain SCC repeated in L-Box tests despite its outstanding effects on mixes containing FA with or without CNT.
- NS accelerated the strength gaining at early ages by creation of nucleation sites due to its higher surface area, despite FA which retarded the process as a result of creation of nucleation site on its surface and retarding reaction of alite at early ages. Interestingly, CNT improved this retardation in FA mix groups.
- According to weak fresh state results of mix groups with 2% NS but without FA, the extra voids of deficient self-compaction worsened the 3 day compressive strength. In presence of FA however, the improving effect of NS appeared. A 14% retardation influence of CNT was may be due to agglomeration of the particles. A total reduction of 3 day strength of samples by inclusion FA might be worth to be paraphrased.
- Accelerating attribute of NS showed even an improvement in 7 days despite the surplus voids of inadequate self-compacting. A small rise happened by CNT as well. On

the other hand, NS and CNT demonstrated again their outstanding influences together with FA and the maximum 7 days rise of strength was seen in a synergic mix of them.

- The improving effect of NS continued on 28 days and continued to recompense the weak points produced by insufficient fresh quality of SCC mixes without FA. CNT showed its slight influence in accordance with its small proportion or maybe due to its helpful role during fresh tests. In SCC mixes including FA, the main role of highlighted again. SCC mixes containing one or both CNT and NS by introduction FA gained the best compressive strength in 28 days.
- The highest load bearing capacity in flexural toughness test recorded for mix groups containing CNT. It was expectable due to tubular shape of CNTs which provide bridging between crack spans and tolerate the tension stresses induced through moment of loading by means of their incredible tensional strength.
- For all mix groups we had: $I_5=I_{10}=I_{20}=I_{30.}$ It was predictable since the ultimate displacement of a concrete with neither steel bar nor any kind of fiber would not reach to the threefold value of the displacement corresponding to the first crack.
- CNT demonstrated the maximum improvements on flexural toughness indices about 21% and 18% for SCC mixes both with and without FA, respectively. NS made its own rise but not comparable to that of CNT. The synergic effects of them were promising as well.
- Considering all mentioned above, it could be concluded that the mix group number 8 which contained 40% FA, 2% NS and 0.08% CNT can be determined as the best SCC mixture. The advantage of 40% replacement of FA can help to development of environment friendly and sustainable construction by reducing cement consumption. Furthermore, it helps SCC mix to be more cohesive and balance the weak points of fresh state properties of the mix including NS. On the other hand, NS not only help fresh SCC to avoid segregation or bleeding in presence of FA, but also remove the retardation effects of FA in early ages. In addition, NS help the SCC mix improve its compressive strength remarkably beside its sensible rising effect on flexural toughness indices. Finally, CNT helps in correction of all fresh properties of SCC mix but its main role appears in flexural toughness. In spite of the tiny proportion of CNT, it is able to rise the flexural indices more than 20% and provide the advantage of more elastoplastic

SCC mix by restraining cracks and avoiding their propagation due to its bridging influences. Moreover, CNT similar to NS could improve ITZ and microstructure of SCC significantly to result in such improvements in hardened properties.

- The usage of LVDT and Yoke is strongly recommended to avoid effects of seating or twisting of specimens during flexural test.
- It could be recommended that the durability of this mix of SCC to be investigated and permeability tests to be fulfilled as the proof of microstructure improvements.

REFERNCES

Anderson Materials Evaluation, Inc., 2014. Thermogravimetric Analysis (TGA). http://wwwandersonmaterials.com/tga/html.

ASTM C 1018, 1990. Standard Test Method for Flexural Toughness and First Crack Strength of Fiber Reinforced Concrete.

ASTM C 1585-04, 2007. Standard Test Method for Measurement of Rate of Absorption of Water by Hydraulic-Cement Concretes.

ASTM C 666/C 666M – 03, 2008. Standard Test Method for Resistance of Concrete to Rapid Freezing and Thawing.

Aydin A. C., 2007. Self Compactability of High Volume Hybrid Fiber Reinforced Concrete. Construction and Building Materials 21 (2007) 1149-1154,

Banthia N. and Gupta R., 2004. Hybrid Fiber Reinforced Concrete (HyFRC): Fiber Synergy in High Strength Matrices. Materials and Structures 37 (2004) 707-716.

Banthia N. and Trottier J., 1995. Test Methods for Flexural Toughness Characterization of Fiber Reinforced Concrete: Some Concerns and a Proposition. ACI Materials Journal/ January-February (1995) 48-57

Behfarnia, K. and Salemi, N., 2013. The effects of nano-silica and nano-alumina on frost resistance of normal concrete. Construction and Building Materials 48 (2013) 580–584.

BIBM, CEMBUREAU, ERMCO, EFCA and EFNARC, 2005. SCC 028. The European Guidelines for Self-Compacting Concrete Specification, Production and Use.

Birgisson, B., Mukhopadhyay, A.K., Geary, G., Khan, M. and Sobolev, k., 2012. Nanotechnology in concrete materials: A synopsis. Transportation Research Materials E-C170.

Brouwers, H.J.H. and Radix, H.J., 2005. Self-Compacting Concrete: Theoretical and experimental study. Cement and Concrete Research 35 (2005) 2116 – 2136.

Controls Group Company, 2014. Testing equipment for the construction industry. Http://http://www.controls-group.com.

Dinakar, P. and Manu, S.N., 2014. Concrete mix design for high strength self-compacting concrete using metakaolin. Materials and Design 60 (2014) 661–668.

Domone P.L., 2005. Self-compacting concrete: An analysis of 11 years of case studies. Cement & Concrete Composites 28 (2006) 197–208

Domone, P.L., 2006. A review of the hardened mechanical properties of self-compacting concrete. Cement & Concrete Composites 29 (2007) 1–12.

Dransfield, J., 2003. Admixture for concrete, mortar and grout. Advanced Concrete Technology Constituent Materials, Newman J. and Choo B.S.. Elsvier, UK,4/1-3/36.

Duzgun O. A., Gul R. and Aydin A. C., 2005. Effects of Steel fiber on the Mechanical Properties of Natural Light Weight Aggregate Concrete.

Efnarc, 2002. Specification and Guidelines for Self-Compacting Concrete.

Efnarc, ENC 180VMA, 2006. Guidelines for Viscosity Modifying Admixtures For Concrete.

Farzaneh, O.J. Nasiri, J.R. and Bahari, A., 2009. The role of nano particles in self Compacting concrete. Excellence in Concrete Construction through Innovation.

Ferro, G., Tulliani, J., and Musso, S., 2011. Carbon nanotubes cement composites. Frattura ed Integrità Strutturale, 18 (2011) 34-44.

Gaimster, R. and Dixon, N., 2003. Self-Compacting Concrete. Advanced Concrete Technology Processes, Newman J. and Choo B.S.. Elsvier, UK,9/1-9/23.

Gieshe, H., 2006. Mercury Porosimetry: a General (Practical) Overview. Part. Part. Sys. Charact. 23 (2006) 1-11.

Hafner, B., 2007. Scanning Electron Microscopy Primer. Characterization Facility, University of Minnesota—Twin Cities.

Hongjian D., Suhuan, D. and Xuemei, L., 2014. Durability Performances of Concrete With Nanosilica. ACI Materials Journal

Lewis R., Sear L., Wainwright P. and Ryle R., 2003. Cementitious additions. Advanced Concrete Technology Constituent Materials, Newman J. and Choo B.S.. Elsvier, UK,3/1-3/66.

Micromeritics Instrument Corporation, 2014. Mercury Intrusion Porosimetry Theory. http://www.micromeritics.com

Nataraja M.C., Dhang N. and Gupta A.P., 2000. Toughness Characterization of Steel Fiber-Reinforced Concrete JSCE Approach. Cement and Concrete Research 30 (2000) 593-597.

Nazari, A. and Riahi, R., 2010. Microstructural, thermal, physical and mechanical behavior of the self-compacting concrete containing SiO2 nanoparticles. Materials Science and Engineering A 527 (2010) 7663–7672.

Nazari, A. and Riahi, R., 2011. Effects of CuO nanoparticles on compressive strength of self-compacting concrete. Sa¯dhana¯ Vol. 36, Part 3, June 2011, pp. 371–391.

Newman J., 2003. Strength-testing Machines for Concrete. Advanced concrete Technology-Testing and Quality, Newman J. and Choo B.S. Elsvier, UK, 2/1-2/11.

NT BUILD 492, 1999. Chloride Migration Coefficient from Non-Steady-State Migration Experiments.

PerkinElmer, Inc., 2010. Thermogravimetric Analysis (TGA) A Beginner’s Guide. http://www.perkinelmer.com.

Quercia, G., and Brouwers H.J.H., 2010. Application of nano-silica (nS) in concrete mixtures. 8th fib PhD Symposium in Kgs. Lyngby, Denmark.

Quercia, G., Spiesz P., Hüsken G. and Brouwers H.J.H., 2013. SCC modification by use of amorphous nano-silica. Cement & Concrete Composites 45 (2014) 69–81.

Raki, L., Beaudoin, J., Alizadeh, R., Makar, J. and Sato, T., 2010. Cement and Concrete Nanoscience and Nanotechnology. Materials 2010, 3, 918-942.

Sahmaran M. and Yaman I.O., 2005. Hybrid Fiber Reinforced Self-Compacting Concrete with a High-Volume Coarse Fly Ash. Construction and Building Materials (2005)

Sfikas, L.P., Badogiannis E.G. and Trezos K.G., 2014. Rheology and mechanical characteristics of self-compacting concrete mixtures containing metakaolin. Construction and Building Materials 64 (2014) 121–129.

Shaikh, F.U.A., Supit, S.W.M. and Sarker, P.K., 2014. A study on the effect of nano silica on compressive strength of high volume fly ash mortars and concretes. Materials and Design 60 (2014) 433–442.

Testing-SCC, 2005. Guidelines for testing fresh self-compacting concrete.

Transportation Research Circular E-C170, 2012. Nanotechnology in Concrete Materials.

Türkel, S. and Kandemir, A., 2010. Fresh and Hardened Properties of SCC Made with Different Aggregate and Mineral Admixtures. Journal Of Materials In Civil Engineering, 1025-1032.

Wang, X., Rhee, I., Wang, Y. and X+C15i, Y., 2014. Compressive Strength, Chloride Permeability, and Freeze-Thaw Resistance of M+C42WNT Concretes under Different Chemical Treatments. Scientific World Journal Volume 2014, Article ID 572102, 8 pages.

Yu, R., Spiesz, P., Brouwers, H.J.H., 2014. Effect of nano-silica on the hydration and microstructure development of Ultra-High Performance Concrete (UHPC) with a low binder amount. Construction and Building Materials 65 (2014) 140–150.

Zhang, P., Zhao, Y., Li, Q., Wang, P. and Zhang, T., 2014. Flexural Toughness of Steel Fiber Reinforced High Performance Concrete Containing Nano-SiO2 and Fly Ash. The Scientific World Journal, Volume 2014, Article ID 403743, 11 pages

CURRICULUM VITAE

Vahid Jalilzadin Nasl was born in Maragheh/Iran, in 1978. He received his bachelor degree in Civil Engineering from Technical and Engineering Faculty of Urmia University, Iran. Before attending his Master degree in Ataturk University of Turkey in 2013, he had been working in various construction projects as civil engineer and construction manager.